

# Speed-dependent interaction of sensory signals and local, pattern-generating activity during walking in *Drosophila*

Inaugural-Dissertation

zur

Erlangung des Doktorgrades

der Mathematisch-Naturwissenschaftlichen Fakultät

der Universität zu Köln



vorgelegt von

**Volker Berendes**

aus Bensberg

Köln

Mai

2016

Berichtersteller: Prof Dr. Ansgar Büschges  
(Gutachter) PD Dr. Silvia Daun (ehem. Gruhn)

Tag der mündlichen Prüfung: 08.07.2016



## Table of Contents

|  |     |
|--|-----|
| Abstract .....   | III |
| Zusammenfassung.....   | V   |
| 1. Introduction.....   | 1   |
| 1.1 Central pattern generators (CPGs) and coordination .....           | 2   |
| 1.2 Inter-leg coordination at different walking speeds.....            | 3   |
| 1.3 Amputation experiments and the control mechanisms of walking ..... | 5   |
| 1.4 Studying walking in <i>Drosophila</i> .....                        | 5   |
| 1.5 The present thesis.....  | 7   |
| 2. Material and Methods.....   | 9   |
| Animals .....  | 9   |
| 2.1 Experiments on leg kinematics and inter-leg Coordination .....     | 9   |
| Experimental setup.....  | 9   |
| Video acquisition.....   | 12  |
| Data Analysis .....  | 14  |
| Software .....   | 18  |
| 2.2 Walking Speed and Activity Assay.....                              | 19  |
| Experimental setup.....  | 19  |
| Data analysis .....  | 20  |
| Software .....   | 21  |
| 3. Results .....   | 25  |
| 3.1 Experiments on leg kinematics and interleg coordination .....      | 25  |
| 3.1.1 Experiments on the side-view setup.....                          | 25  |
| Intact flies.....  | 25  |
| R1 amputees:.....  | 29  |
| R2 amputees .....  | 32  |
| R3 amputees .....  | 36  |
| 3.1.2 Experiments on the top-view setup .....                          | 42  |
| Intact flies.....  | 44  |
| R1 amputees .....  | 46  |
| R2 amputees .....  | 51  |
| R3 amputees .....  | 54  |
| 3.2 Animal Speed and Activity Assay .....                              | 58  |
| Intact animals .....   | 59  |

---

|  |     |
|--|-----|
| R1 amputees .....  | 61  |
| R2 amputees .....  | 62  |
| R3 amputees .....  | 64  |
| 4. Discussion .....  | 66  |
| 4.1 Rhythmic Motor Activity of Leg Stumps in Walking <i>Drosophila</i> ..... | 67  |
| 4.2 Descending Control of Walking Speed in <i>Drosophila</i> .....           | 69  |
| 4.3 Speed-dependence of coordination strength .....                          | 70  |
| 4.4 Differences between the ball setups .....                                | 71  |
| 4.5 Differences between free and tethered walking .....                      | 72  |
| 4.6 New insights and open questions .....                                    | 75  |
| Bibliography .....   | 77  |
| Appendix .....   | 88  |
| List of Figures .....  | 108 |
| Danksagung .....   | 111 |
| Mein Besonderer Dank gilt: .....   | 111 |
| Teilpublikationen .....  | 112 |
| Conference abstracts .....   | 112 |
| Erklärung .....  | 113 |
| Curriculum vitae .....   | 114 |
| Ausbildung .....   | 114 |
| Praktika .....   | 115 |

## Abstract

Locomotion in six legged insects requires effective mechanisms for inter-leg coordination. Such mechanisms could be realized by mechanical coupling of the legs via the ground during stance phase, by direct connections between the rhythm generating networks in the ventral nerve cord (VNC) of these animals, or they could rely on an intersegmental exchange of phasic sensory feedback. This thesis investigates the role of local pattern-generating networks and inter-leg sensory influences for the generation of rhythmic motor activity during walking at different speeds in *Drosophila*. For this purpose, a series of already existing techniques was used in combination for the first time in the model organism *Drosophila melanogaster*. Single leg amputation was used to reduce sensory feedback of one leg allowing the residual stump to move freely and thereby providing insight into the rhythmic activity of motor pattern-generating networks in the VNC. This approach has already been used to investigate the control mechanisms of walking in several animals, including stick insects (e.g. Wendler, 1964) and cockroach (e.g. Delcomyn, 1988). In the present thesis, oscillation periods, phases, and absolute inter-segmental intervals of movements in the intact legs and single leg stumps were quantified in tethered flies walking on top of an air-cushioned ball. A similar setup has previously been used for several other animals such as cockroaches (Spirito and Mushrush, 1979) and also *Drosophila* (Seelig and Jayaraman, 2013; Seelig et al., 2010). High-speed video analysis of the walking behavior was performed manually (Strauss and Heisenberg, 1990; Wosnitza et al., 2013) as well as in semi automatic fashion (Branson et al., 2009; Mendes et al., 2013). The *nan[36a]* mutant (Kim et al., 2003), which has defective chordotonal organs, was used to investigate the influence of sensory feedback from chordotonal organs in the intact legs on movements of the stump.

Consistent with findings in cockroaches and stick insects rhythmic oscillatory movements were found for stumps of single front, middle and hind legs during tethered walking in *Drosophila*. The stumps oscillated with a frequency of approximately 10 Hz that was largely consistent for the whole range of recorded walking speeds. Intact legs showed step periods of 100 ms only during relatively fast walking, thus, during slow walking sequences multiple stump oscillations were found for one step period of the intact legs. Consequently, the phase relation between stumps and intact legs was very variable at low walking speeds. Nevertheless, preferred absolute time intervals were found between intact leg liftoff and subsequent levation or depression onset in the stump, even if the frequency of stump oscillations was much higher than the step frequency of intact legs. With increasing walking speed the stump oscillations became highly coordinated with respect to the intact legs. Interestingly, the transition range to strong coordination occurred at the point where the stepping period in intact legs becomes very similar to the base frequency of the stump oscillations.

Single middle leg stumps of *nan[36a]* mutant flies showed the same high frequency oscillations that were found during experiments with wild type flies. The stumps oscillated almost independently of

walking speed with a movement period of about 100 ms. In contrast to wild type flies stump oscillations in the mutant flies failed to entrain to the stepping behavior of the intact legs at high walking speeds and the absolute time intervals between liftoff events in intact legs and subsequent onset of levation or depression in the stump were more variable.

These results lead to the following four conclusions: First, a putative descending control of walking speed does not target the rhythm generating networks directly but it probably has an indirect influence by changing the gain factor of sensory signals, for instance. Second, if the relatively high frequency of stump oscillations reflects a high natural frequency of the investigated pattern generating networks this would facilitate the coordination at high walking speeds, where precise coordination is very important. Fourth, coordinating signals from the intact legs influences the stump movements even during slow walking, but it is probably more effective during fast walking where the stump shows a cycle to cycle coupling to the intact legs. This indicates a stronger inter-leg coordination at high walking speeds. Fourth, the chordotonal organs in the intact legs play an important role for this coordination.

During the second part of this thesis the speed range and activity pattern of intact *Drosophilae* and single leg amputees were studied during voluntary untethered walking. For this purpose, a behavioral paradigm was created that allowed for the study of walking behavior in nine individual flies in separate petridish enclosures. Additionally, software was developed to provide a semi- automatic analysis of the recorded videos. It was found that compared to intact animals the occurrence of walking speeds above 5 mm/s was strongly reduced in amputees. During voluntary untethered walking hindleg amputees showed the highest speed range of all amputees. A reduced level of walking activity was found in frontleg and hindleg amputees, whereas middleleg amputees showed the same probability to walk as the intact animals. The flies walked in short bouts of mostly less than two seconds. As previously shown in the literature (Martin, 2004; Valente et al., 2007) the probability for fast walking was higher in the center of the walking arena compared to the area close to the wall of the enclosures, where the flies spend most of the time. In any case walking activity was only found for a maximum 30 % of the recorded time (in R2 amputees).

## Zusammenfassung

Die Fortbewegung von sechsbeinigen Insekten erfordert effektive Mechanismen um die Bewegung der Einzelbeine miteinander zu koordinieren. Solche Mechanismen könnte realisiert sein, durch mechanische Kopplung der Einzelbeine über den Boden während der Stemmphase, durch direkte Verbindungen zwischen den Rhythmus erzeugenden Netzwerken im ventralen Nervensystem dieser Tiere oder durch intersegmentalen Austausch von phasischer sensorischer Information. Die vorliegende Arbeit untersucht die Rolle von lokalen Rhythmus generierenden Netzwerken und dem Austausch von sensorischer Information zwischen den Beinen auf die Entstehung rhythmischer motorischer Aktivität beim Laufen mit verschiedenen Geschwindigkeiten bei *Drosophila*. Zu diesem Zweck wurde eine Reihe von bereits existierenden Techniken das erste Mal in Kombination am Modellorganismus *Drosophila* verwendet. Amputationen einzelner Beine wurden durchgeführt um die sensorische Rückmeldung von einem Beines zu reduzieren, der Stumpf kann sich dabei frei bewegen und erlaubt dadurch Einblicke in die rhythmische Aktivität der mustergenerierenden Netzwerke im ventralen Nervensystem. Diese Methode wurde bereits bei verschiedenen Tieren eingesetzt um die Kontrollmechanismen des Laufens zu untersuchen dazu gehören Stabheuschrecken (z.B. Wendler, 1964) und Schaben (z.B. Delcomyn, 1988). In der vorliegenden Arbeit wurden Oszillationsperiode, Phasenlage und absolute intersegmentale Zeitintervalle bei der Bewegung von intakten Beinen und Stümpfen quantifiziert während die Tiere gehaltert auf einem Ball laufen, der auf einem Luftkissen schwebt. Ein ähnlicher experimenteller Aufbau wurde bereits bei verschiedenen anderen Tieren wie Schaben (Spirito and Mushrush, 1979) und auch *Drosophila* (Seelig and Jayaraman, 2013; Seelig et al., 2010) benutzt. Hochgeschwindigkeitsvideos des Laufverhaltens wurden manuell (Strauss and Heisenberg, 1990; Wosnitza et al., 2013) und halbautomatisch (Branson et al., 2009; Mendes et al., 2013) ausgewertet. Die *nan[36a]* Mutante, welche defekte Chordotonalorgane hat, wurde benutzt um den Einfluss sensorischer Information von den Chordotonalorganen in den intakten Beinen auf die Bewegungen des Stumpfes zu untersuchen.

In Übereinstimmung mit Ergebnissen von Schaben und Stabheuschrecken wurden rhythmische oszillatorische Bewegungen der Einzelbeinstümpfe von Vorder-Mittel und Hinterbein beim gehalterten Laufen von *Drosophila* gefunden. Die Stümpfe oszillierten mit einer Frequenz von etwa 10Hz und das relativ konstant über den gesamten Bereich der aufgezeichneten Laufgeschwindigkeiten. Intakte Beine zeigten eine Schrittdauer von 100 ms nur bei relativ schnellem Laufen, so dass bei langsamen Laufsequenzen häufig mehrere Oszillationen des Stumpfes während einer Schrittperiode der intakten Beine gefunden wurden. Als Konsequenz war die Phasenlage zwischen Stümpfen und intakten Beinen bei langsamen Läufen sehr variabel. Nichtsdestotrotz gab es vorherrschende Zeitintervalle zwischen dem Abheben der intakten Beine und direkt darauffolgenden Levationen oder Depressionen des Stumpfes, selbst wenn die Frequenz der Stumpfoszillationen viel höher war als die

Schrittfrequenz der intakten Beine. Mit ansteigender Laufgeschwindigkeit wurden die Stumpfoszillationen im Bezug auf die intakten Beine sehr koordiniert. Interessanterweise lag der Übergangsbereich zu hoher Koordinationsstärke in dem Geschwindigkeitsbereich in dem die Schrittperiode der intakten Beine sich der Grundfrequenz der Stümpfe näherte. Einzelne Mittelbeinstümpfe der *nan[36a]* Mutante zeigten die gleichen hochfrequenten Oszillationen die auch während der Experimente mit wildtypischen Fliegen gefunden wurden. Die Stümpfe oszillierten fast unabhängig von der Laufgeschwindigkeit mit einer Periodendauer von um die 100 ms. Im Gegensatz zu wildtypischen Fliegen gab es keine Ankopplung der Stumpfoszillationen an die Schreitbewegungen der intakten Beine bei hohen Laufgeschwindigkeiten und die die absoluten Zeitintervalle zwischen dem Abheben der intakten Beine und direkt darauffolgenden Levationen oder Depressionen des Stumpfes waren variabler.

Diese Ergebnisse führen zu den folgenden vier Annahmen: Erstens, eine mögliche zentrale Kontrolle der Laufgeschwindigkeit beeinflusst die CPGs nicht direkt sondern hat einen indirekten Einfluss, zum Beispiel auf die Verstärkungsfaktoren von sensorischen Signalen. Zweitens, wenn der relativ hohen Frequenz der Stumpfoszillationen eine hohe natürliche Frequenz der mustergenerierenden Netzwerke zugrunde liegt dann würde das die Koordination bei schnellem Laufen erleichtern, da dort eine präzise Koordination sehr wichtig ist. Drittens, ein koordinierendes Signal von den intakten Beinen beeinflusst die Bewegungen des Stumpfes auch beim langsamen Laufen, aber es ist effektiver beim schnellen Laufen, wo der Stumpf von Zyklus zu Zyklus an die intakten Beine gekoppelt ist. Viertens, die Chordotonalorgane in den intakten Beinen sind eine wichtige Quelle für diese koordinierenden Signale.

Für den zweiten Teil dieser Arbeit wurde der Geschwindigkeitsbereich und die Häufigkeit des Laufverhaltens von intakten und Einzelbein amputierten Tieren während spontanen ungehaltertem Laufens untersucht. Zu diesem Zweck wurde ein Verhaltensparadigma entwickelt das es erlaubte das Laufverhalten von 9 Fliegen in separaten Petrischalen zu untersuchen. Zusätzlich wurde Software entwickelt die eine teilautomatisierte Auswertung der aufgezeichneten Videos erlaubte. Es wurde herausgefunden, dass im Vergleich zu intakten Fliegen das Auftreten von Laufgeschwindigkeiten über 5mm/s, bei Fliegen mit Einzelbeinamputationen stark reduziert war. Bei spontanem ungehaltertem Laufen zeigen hinterbeinamputierte Tiere den größten Geschwindigkeitsbereich aller amputierten Tiere. Vorder und hinterbeinamputierte Tiere zeigten eine reduzierte Laufaktivität währenddessen mittelbeinamputierte Tiere mit der gleichen Wahrscheinlichkeit Laufen wie intakte Tiere. Die Fliegen laufen in kurzen Bouts von meist weniger als zwei Sekunden. Wie bereits in der Literatur gezeigt (z.B. Martin, 2004; Valente et al., 2007) war die Wahrscheinlichkeit für schnelle Läufe in der Mitte der Laufarena höher verglichen mit dem Rand, wo die Fliegen sich die meiste Zeit aufhalten. In jedem Fall wurde Laufaktivität nur in maximal 30% der aufgezeichneten Zeit beobachtet.

## 1. Introduction

Parts of this section are included in a paper draft with the working title: "**Speed-dependent interplay between local, pattern generating activity and sensory feedback during walking in *Drosophila***" that has recently been submitted for publication in Journal of Experimental Biology.

Locomotion is important in the animal kingdom to explore the environment, find food, escape predators and fulfill the requirements for reproduction (Dickinson et al., 2000). Walking is an important form of locomotion for many animals and therefore walking behavior has been studied in a vast variety of species (for review see Büschges, 2005; Orlovsky, 1999; Pearson, 1993).

Walking animals use body appendages known as limbs or legs to produce a cyclic behavior consisting of two phases: A stance phase during which the legs have contact to the ground and generate propulsion and a swing phase that is used to return the appendages back to their starting position in order to generate the next stance phase (for review see Büschges and Gruhn, 2007; Graham, 1985a). For neuroscientists, walking is of particular interest because it poses a series of rather complicated tasks to the neural circuitry controlling this behavior. There are several levels of increasing complexity. On the lowest level it requires motor output to be generated for each of the leg's joints that results in coordinated swing and stance phases (intra-leg coordination). On an intermediate level, all legs of an animal have to be coordinated with each other (inter-leg coordination). On the highest level, the walking pattern has to be adaptable with regard to walking speed or direction.

Insects such as cockroaches, locusts and stick insects have proven to be particularly useful for locomotor studies, because compared to most vertebrates they are small in size and their nervous system is relatively simple and easily accessible (for review see Büschges and Bässler, 1998; Büschges, 2005; Pearson, 2004).

## 1.1 Central pattern generators (CPGs) and coordination

For insects (e.g. stick insect: Büschges et al., 1995; hawk moth: Johnston and Levine, 1996a) and several other animals for example leech (Nusbaum et al., 1987), turtle (Robertson et al., 1985), lamprey (Wallén and Williams, 1984) and other vertebrates (Brown, 1911; for review see Grillner, 1985) the existence of rhythmic central neural networks (also called CPGs) has been demonstrated in the past. CPGs are relatively small and autonomous neural networks that are able to provide the timing for motoneuron discharge, without rhythmic central or sensory input, albeit sensory information may be essential to shape the CPG output for behavioral needs of the animal (for review see Marder and Calabrese, 1996).

During walking CPGs are believed to provide rhythmic activity that is modulated on a cycle to cycle basis by sensory afferents (e.g. stick insect: Borgmann et al., 2009; cockroach: Fuchs et al., 2012) to generate the magnitude and timing of the motor output (for review see Büschges, 2005). The coupling between different segments of a leg (intra-leg coupling) is probably achieved indirectly by sensory signals that connect the CPGs controlling individual leg joints (stick insect: Akay et al., 2001; 2004; Chung et al., 2015; Daun-Gruhn and Toth, 2011; Hess and Büschges, 1999; crayfish: Bacqué-Cazenave et al., 2015).

In this regard the system that controls stepping in insects can be seen as a set of oscillators that are weakly and indirectly coupled via sensory feedback (locust: Laurent and Burrows, 1989; stick insect: Ludwar, 2004; cockroach: Pearson and Iles, 1973). The nature of this coupling is not entirely clear and it is possible that an additional and more direct coupling of the CPGs via interneurons exists.

Apart from intra-leg coordination walking also requires coordination between the different legs of an animal (inter-leg coordination). Studies in cockroaches (Delcomyn, 1989; Delcomyn, 1991a; 1991c) and stick insects (Foth and Bässler, 1985a; 1985b) suggest a set of behavioral rules for inter-leg coordination (Cruse, 1990; Dürr et al., 2004) that are active locally between neighboring legs. The rules are numbered from 1-6 (Cruse et al., 1995).

1. If a posterior leg is in swing phase, it inhibits the start of a swing phase in its anterior neighboring leg.
2. If a posterior leg starts its stance phase it excites the start of a swing phase in the anterior leg.
3. If a leg has reached an increasingly posterior position during its stance phase it excites the start of a swing phase in its posterior neighbor.
4. During swing phase the posterior leg targets the resting position of the anterior legs tarsus.
5. An increased resistance increases force during stance (co-activation) and an increased load prolongs the stance phase.
6. If a leg steps on the tarsus of its neighboring leg the trod-on leg tells the one on top to step off.

(Dürr et al., 2004)



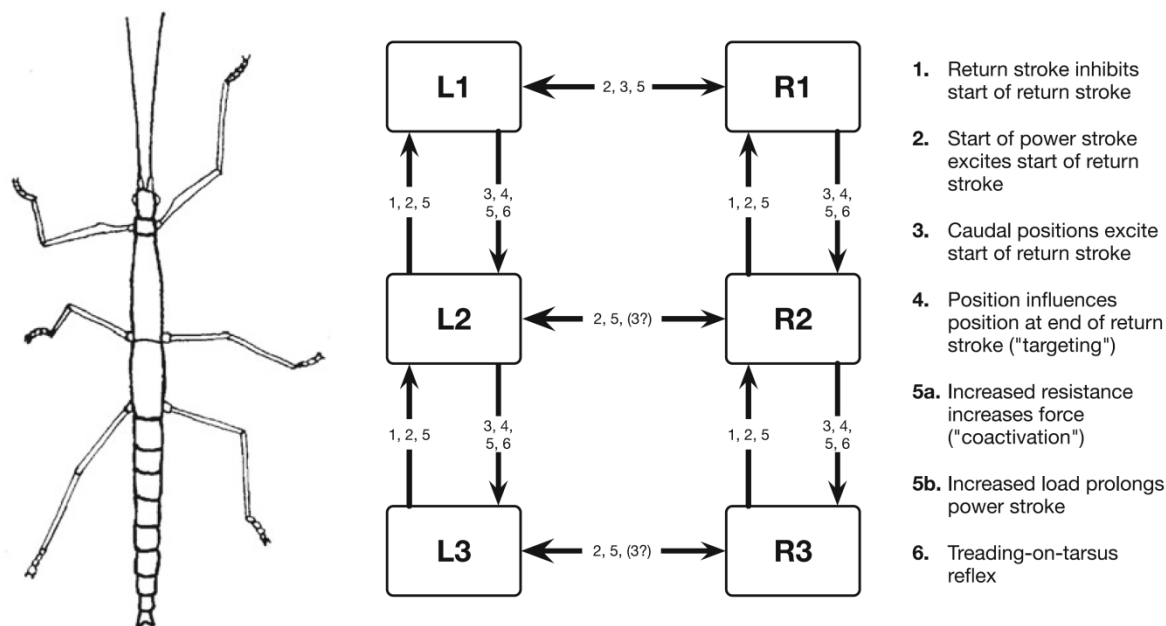


**Fig. 1:** " Leg modules and their connection via coordination rules (from Dürr et al. 2004). L1, L2, L3 left front, middle, and hind leg, respectively. R1, R2, and R3 stand for the corresponding right legs. The question mark indicates that there are ambiguous data concerning this influence." (Figure and caption literally quoted from Schilling et al., 2013 Fig. 3)

Similar to intra-leg coordination these rules are based on sensory afferents providing feedback about the current state of the locomotor system (Borgmann et al., 2009; 2012; Daun-Gruhn et al., 2012; Ludwar, 2004). Additionally, all legs of an animal that are simultaneously in stance phase are mechanically coupled through the ground, which may have a strong influence on inter-leg coordination (Zill et al., 2009).

General activation of the CPGs and the control of locomotion frequency is believed to be provided by a descending tonic excitatory input whose magnitude can vary in order to allow for control of walking speed (Gal and Libersat, 2006; Ridgel and Ritzmann, 2005; Roeder, 1937).

The origin of such a tonic excitation in insects is believed to be the gnathal (former: sub-esophageal) ganglion (Graham, 1979; Kien and Altman, 1984; Kien and Williams, 1983). How these signals work in detail and if they target CPGs directly or indirectly is so far unknown, but there is evidence that they influence the way sensory feedback is processed (Gabriel and Büschges, 2007; Sauer et al., 1996).

## 1.2 Inter-leg coordination at different walking speeds

Walking speed has an influence on temporal coordination between the legs of an insect, which leads to different coordination patterns for different speed ranges (Graham, 1972; Gruhn et al., 2009; Mendes et al., 2013; Wendler, 1964; Wosnitza et al., 2013).

During slow walking many insects use a coordination pattern called *wave gait* (Hughes, 1952), where only one of the six legs is in swing phase at a given time (Fig. 2 A). When the walking speed is increased a coordination pattern called *tetrapod gait* (Burns, 1973; Graham, 1972) was described where four legs of the animal are in swing phase at the same time (Fig. 2 C and D). Fast walking insects mostly use the so called *tripod gait* (Delcomyn, 1971; Graham, 1972; Mendes et al., 2013; Strauss and Heisenberg, 1990; Wahl et al., 2015; Wosnitza et al., 2013), where the middle leg on one body side and the front and hind leg on the contralateral side are simultaneously in swing phase (Fig. 2 B). However, the aforementioned patterns should not be regarded as strict states of the locomotor system, as studies indicate that they form a speed dependent continuum with rather seamless transitions between them (Spirito et al., 1979; Wendler, 1965; for review see Graham, 1985; Wilson, 1966).

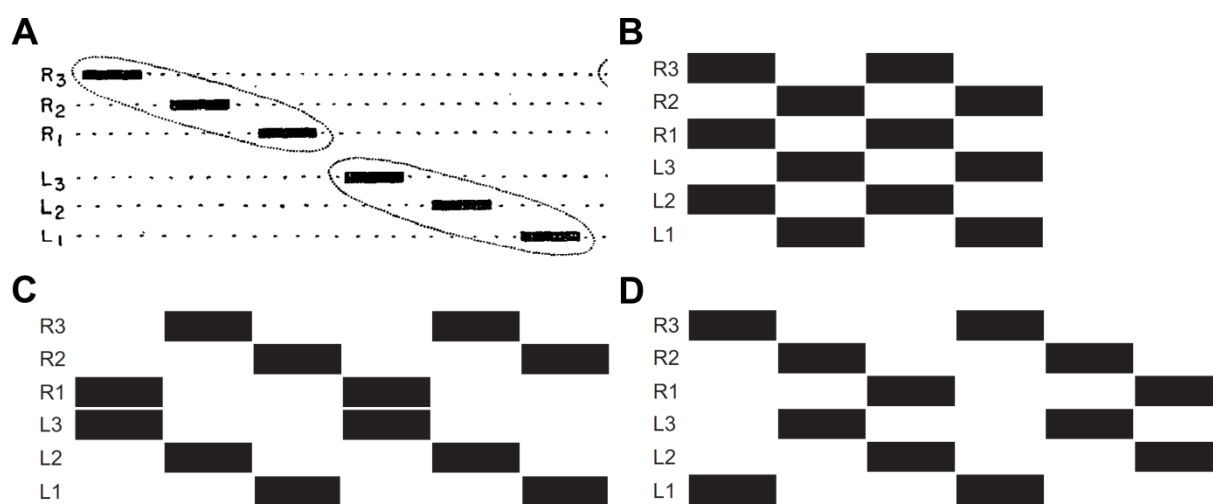


**Fig. 2: Stereotypic footfall patterns of hexapedal animals. Black bars indicate swing phases of the legs. (A) *wave gait*: Only one of the six legs of the animal is in swing phase at a given time. (A modified from Wilson, 1966 Fig. 1 A). (B) *tripod gait*: middle leg on the ipsilateral side swings in synchrony with front and hind leg on the contralateral side (C, D) *Tetrapod gait*: two diagonal legs swing synchronously. (B,C and D modified from Grabowska et al., 2012 Fig. 1)**

An increase in stepping frequency and walking speed in insects is achieved by a decrease in stance duration (retraction time), while the swing duration (protraction time of the legs) of the legs is kept almost constant (Burns, 1973; Mendes et al., 2013; Wendler, 1964; Wosnitza et al., 2013; for review see Wilson, 1966; Büschges, 2012). Intracellular recordings in stick insects (Gabriel and Büschges, 2007) provide evidence that stepping velocity is controlled by synaptic inputs that act on stance phase motor neurons exclusively during stance. As stance phase motor neurons are influenced by sensory feedback signaling ground contact (Berendes et al., 2013; Schmitz et al., 2015; for review see Zill et al., 2004) it is possible that modifications in the gain of these sensory feedback loops contribute to the changes in stance duration and thereby cycle period and speed .

Behavioral observations show that two neighboring legs are never in swing phase at the same time (equivalent to Cruse rules 1 to 3, Cruse, 1990; for review see Dürr et al., 2004) consequently the occurrence of swing phases has to be timed precisely at high walking speeds to coincide with the

comparatively short stance phases of the neighboring legs. This implies a rather strict inter-leg coordination at high walking speeds.

### **1.3 Amputation experiments and the control mechanisms of walking**

One of the oldest methods to investigate the control mechanisms of walking behavior is leg amputation (e.g. Buddenbrock, 1921). A leg stump that cannot contact the walking substrate is mechanically uncoupled from the intact walking legs. Furthermore, sensory feedback from all leg segments distal to the lesion is gone and load sensors proximal to the lesion cannot provide a ground contact signal.

Previous amputation studies in cockroaches (Delcomyn, 1988; Delcomyn, 1991b; Delcomyn, 1991c; Hughes, 1957; Noah et al., 2004) and stick insects (Graham, 1977; Wendler, 1964) revealed that the animals still show coordinated walking behavior with their remaining intact legs, while the stumps of single legs show rhythmic patterns of motor activity, despite the lack of sensory input created by the amputation. However, many of these studies report multiple burst of motor activity in the stump during single steps of the adjacent intact legs, especially during slow walking (Delcomyn, 1988; Noah et al., 2004). These findings provide important hints that sensory feedback mediating ground contact might be crucial to maintain inter-leg coordination. Delcomyn (1988) compared the patterns of motor activity in the stump with those that he found during searching (Delcomyn, 1987). He concluded that the activity of the stump is probably still driven by the interneurons that control the intact leg during walking and that therefore an analysis of the stump motor pattern might reveal important features of the locomotor system.

### **1.4 Studying walking in *Drosophila***

Since in 1910 Thomas Hunt Morgan started his genetic studies on *Drosophila melanogaster* MEIGEN, 1830, fruit flies have become an important model organism, with a large set of genetic tools available (for review see Jennings, 2011; Rubin, 1988). These genetic tools allow experimenters to find and specifically activate (e.g. Hamada et al., 2008; Klapoetke et al., 2014; Zhang et al., 2007) or inhibit (e.g. Chuong et al., 2014) sense organs (e.g. Kim et al., 2003) and neurons (e.g. Bidaye et al., 2014) that are necessary to control or maintain walking behavior. Albeit electrophysiology is difficult to perform in *Drosophila*, mainly due to its small body size, genetically encoded calcium indicators can be used to study the firing patterns of neurons (e.g. Berlin et al., 2015). High-speed video recording can be used in concert with computer based tracking and classification algorithms to quantify many behavioral parameters (e.g. Branson et al., 2009; Kain et al., 2013; Mendes et al., 2013; Valente et al., 2007). As *Drosophila* is a vigorous walker with a large range of different walking speeds, all those

tools taken together could provide new insights for still unanswered questions regarding walking behavior in insects.

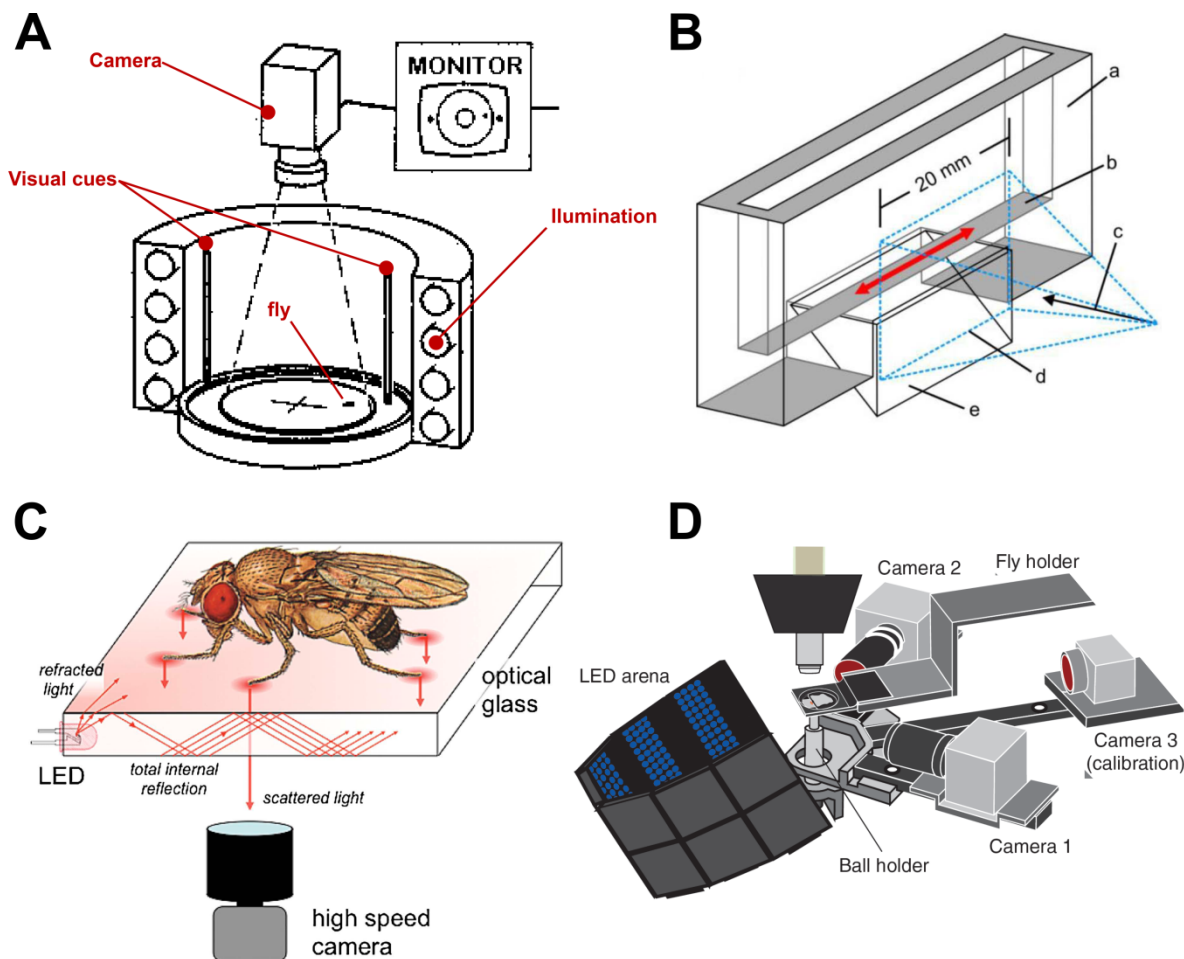


**Fig. 3:** Setups used to study the walking behavior in fruit flies. (A) Schematic diagram of Buridan's paradigm, a circular luminous arena where a wingless fly is placed on disc surrounded by water. The fly patrols between two dark optical cues placed opposite from each other. Videos of the flies' behavior are taken by a camera mounted above the setup. (modified from Bühlhoff et al., 1982 Fig. 2) (B) Schematic diagram of the tunnel setup. Walking behavior of the flies on a walkway (red arrows) was recorded with a high-speed camera through a 20 mm wide window simultaneously from one side and from below (a: acrylic glass, coated on the inside with a layer of Fluon to prevent the flies from scaling the glass; b: 5 mm wide transparent walkway; c: camera viewpoint; d: camera field of view, free of Fluon; e: glass prism, providing a ventral view of the walkway) (modified from Wosnitza et al., 2013 Fig. 1A). (C) Schematic overview of the FTIR setup. The flies walk on a glass surface that has LEDs attached at the edges. The light propagates within the optical glass via total internal reflection. Tarsal contact causes Light scattering, which is observed by a high-speed camera mounted below the fly. (figure modified from Mendes et al., 2013 Fig. 1A) (D) Modified schematic overview of the setup used by Seelig and colleagues (2010) for two-photon imaging from the brain of head-fixed flies walking on a ball. The ball is floating on air. Movement and velocity around each of the ball three rotational axes was recorded by two optical sensors (called camera 1 and camera 2 in the scheme).

However, so far only few studies exist that investigate the kinematics and coordination of the legs during walking behavior in the fruit fly *Drosophila melanogaster* (Mendes et al., 2013 and 2014; Strauss and Heisenberg, 1990a; Wosnitza et al., 2013). Strauss and Heisenberg 1990 studied voluntary walking of untethered *Drosophila* in the Buridans paradigm, a uniform white arena were the flies patrolled between two inaccessible black landmarks (Fig. 3 A). Using high-speed video analysis they found that flies walk in alternating tripod coordination during fastest walks and that the strictness of this tripod coordination depends on walking speed. Wosnitza and colleagues 2013 analyzed high-speed videos of flies walking in a tunnel setup (Fig. 3 B) and found that flies also use wave-gait like and

tetrapod walking patterns at low speeds. These findings suggest that inter-leg coordination in *Drosophila* is flexible and dependent on walking speed. During some experiments the authors amputated a single hind leg of the flies and found that they show immediate adaptations in body posture, leg kinematics and inter-leg coordination, and were still able to walk coordinately. They conclude that the neural system that controls walking behavior in *Drosophila* allows for a modular control of single leg stepping, thus that individual legs of fruit flies are largely independent from each other and only loosely coupled. Mendes and colleagues (2013) used a setup where light travels through a glass plate on which the flies walk (Fig. 3 C). While the tarsi of the flies contacted the glass surface during stance phase of walking they light up due to a phenomenon called frustrated Total Internal Reflection (fTIR). This was used to automatically detect tarsi position and stance phase timing with a computer based approach. A tripod coordination pattern was found for most walking speeds with gradually diminishing frequencies for slower flies, abrupt gait transitions, known for example from horses (Hoyt and Taylor, 1981), were not found in *Drosophila*. Furthermore, Mendes and colleagues (2013) found that genetically modified flies, which lack most of the proprioceptive feedback from sensory structures in the leg, including the chordotonal organs, hair plates, campaniform sensilla and mechanosensory bristles, have a deficient step precision, but are still able to walk in tripod coordination pattern. On the other hand a more recent study of the same group showed that functional chordotonal organs are important for the flies to respond kinematically to changes in walking conditions, such as carrying an additional weight (Mendes et al., 2014).

This poses the question to which extent *Drosophila* relies on sensory feedback during walking, especially in the light of results from Chung and colleagues (2001), who showed that flies cannot walk at all if they lack sensory feedback from both their chordotonal organs and campaniform sensilla (Chung et al., 2001 Fig. 3 B).

Currently the role of sensory feedback during walking in *Drosophila* is far from being fully understood. Further investigations are necessary to disentangle the influence of rhythmic neural networks and sensory influence on the motor output during walking.

## **1.5 The present thesis**

For the present thesis single leg amputations were used as a method to investigate the role of local pattern generating networks and inter-leg sensory influences on the generation of rhythmic motor activity during walking in *Drosophila*. As indicated by previous experiments, fruit flies are still able to walk coordinately with only five legs, although inter-leg coordination becomes more variable (Wosnitza et al., 2013). In the first part of this thesis high-speed video analysis was used to investigate the movements of single front, middle and hind leg stumps during tethered walking on an air-

cushioned ball. The ball setup was adapted from the literature (Fig. 3 D) and allowed to infer the walking path of the fly from the movements of the ball around its three rotational axes (Seelig et al., 2010). Coordination among the remaining intact legs was analyzed as well as the coordination of the stump movements with respect to these intact legs. A special focus was drawn here on changes that occur with increasing walking speed. If the stump movements largely reflect the activity of central pattern generating networks and if a central descending drive directly influences these networks to modulate a change in walking speed this influence should affect stump movements when speed increases. As the stump is not mechanically coupled to the intact walking legs a possible coupling between its movements and the stepping behavior of the intact legs should be a result of inter-leg coordinating signals. Previous studies in intact flies and hind leg amputees found that inter-leg coordination becomes stricter with an increase in walking speed (Wosnitza et al., 2013). If this increase in coordination is not mediated by mechanical coupling of the legs via the ground, it should be reflected in the stump movements. A putative neural inter-leg coupling might be realized via interneurons that directly connect the rhythm generating networks responsible for the legs movements. Alternatively, inter-leg coupling might be achieved by an exchange of sensory information between the legs (Borgmann et al., 2009). Both motor activity and, consequently, sensory information are correlated with the rhythmic activity of the pattern generating network. In order to distinguish between these two alternatives some experiments of the current thesis were conducted with *nan[36a]* mutant flies that lack sensory feedback from chordotonal organs (Kim et al., 2003). As previous studies indicate chordotonal organs might play an important role for leg coordination during walking in fruit flies (Chung et al., 2001; Mendes et al., 2014). The mass of the air-cushioned ball (see materials and methods) that has to be moved by the fly might reduce the range of recorded walking speeds. These issues were addressed in the second part of this thesis, which uses a custom made behavioral paradigm and a semi automatic computer based approach to analyze the speed range and activity frequency of intact and single leg amputated *Drosophila* during voluntary untethered walking. The goal of these experiments was to unravel possible differences between the speed range and activity level that flies exhibit during tethered walking on a ball, compared to untethered voluntary walking in an arena. Concerning the amputees such a comparison is particularly useful because tethered flies do not have to carry their own body weight therefore amputation of a leg does not affect the stability of an animal during walking. This situation is quite different during untethered walking where the impact of a single leg amputation on the stability of an animal during walking might differ depending on the amputated leg. Several previous studies (Mendes et al., 2013; Strauss and Heisenberg, 1990; Wosnitza et al., 2013) have shown that *Drosophila* uses the tripod coordination pattern during fast walking, therefore one might assume that an amputation of the middle leg has a strong impact on the ability of the animal to walk.

## 2. Material and Methods

### Animals

For all experiments 4 to 6 day old males of the *Drosophila melanogaster* wild-type strain *Canton-S* (*wt<sup>CS</sup>*) or the mutant strain *nan* [36a] were used. The flies were raised on standard medium with cornmeal, yeast, agar and molasses (Zoological Institute, Univ. of Cologne, Cologne, Germany). Flies were kept at 23-25°C and 60% humidity on a 12h light /12h dark cycle.

### 2.1 Experiments on leg kinematics and inter-leg Coordination

Parts of this section are included in a paper draft with the working title: "**Speed-dependent interplay between local, pattern generating activity and sensory feedback during walking in *Drosophila***" that has recently been submitted for publication in Journal of Experimental Biology.

#### Experimental setup

Flies were cold anesthetized and isolated from each other 1-2 hours prior to an experiment. Under anesthesia the flies were transferred to separate enclosures, where they were kept at room temperature for the next 1-2h. Each enclosure contained a wet filter paper to provide water without food. The starvation was done to increase the activity level of the flies by inducing food searching behavior (Knoppien et al., 2000). In the cases where amputations were made, leg or leg parts were amputated with micro scissors during cold anesthesia.

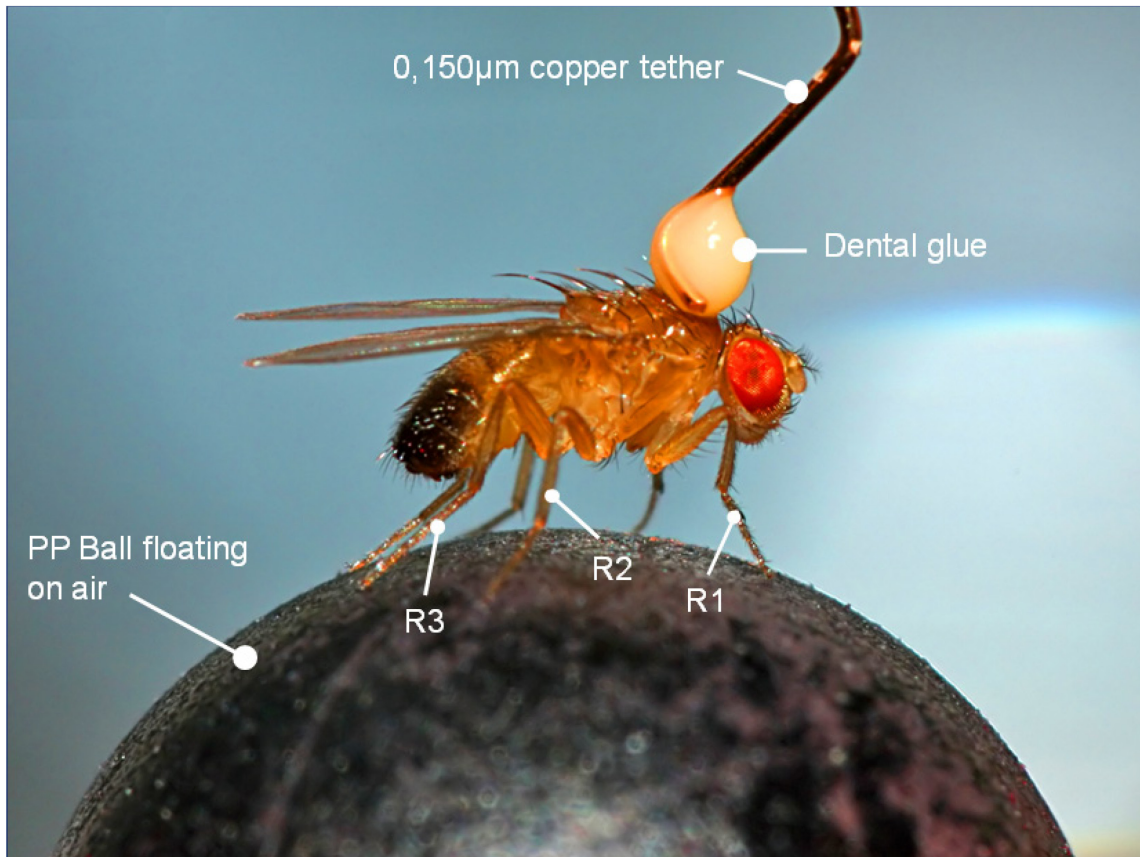


**Fig. 4:** Exemplary image of a male *Drosophila* tethered with dental glue and a copper wire on top of a 6 mm polypropylene (PP) ball.

The flies that were used for the experiments had either all six legs intact (Fig. 5A) or one leg amputated (front, middle, or hind leg) at the proximal half of the femur so that only a stump remained (see Fig. 5 B, C and D).

For all experiments with tethered animals the flies were cold anesthetized again immediately before the experiment and placed ventral side down in the groove of a custom build aluminum block (Electronics workshop, Zoological Institute, Univ. of Cologne, Cologne, Germany). A copper wire with a diameter of 0.150 mm was glued with a light curing composite dentist glue (ESPE Sinfony, 3M ESPE AG, Seefeld, Germany) on the thorax of the animal under a dissecting microscope. The glue was cured with a curing light (wavelength 420 nm to 480 nm).

The tethered flies were then mounted on top of an air-suspended 6 mm Polypropylene (PP) ball (Fig. 4), with a mass of approximately 100 mg. Movements of the ball around all three rotational axes were monitored by two sensors derived from optical computer mice with a method similar to the one described by Seelig and colleagues (2010). The original setup can be seen in the Introduction (Fig. 3 D).



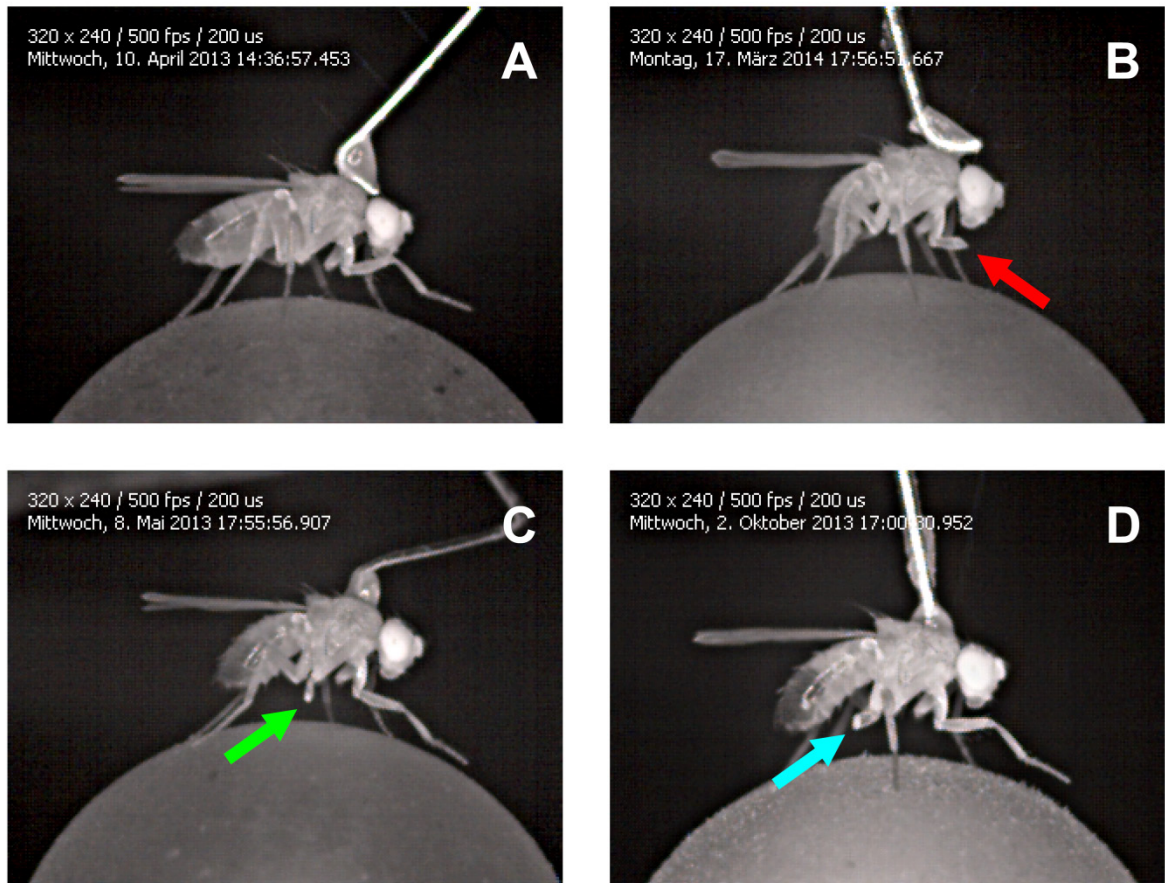


**Fig. 5: Flies used had either all legs intact or one leg amputated. (A) Intact animal on the ball, lateral view showing the right body side. (B) Fly with amputated right front leg (red arrow). (C) Fly with amputated right middle leg (green arrow). (D) Fly with amputated right hind leg (blue arrow).**

Two synchronized optical sensors measured (ADNS-9500, Avago Technologies, San José, CA, USA) optic flow on the ball's surface. Each sensor measured the horizontal and vertical movement velocity of a small patch of surface at the equator of the ball with a temporal resolution of 50 Hz. This patch was illuminated by a red diode laser (LG series, 1 mW, 660 nm, Lasertechn, Aschaffenburg, Germany). The four sensor values were used to reconstruct the movement velocities of the ball's three rotational axes. Assuming that all movements of the ball were caused by the fly walking atop it was possible to reconstruct the fly's virtual walking trajectories and walking speed. Acquisition of ball motion data was synchronized with high-speed video acquisition via a TTL trigger in a 1:10 ratio: for every ten video frames one motion measurement of the ball was acquired. Low-level control of the optical sensors and synchronization to the high-speed camera was implemented with custom-made hardware (Electronics workshop, Zoological Institute, University of Cologne); high-level control was implemented by Dr. Till Bockemühl (Zoological Institute, University of Cologne, Cologne, Germany) with custom-written software in MATLAB 2011b (The Mathworks, Inc., Natick, MA).

## Video acquisition

Two versions of the ball setup were used during this study:

The first setup had the camera mounted on the animal's right body side, which allowed capturing videos of the protraction, retraction, levation, and depression movements of ipsilateral legs or stumps. Video resolution was 320x240 pixels. This setup will be referred to as the side-view setup in the following text (Fig. 6).

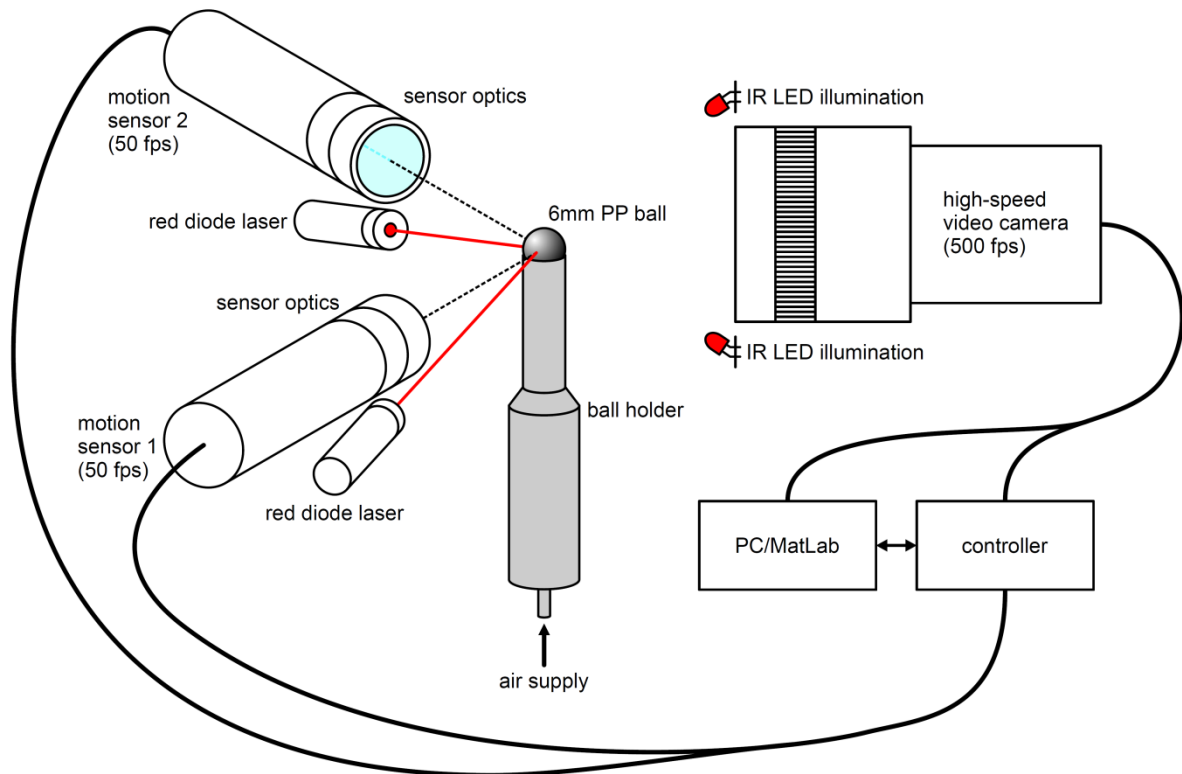


**Fig. 6:** Schematic overview of the side-view setup (courtesy of Dr Till Bockemühl). Flies were tethered and placed atop an air-suspended 6 mm PP ball. Flies were recorded with a high-speed video camera at 500fps from the right body side. A custom-built pulsed IR-LED ring around the camera objective was used to illuminate the scene. Movements of the ball around all three rotational axes were monitored by two sensors derived from optical computer mice with a method similar to the one described by Seelig and colleagues (2010). The ball surface was illuminated for the motion sensor by red diode lasers (660 nm).

For the second setup the camera was mounted above the fly. Additionally, slanted mirrors were attached to the ball holder on both sides of the animal. The angle of 25° to the main camera axis allowed capturing the protraction and retraction movements of all 6 legs without occlusion by the wings or the body (Fig. 7). Videos were recorded at a resolution of 1280x700 pixels in this setup in order to cover the top-view of the fly and the two mirror views (Fig. 9). The second setup will be called the top-view setup in the following text.

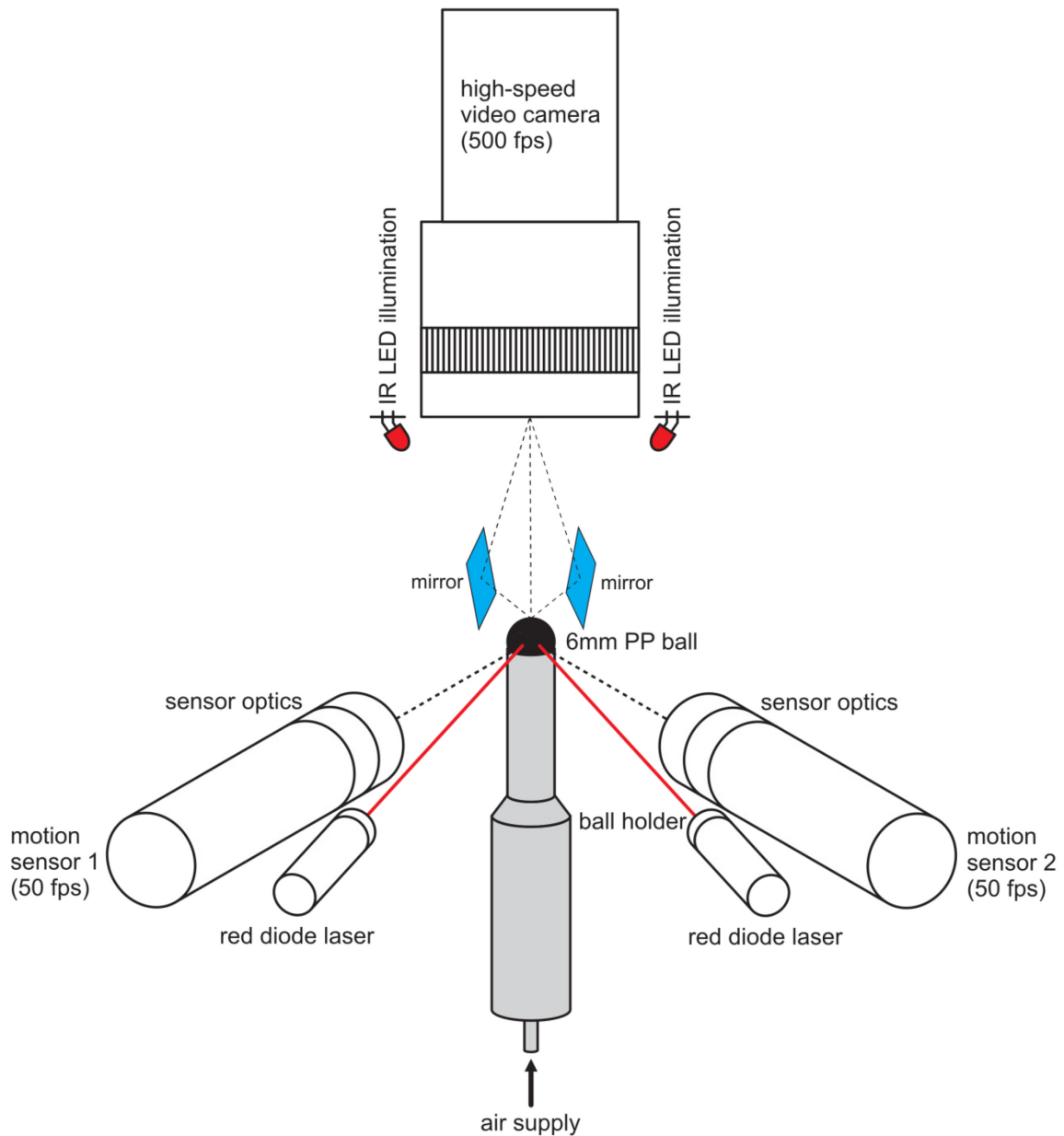


**Fig. 7:** Schematic overview of the top-view setup (courtesy of Dr Till Bockemühl). The setup was technically identical to the side-view setup but the camera was mounted above the ball. Additionally, two mirrors were attached above the ball holder. The mirrors were slanted 25° with regard to the main camera optical axis providing the camera with a view of the right and the left body side of the walking fly additional to the top-view.

For both setups a high-speed camera (AOS S-PRI High-Speed Color 5.2, AOS Technologies AG, Baden Daettwil, Switzerland) was used to record videos of the walking fly at 500 fps with a shutter time of 200  $\mu$ s. A custom-built IR-LED ring ( $\lambda=880$  nm, Siemens AG, Munich, Germany) around the camera objective was used to illuminate the scene (Electronics workshop, Zoological Institute, University of Cologne). Infrared light of 880 nm is invisible to the flies (Yamaguchi et al., 2010). The LEDs were synchronized with the camera shutter and were active only during actual image acquisition (shutter time: 200  $\mu$ s). As videos were recorded at a frame rate of 500 fps the maximum accuracy for determining time points in the analyses is 2 ms.

## Data Analysis

With regard to the walking behavior of the animals the following terms are used:

**AEP** (Anterior Extreme Position): The touchdown of a leg during walking.

**PEP** (Posterior Extreme Position): The lift-off of a leg during walking.

**VEP** (Ventral Extreme Position): The most depressed position of the stump during its oscillation.

**DEP** (Dorsal Extreme Position): The most elevated position of the stump during its oscillation.

**Swing duration:** The time between PEP and the following AEP of the same leg.

**Stance duration:** The time between AEP and the following PEP of the same leg.

**Leg period:** The time between two consecutive PEP events of the same leg.

**Stump oscillations period:** The time interval between two DEPs.

**DF** (Duty Factor): Stance duration divided by cycle period for intact legs or the time between DEP and subsequent VEP divided by stump oscillation period for stumps.

**R1:** right front leg.

**R2:** right middle leg.

**R3:** right hind leg.

**Z-scores:**  $(\text{value} - \text{mean}) / \text{Standard Deviation}$

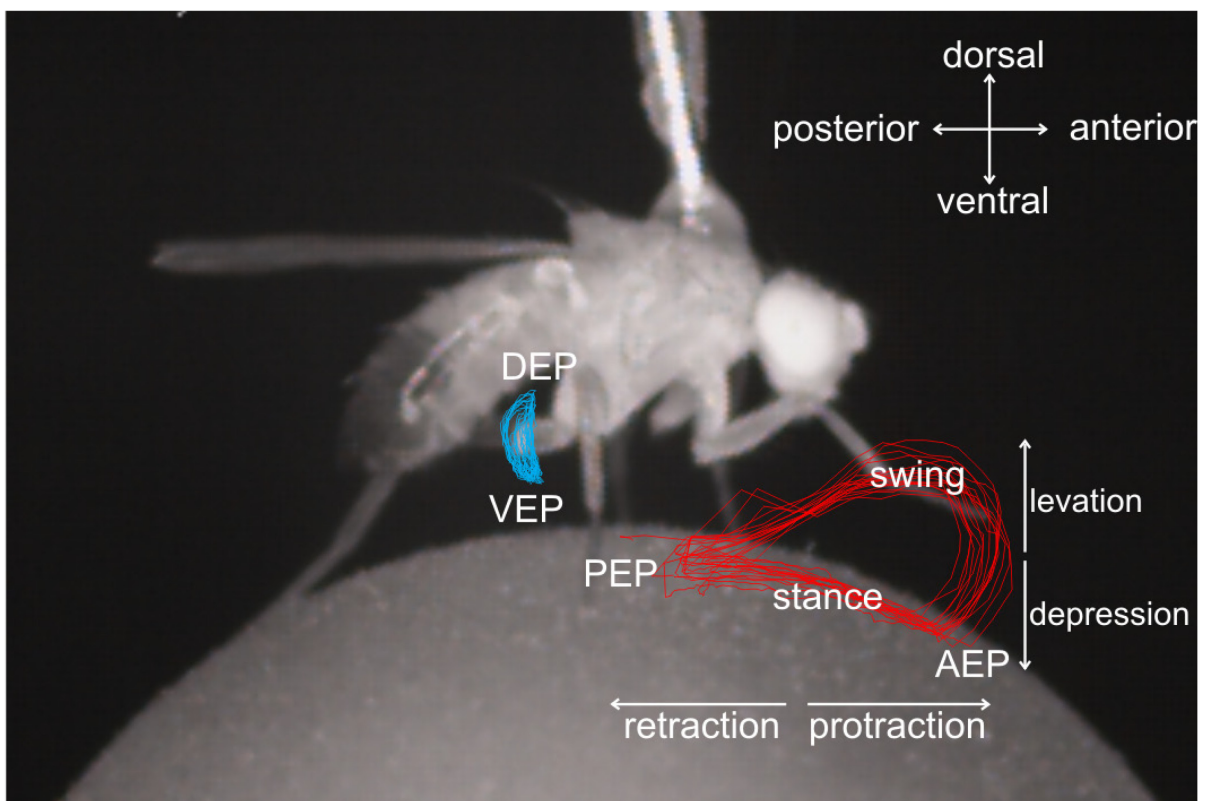


**Fig. 8:** Scheme illustrating the spatial conventions used in the text. The picture shows a single video frame obtained from a single walk of a hind leg amputee. Trajectories of intact front leg (red) and hind leg stump (blue) were superimposed on the video frame.

For the intact ipsilateral legs (right body side) the movements of the tarsi were tracked manually for each video frame recorded in the side-view setup. In the top-view setup, the same was done in a semi-automatic fashion for all intact legs of the animal (right and left body side). Additionally, the points in time of touch-down (anterior extreme position, AEP) and lift-off (posterior extreme position, PEP) were determined. The AEP was defined as the first video frame during a stance period that showed the tarsus touching the ball. The PEP was defined as the last video frame of a given stance period in which the tarsus still touched the ground. For leg stumps the movement of the stump tip was tracked manually in both setups.

In the side-view setup protraction and retraction as well as levation and depression movements of the stump were visible in the videos. The data evaluation for the side-view experiments in this thesis was focused on levation and depression movements of the stump as they were larger and easier to track compared to the stumps' protraction and retraction. For all experiments performed in this setup the ventral and dorsal extreme positions (VEP and DEP) for each complete stump oscillation were determined as the minima (VEP) and maxima (DEP) of the levation and depression movement of the stump.

In the top-view setup only protraction and retraction movements of the stump were visible in the videos. For all experiments performed in this setup the last video frame before the stump switched from retraction to protraction was determined. This event will be called sPEP in the current text to distinguish it from a PEP in an intact leg, which is defined differently (see above).

For all analysis regarding leg coordination either AEP or PEP was used as a reference point in time for the intact legs. For leg stumps either VEP or DEP (side-view setup) or sPEP (top-view setup) events were used as a reference.

The ball-tracking system delivered the data on the fly's speed and position in mm, whereas the tracking information obtained for the leg movements from the high-speed video was in pixel. Therefore, the ball radius served as a calibration to convert pixels to mm. With this calibration, it was possible to calculate the body length (BL, head to abdomen) of each individual fly and then convert the corresponding data on speed in from mms/s to BL/s. This was done to obtain a normalized speed value that accounts for possible differences in body size and therewith step length of the flies.

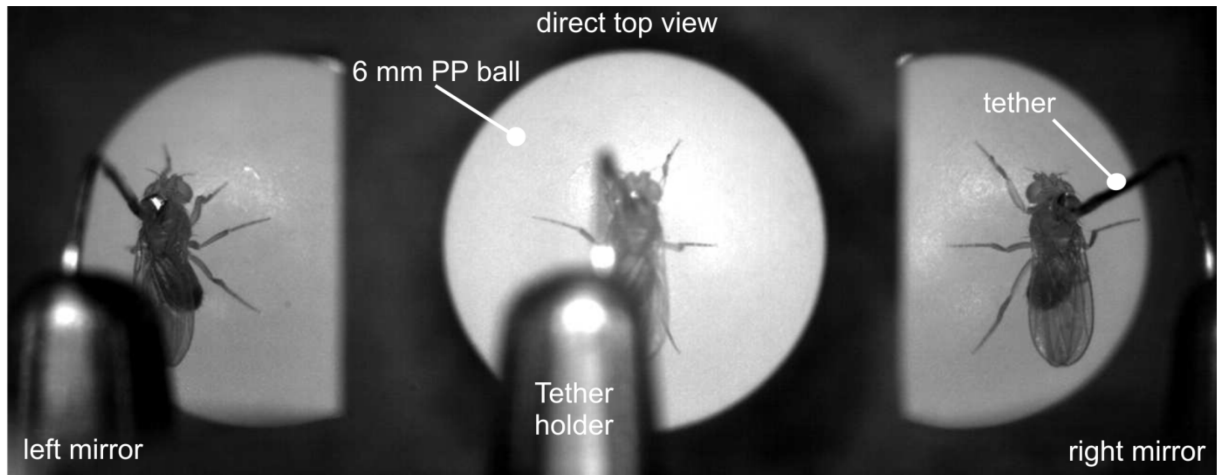


**Fig. 9:** Single video frame of an intact fly walking on a 6 mm polypropylene ball in the top-view setup. The camera is mounted above the fly. The direct top-view on the fly can be seen in the center of the frame. Reflections of the fly in the two slanted mirrors, which were attached to the ballholder, can be seen on the left and on the right side of the center.

As a measure for coordination and coordinateness the time between the occurrences of an event in an investigated leg relative to the time that elapsed between two consecutive events in a reference leg was calculated. Technically, it is the percentage of the reference cycle at which the event in the investigated leg occurred. This value is called phase relation throughout the present study (Fig. 10). A phase of 0 would mean that an event would be in-phase with the reference. A phase relation value of 0.5 would mean that the events are in exact anti-phase.

The phase values were calculated for each experimental condition. In order to show general trends, circular mean values for the dataset were calculated using a gliding window with a size of 15 values and a step size of 1 (Fig. 11). The mean resultant vector (r-vector) was used to quantify the circular spread of the phase data; it was calculated with the same gliding window approach that has been used for the phase values.



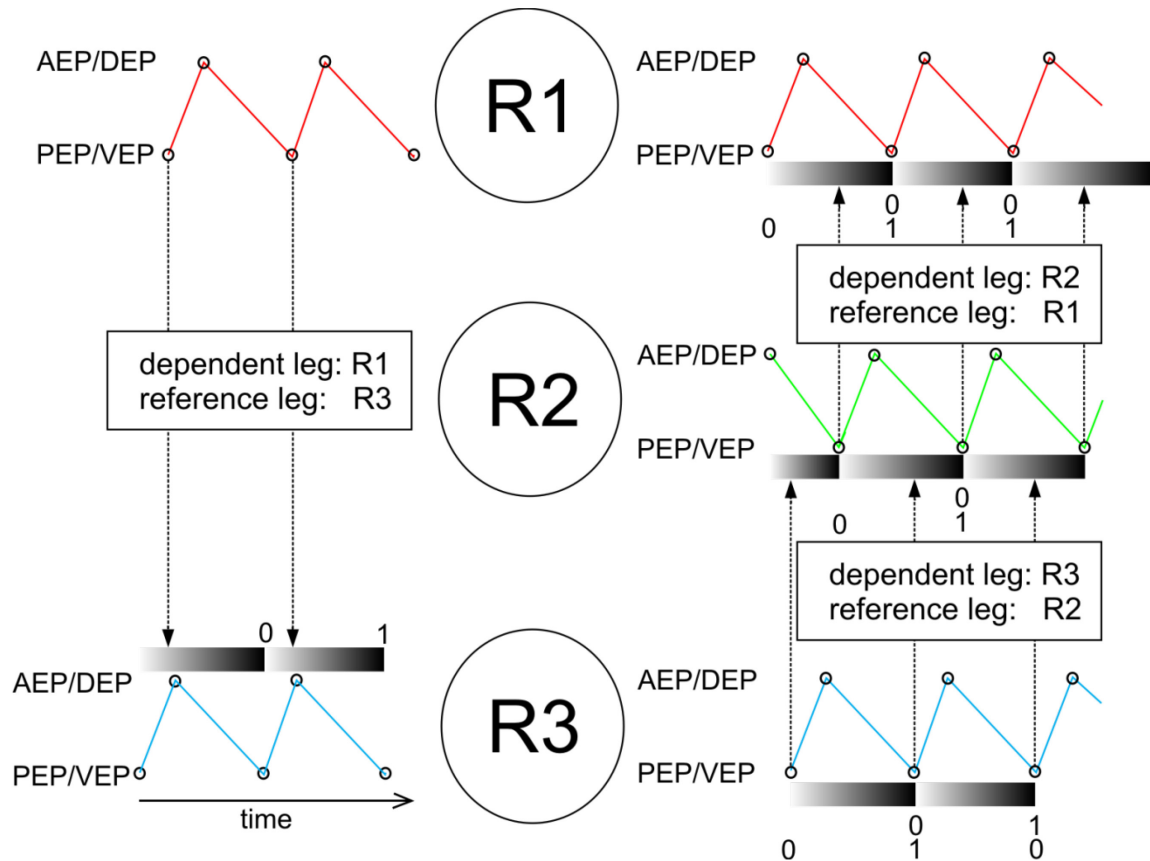


**Fig. 10:** Schematic drawing to illustrate the calculation of phase relations in between legs. R1, R2 and R3 refers to the right front-, middle- and hind leg. The colored traces illustrate movements of the legs (red: movement of R1, green movement of R2 and blue movement of R3). Black circles in the traces indicate the occurrence of extreme positions that could be used as a reference- or dependent event for the calculation of phases. Phase calculation works as follows: The time between two adjacent reference events in a given dependent leg is separated in values increasing from 0 to 1, each time a control event in the dependent leg occurs the current value between 0 to 1 of the reference leg is chosen. This value called the phase between the reference leg and the dependent leg.

To further investigate if the occurrence of the reference events AEP and PEP in intact legs has an influence on the stump movement, traces of levation and depression movements in the stump was superimposed for a time window of 100 ms before and after a PEP event in an intact reference leg (Fig. 24).

Additionally, bee swarm plots of the absolute time intervals between events in the stump (DEP or VEP) and subsequent reference events in intact legs (PEP) and vice versa were created (Fig. 23 and Appendix Fig. 44). To investigate the effect of walking speed on these intervals the data were divided into two subsets; the first subset refers to time intervals at walking speeds lower or equal to 5 BL/s the second refers to time intervals at walking speeds higher than 5 BL/s. The investigated time intervals are named in the present text according to the form  $X > Y$ , where X refers to a PEP in a given intact leg and Y to a VEP or DEP in a given stump. For instance,  $R2 > VEP$  refers to the time that elapsed between a PEP in the middle leg (R2) and the next VEP in the front leg stump.

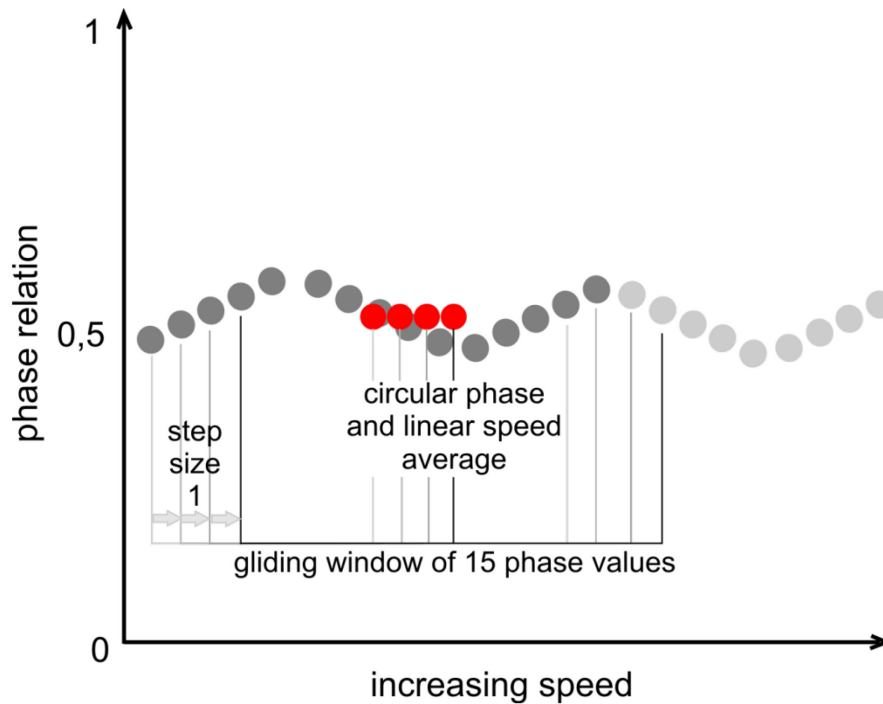


Fig. 11: Scheme illustrating the gliding window approach used to calculate mean phase values for the dataset. Gray dots represent the phase relation values that were sorted for increasing speed. Each red dot represents a linear mean value for the speed and a circular mean value for the phase relation of 15 gray dots. This window of 15 values was shifted with a step size of 1 towards increasing speed.

## Software

AOS imaging studio v3 (AOS Technologies AG, Baden Daettwil, Switzerland) was used to operate the AOS S-PRI High-Speed Color 5.2 camera, and to download videos to the computer in proprietary .raw3 format. The videos were later converted to AVI files with either AOS Imaging studio v3 or a MATLAB function called RAW3Dir2AVI written by Dr. Till Bockemühl.

For all experiments, conducted with the side-view setup tracking was done manually on a frame by frame basis using ProAnalyst 3D Professional edition 1.5.4.0 Software (XCitex, Inc., Cambridge, MA, USA). The tracking information was exported to Excel 2007 (Microsoft Corporation, Redmond, WA, USA) and then imported to MATLAB 2011b (MathWorks, Inc., Natick, MA, USA) to be further analyzed with custom written functions. All functions that are mentioned by name during the given text are available in digital form on a CD, which is part of the Supplementary Material.

For all experiments, conducted on the top-view setup tracking was done semi-automatically with a custom written MATLAB function called FlyMoCap written by Dr. Till Bockemühl. In this case the data were already accessible in MATLAB.

For the detection of maxima and minima the MATLAB function peakfinder (Nathanael C. Yoder 2011) available on the Matlab File Exchange was used.



Due to their circular nature all phase data were processed with the CircStat Toolbox (Berens, 2009), which was downloaded from the Matlab File Exchange.

Figures and graphs were created in MATLAB 2011b, Origin 8.5G (OriginLab Corporation, Northampton, MA, USA), and Corel Draw X4 (Corel Corporation, Ottawa, ON, Canada).

## **2.2 Walking Speed and Activity Assay**

### **Experimental setup**

The animals were handled in the same way as described in section 2.1 but without a second cold anesthesia because they were transferred from the separate enclosures to the experimental setup with an aspirator (Dhooria, 2008). The experimental setup for behavioral analysis consisted of walking arenas for single flies. The arenas were made from a 290 x 290 x 8 mm (length x width x height) Plexiglas board which had 3 x 3 milled circles on it (Fig. 12). The circles had an inner diameter of 53 mm and a depth of 2 mm. The space between neighboring circles was 3 mm. The lids of petri dishes with an outer diameter of 54 mm tightly fitted into them, forming a round enclosure with a height of 4 mm and a diameter of 53 mm. The setup was illuminated from below with an IR spotlight consisting of a 96 LED Matrix (wavelength 850 nm). Additional light was provided by the fluorescent lamps of the ambient light in the laboratory.

A Marlin F 145B2 Camera (Allied Vision Technologies, Stadtroda, Germany) was mounted above the setup. Videos of the flies' behavior inside the petri dishes were taken for about 30 min at a frame rate of 10 fps during each experimental trial. To ensure a stable frame rate the camera was externally triggered with square pulses (interval 100 ms, 5 V) from a pulse generator (Model MS501, Electronics workshop, Zoological Institute, Cologne). Videos were recorded at a resolution of 940x940 Pixels and a shutter time of 50 ms.

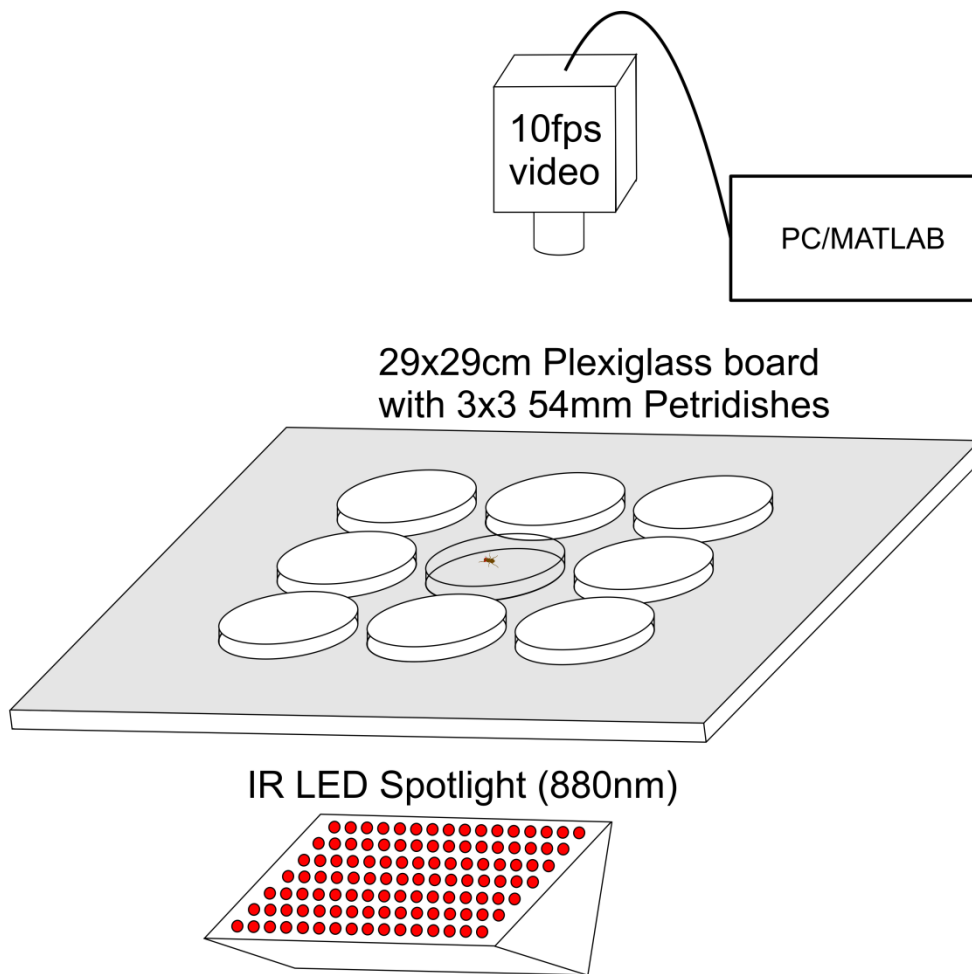


**Fig. 12:** Schematic overview of the setup for activity and speed monitoring during voluntary walking. The setup consists of a 290 x 290 mm Plexiglas board with an array of 3 x 3 lids of 54 mm petri dishes on it. Single flies were placed in the petri dishes. Videos of the flies' behavior inside the petri dishes were taken at 10 fps. The setup was illuminated from below by a spotlight of 96 IR LEDs (880 nm) which was constantly on.

### Data analysis

The datasets for a particular experimental situation, e.g. intact *Canton-S* flies were pooled and histograms, which showed the probability of occurrence for several parameters, were created. Those parameters were speed during walking (Fig. 38 and Fig. 39), length of single walking bouts (Fig. 40 and Fig. 41) and walking activity during the 30 min of the recording (Fig. 42 and Fig. 43). The activity was displayed in the following way: If an animal showed walking activity during a video frame in any of its recorded trials the activity was counted as 1. If all animals would show walking activity in at least 1 frame of a video the histogram bin of that frame would have a value that equals the number of animals, if no animal would be active at that time point the value would be 0.

## Software

Custom made MATLAB software called AVTRecorder (Dr. Till Bockemühl) was used to operate the F 145B2 Camera and to record videos to the PC.

The position of the flies was detected automatically for each video frame with a custom written MATLAB function called flytrackingparadigm. This function was developed during this study using background subtraction to detect the fly as a moving object in front of a static background (for review see Emile et al., 2008).

The first step during image processing was to fit a grid on the video image with a separate rectangle for each enclosure that contained a fly to be tracked (Fig. 13 A). An average frame was calculated from all frames in the video or a subsample of them using a custom written MATLAB function called avgFrame 2 (modified from Dr. Till Bockemühl). This average frame only shows objects that were static throughout the video (Fig. 13), i.e. the enclosures without the flies. For further processing the gray values of the average frame were inverted. If a fly did not move in most of the video frames it would also appear in the average frame (see magenta arrow in Fig. 13B). The average frame could be exported as a portable network graphics (.png), thus that the fly could be removed by cloning the neighborhood surrounding pixels in the flies' location with the help of the image processing software GIMP Portable 2.8 (open source program obtained from portableapps.com). The modified average frame was then re-imported to the MATLAB function.

Next, the video was calibrated to pixels per mm to convert the walking speed from pixels/s to mm/s later. As all petri dishes used on the setup had a radius of 27 mm, calibration was achieved by fitting a circle to one of the petri dishes with a MATLAB function called Circle Fit by Pratt (Matlab File Exchange). A pixel per mm value was obtained by dividing the radius of that circle in pixel by the radius of the petri dishes in mm.

For all further processing steps the original video image and average frame were cropped according to the rectangles that were selected in the first step (Fig. 13C). Each rectangle should contain an enclosure with just one fly. The program processed the rectangles one by one.

Isolating the fly in every video frame was done by subtraction of the cropped average frame from each video frame. This method led to a deletion of the background from each video frame, leaving only the fly. As both average and video frame had been inverted before subtraction the fly appears as a white dot in the resulting image (Fig. 13D). The image was then converted to monochrome (Fig. 13E), which means that all luminance values were converted to either black or white depending on whether they were below or above a threshold value which could be chosen in the program interface (Fig. 14). The whole image was now a matrix consisting of one's (white) and zeros (black). The fly's position

detected by the program was the center of the white dots (the ones) within the black background (the zeros) (see red circle Fig. 13 E).

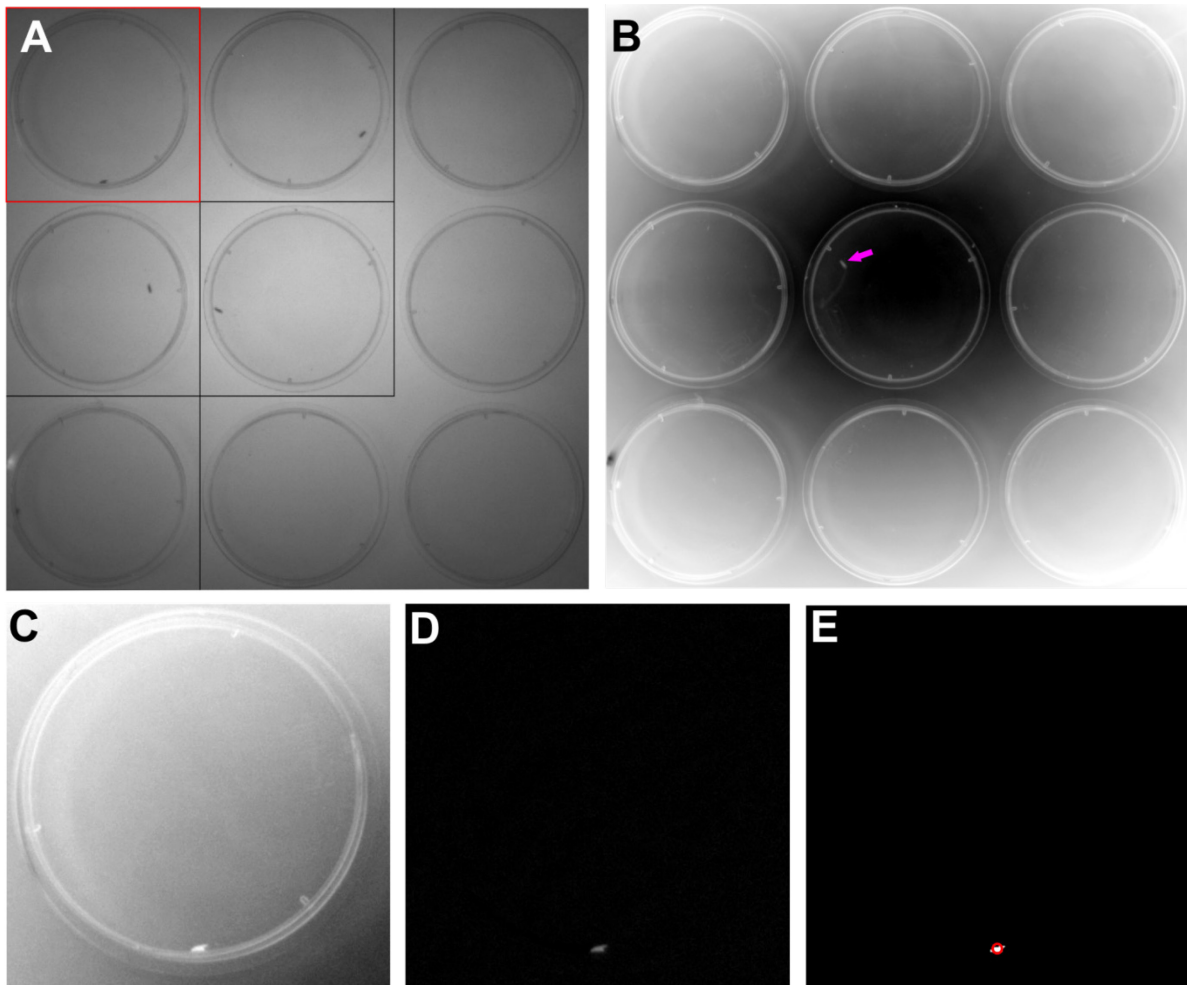


**Fig. 13:** Figure showing the image processing steps involved during background subtraction. (A) Example of a single image captured by the camera during video recording. The image is overlaid with a grid (black rectangles) used to divide the video in smaller images showing one fly enclosure each. From this step on all post processing is done on single enclosures. The red square indicates the fly enclosure shown in C, D, and E. (B) Average frame calculated from all frames of the video shown with inverted gray values. The average frame shows the static background of the recorded video. All enclosures containing moving objects (flies) should be empty in this picture. The magenta arrow indicates a fly that has not moved for most of the video frames and therefore appears in the average frame. (C) Single frame of the video cropped to the red rectangle indicated in A. Gray values of the image have been inverted. The fly appears white in this image. (D) Image obtained by subtraction of the cropped average frame from the video frame shown in C. The whole static background was deleted by this method leaving only the fly behind. (E) Same image as shown in D but with gray values converted to a monochrome picture. Threshold used for conversion: 0.2. The fly position calculated by the program is indicated as a red circle in the image.

The program determined the position of the flies in each video frame. Furthermore, the Euclidean distance of the fly's position between consecutive video frames was calculated and saved as well as the speed of the fly, which was given by the Euclidean distance divided by the time interval between the video frames.

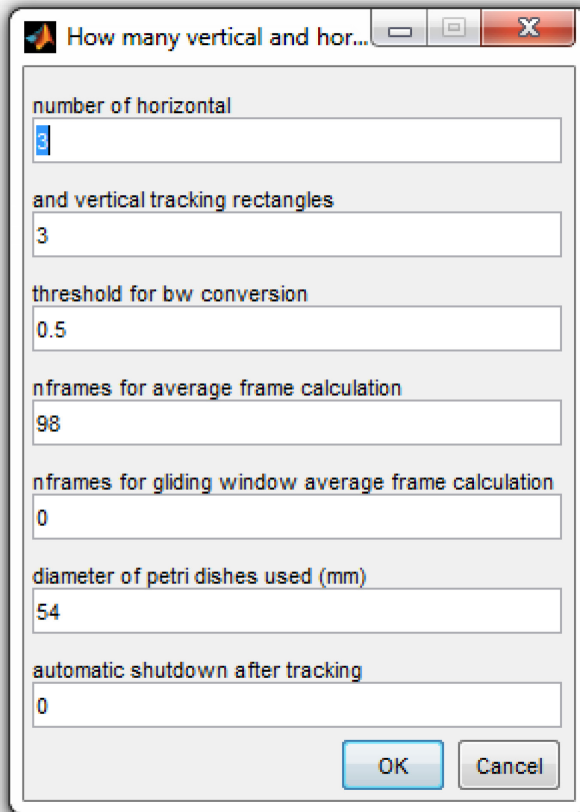


**Fig. 14:** User interface displaying the adjustable parameters of the function flytrackingparadigm. These parameters included:

- (1. field) The number of horizontal and (2. field) vertical rectangles for the grid fitted to the image.
- (3. field) A threshold value used to convert the grayscale image to monochrome (all values below threshold would be black and all values above threshold would be white after conversion).
- (4. field) The number of frames that would be used for calculating an average frame of the video (If the user chose a value below the total number of frames in the video the frames used would be equally distributed in time throughout the video).
- (5. field) The number of frames that would be used for calculating an average frame using a gliding window. (If the lighting condition changed throughout the video the average frame could be calculated in a gliding window approach.)
- (6. field) The diameter of the petri dishes or other round enclosures used in the setup. (This value was used to calibrate the video in order to convert tracked values from pixel to mm)
- (7. field) If the user wished to shutdown the computer after the tracking job was completed a 1 could be inserted in this field.

That time interval was 100 ms for all videos recorded in this setup during this study given by the frame rate of 10 Hz. In order to remove tracking jitter all speed values below 2 mm/s were excluded from the recorded trials. Additionally, all speed values above 50 mm/s have been excluded because they corresponded most likely to jumping or flying instead of walking.

A second function called evaluateflytracking was developed to further process the dataset generated by flytrackingparadigm. This function made it possible to:

- Select each rectangle of the grid that was fitted to the video image.
- Assign an experimental situation to the corresponding fly (e.g. 'R2 amputee')
- Visualize the trajectory of the fly's movement.
- Observe the cropped video for tracking inaccuracies.
- Define a "Free walking zone" in which the fly was most probably not touching the vertical wall of the enclosure with any of its appendages. This was achieved by fitting a virtual circle to the image, which served as a border between the "Wall area" and the "Free walking zone". It was necessary to handle the data from these two zones separately because the flies tend to perform a lot of walks following the walls of the arena (e.g. Martin, 2004). These walks differ in speed and frequency of occurrence from those that were performed in the center of the enclosure without any contact to the wall.

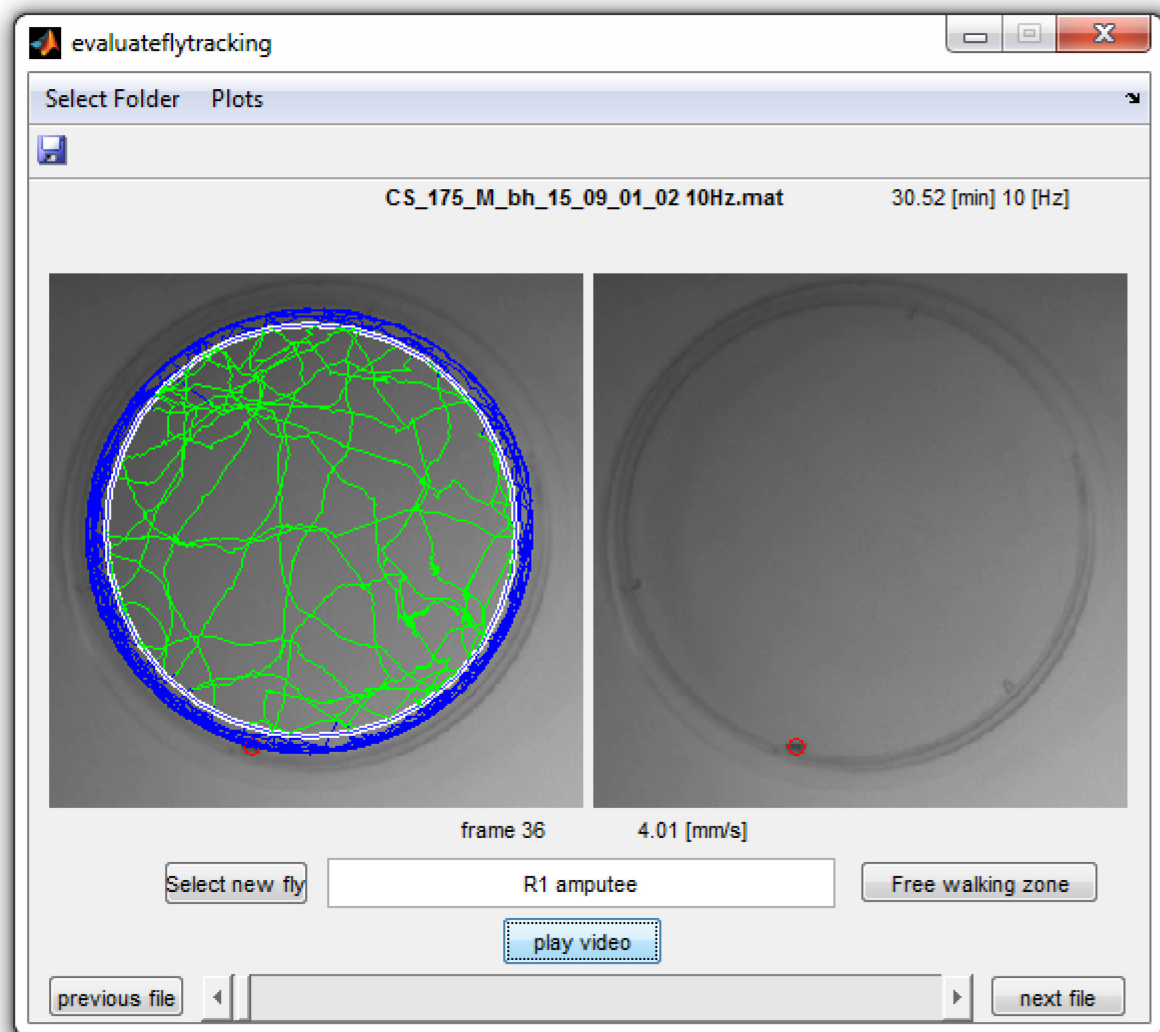


**Fig. 15:** User interface of the `evaluateflytracking` function. Name, duration, and frame rate of the video file were displayed on top of a split screen view of the video image cropped to the enclosure of the fly currently selected. It was possible to play the video or navigate through the timeline using a slider. The red circle in the right image indicates the position of the fly detected by `flytrackingparadigm` for the current video frame. The left image shows the same video frame with an overlay of the fly's movement throughout the entire video. This image was also used to define a "Free walking zone". The fly's trajectory inside this zone is shown in green the Trajectory outside of this zone is shown in blue. The circle that was used to divide between these two zones is displayed in white.

Figures and graphs were created in MATLAB 2011b and Corel Draw. Screenshots were made with Snipping tool, which is part of Microsoft Windows 7 (Microsoft Corporation, Redmond, WA, USA).

## 3. Results

### 3.1 Experiments on leg kinematics and interleg coordination

Parts of this section are included in a paper draft with the working title: "**Speed-dependent interplay between local, pattern generating activity and sensory feedback during walking in *Drosophila***" that has recently been submitted for publication in Journal of Experimental Biology.

#### 3.1.1 Experiments on the side-view setup

Preliminary experiments showed that after leg amputation the residual stump is still active while the animal is walking with its intact legs (Dr. Till Bockemühl, personal communication).

In order to investigate if the stump movements (protraction, retraction, levation and depression) are coordinated with respect to the intact leg's movements a first set of experiments was conducted with a high-speed camera observing the right body side of the animal (Fig. 16, side-view setup Fig. 6).

##### Intact flies

In a first set of experiments the walking behavior of intact flies was studied as a control. Walking sequences of 7 animals were recorded during 10 trials. An example of the trajectories tracked for the intact legs R1, R2, and R3 during a single trial is shown in Fig. 16 A. On average, the animals' walking speeds ranged from 2.2 to 7.5 BL/s. This corresponds to an absolute speed range of 4.1 to 17.9 mm/s. During each trial between 5 and 31 steps of the right front (R1) and middle leg (R2) and between 5 and 33 steps of the right hind leg (R3) were recorded. A total number of 142 steps of R1, 146 steps of the R2, and 153 steps of R3 were analyzed in intact animals.

The average step period was relatively similar for all legs. It was 132 ms (SD = 53 ms) for R1, 129 ms (SD = 63 ms) for R2, and 123 ms (SD = 46 ms) for R3. The step period of all legs decreased with increasing speed (Fig. 19). This finding is in accordance with previous publications (Mendes et al., 2013; Strauss and Heisenberg, 1990; Wosnitza et al., 2013). A comparison (Fig. 17) between the leg periods obtained for intact *CS* flies during tethered walking on the ball setup (this study) and published data for intact flies during untethered walking in a tunnel (Wosnitza et al., 2013) revealed that the flies walked on average slower on the ball setup (12 mm/s on the ball vs. 22 mm/s in the tunnel). The speed



ranges overlapped between 10 and 23 mm/s. The slowest values recorded for flies on the ball were at 3 mm/s (1.4 BL/s) whereas the fastest values recorded for flies in the tunnel were at 31 mm/s (16 BL/s). The leg periods, recorded on the ball setup, ranged between a max of 492 ms for the right middle leg and a minimum of 66 ms recorded for the right hind leg. In the tunnel values ranged from a maximum of 126 ms for R3 to a minimum of 52 ms for R3 (Fig. 17 C). In general, all legs in an intact animal performed approximately the same number of steps in a given time; the stepping frequency in all legs is virtually identical (Fig. 18 A for slow and B for fast walking). This is consistent with the general notion of a metachronal wave of swing phase activity that progresses from posterior to anterior.

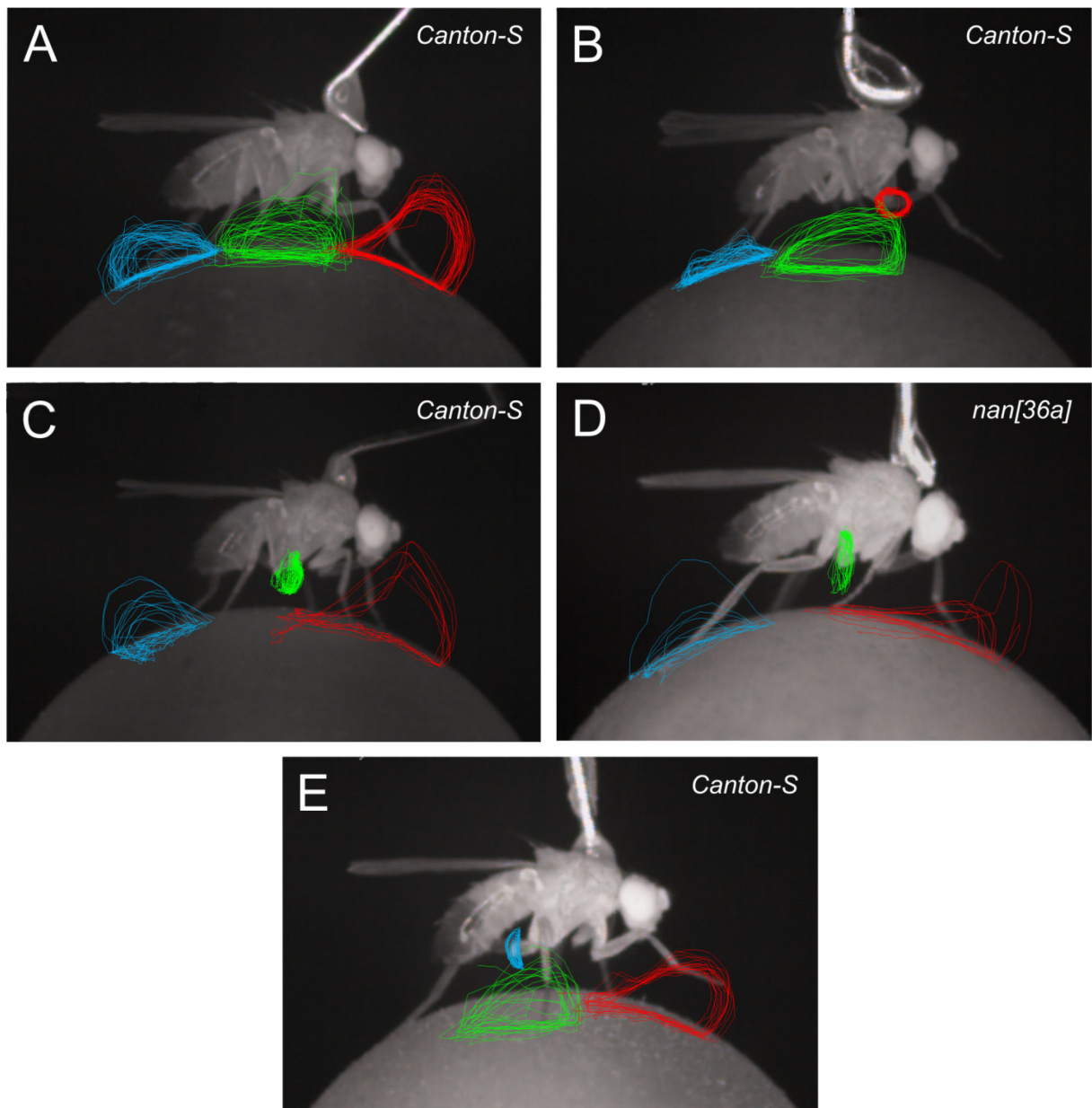


Fig. 16: (A) Trajectories of all legs on the right body side derived from a single walk of an intact animal. (B) Trajectories for intact legs and leg stump of an animal with an amputation of the right front leg. (C) Trajectories for intact legs and leg stump of an animal with an amputation of the right middle leg. (D) Trajectories for intact legs and middle leg stump of an animal with the genotype *nan[36a]*, that has defective Chordotonal organs. (E) Trajectories for intact legs and leg stump of an animal with an amputation of the right hind leg. The trajectories were derived from a single walk and superimposed on a single frame of the corresponding video. (red: front leg or stump trajectory (B), green: middle leg or stump trajectory (C and D), blue: hind leg or stump trajectory (E))



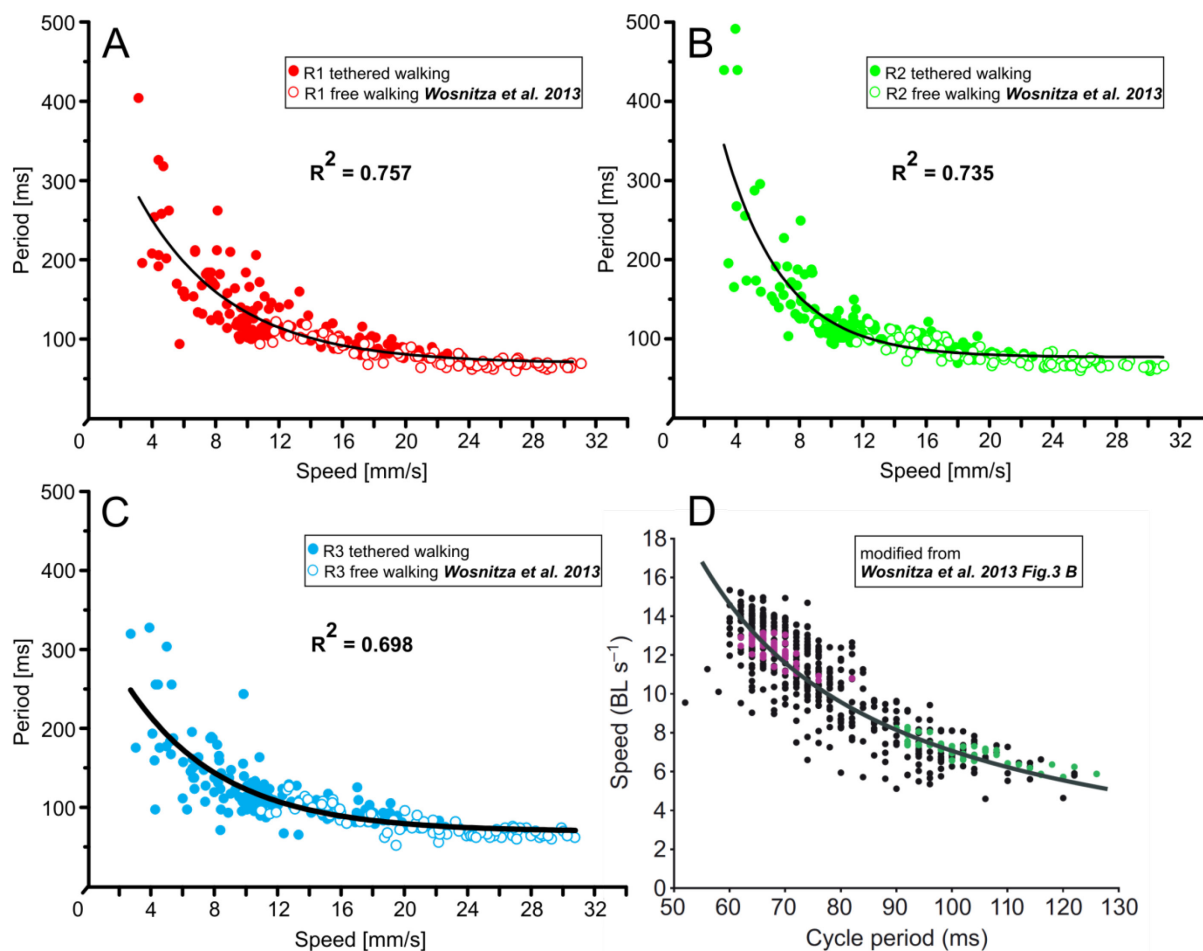


Fig. 17: Periods of leg movement vs. walking speed (in mm per second, mm/s) for intact *Canton-S* flies. Comparison of data obtained for tethered flies on the ball setup (filled circles) and data obtained for free walking flies in a tunnel (Wosnitza et al., 2013) (open circles). Legs are color coded (red: right front leg (A); green: right middle leg (B) and blue: right hind leg (C)) Panel D shows the walking speed (in body length a second, BL/s) as a function of leg period (in ms) for all legs of intact *Canton-S* flies during untethered walking in a tunnel (modified from Fig 3 B Wosnitza et al., 2013).

Although the existence or consistency of metachronal activity waves was not explicitly quantified, qualitative observations confirm that most of the walking activity is consistent with this (see also Fig. 18 A, 400 to 1400 ms for an example).

The duty factor (stance duration divided by leg period) ranged between almost 1 and 0.6 for R1 (Fig. 25 Ai), R2 (Fig. 25 Aii) and R3 (Fig. 25 Aiii), with decreasing values when the speed increased.

The phase difference between R1 and R3 tended to be relatively variable in a speed range between 1.5 and 5 BL/s. It has a value of approximately 0 between 5 and 10 BL/s, which indicates simultaneous swing phase onset (Fig. 21 Ai). Phase relations between R2 and R1 (Fig. 21 Aii) and R3 and R2 (Fig. 21 Aiii) are both approximately 0.5, which is equal to anti-phase swing activity. An analysis of the mean resultant vector length showed that, in general, all legs tended to become more coordinated with

increasing speed (Fig. 22, panels A). The mean resultant vector length of the phase relation between R1 and R3 increased from approx. 0.3 at a speed of 2 BL/s to almost 1 at a speed of 8 BL/s, with two intermittent drops to lower values at 4 and 6 BL/s. The mean resultant vector length of the phase relation between R2 and R1 had a value of approx. 0.7 at a speed of 2 BL/s and increased to 0.9 at about 6 BL/s (Fig. 22 Aii). For the phase relation between R3 and R2 the mean resultant vector length had values of approx. 0.7 at 2 BL/s and increased to values of 0.9 for speeds above 8 BL/s (Fig. 22 Aiii).

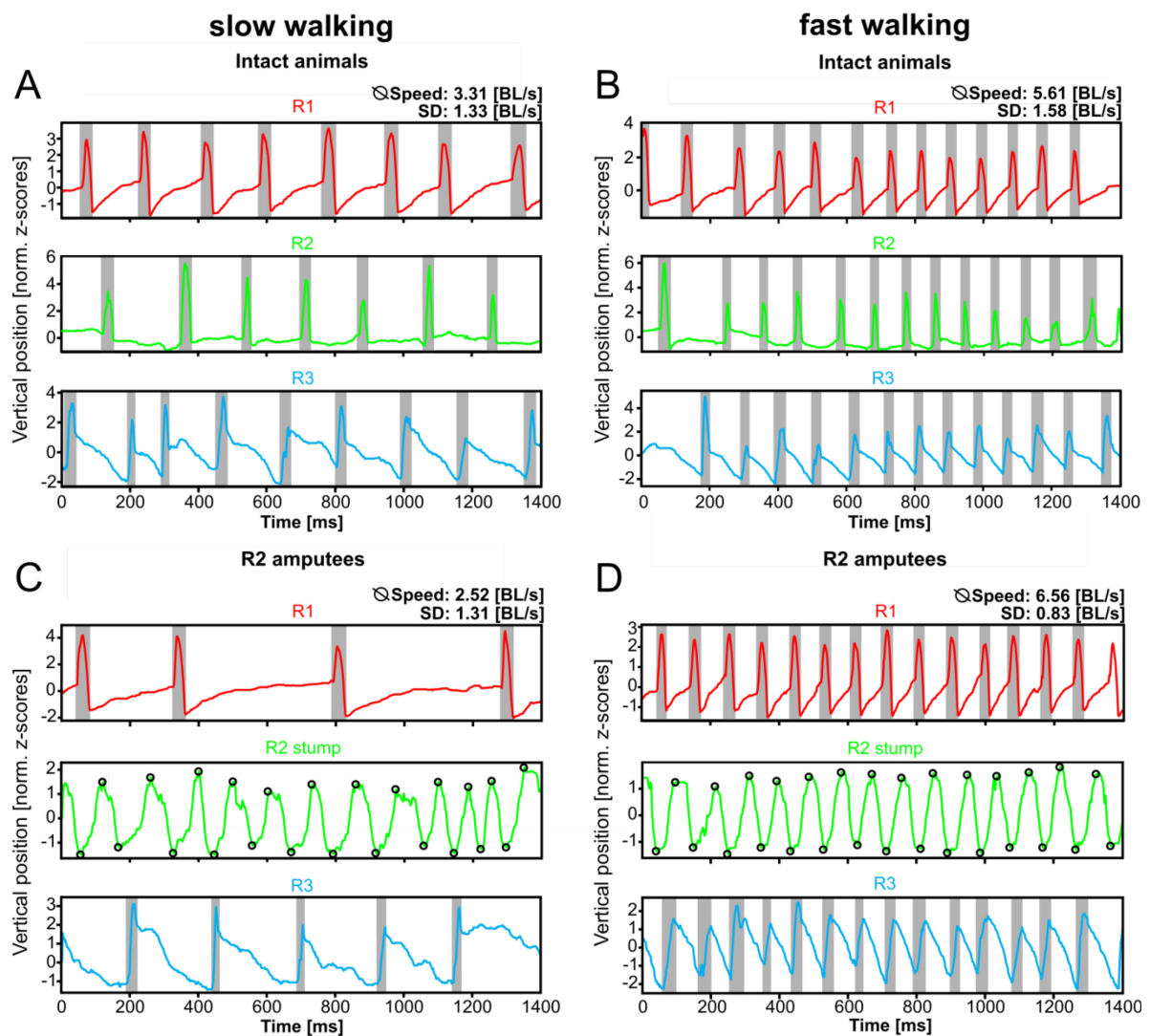


**Fig. 18: Movements (vertical component only) of intact leg tarsi or the tip of stumps, respectively, plotted over time for typical slow (A) and fast walks (B) of an intact and a middle leg amputee (C and D). Grey bars indicate swing phases in traces of intact legs. Black circles indicate ventral extreme positions (VEPs) and dorsal extreme positions (DEPs) in the stump traces. Trajectories have been normalized to their z-scores. Legs and stumps, respectively, are color coded (red: front leg, green: middle leg and stumps, blue: hind leg). (A and B) All legs of an intact animal perform approximately the same number of steps over time, i.e. the stepping frequency in all legs is more or less identical. This is true for slow and fast walking speeds. (C and D) the stump of a middle leg amputee performs oscillations with a relatively high frequency. This frequency is independent of walking speed, thus in slow walking animals the stump performs several oscillations during single steps of the intact legs. Furthermore, the intact hind leg shows a higher stepping frequency than the intact front leg, indicating a change in interleg coordination, which is most likely caused by the amputation.**

**R1 amputees:**

In front leg amputees' straight walking sequences of 7 animals were recorded in 12 trials with average speeds between 2.2 and 7.3 BL/s (equivalent to 4.7 and 15.7 mm/s). Example trajectories for the intact legs R2 and R3 and the stump of R1 obtained during a typical trial are shown in Fig. 16 B. Trials contained between 9 and 28 oscillations of the R1 stump, between 2 and 28 steps of R2, and between 3 and 28 steps of R3. 203 oscillations of the R1 stump (R1s), 99 steps of R2, and 120 steps of R3 were analyzed.

The average step period of R2 was 201 ms (SD = 118 ms), for R3 it was 175 ms (SD = 114 ms), while the average oscillation period of the R1 stump was 111 ms (SD = 51 ms). Step periods of the intact legs R2 and R3 decreased when the walking speed increased (Fig. 19 Bii and Biii). The oscillation period of the R1 stump, however, did not show such a dependence; here average values of approximately 100 ms for the complete range of walking speeds were found ( $R^2 = 0.005$ ). As a consequence, the oscillation frequency of the front leg stump is not identical to the stepping frequency of the intact legs at slow walking (see Fig. 19 Bi to Biii). Multiple oscillations of the stump during single steps of the intact legs (see exemplary data for the R2 stump in Fig. 18 C) occurred frequently during slow walking.

The duty factor (stance duration divided by leg period) ranged between almost 1 and 0.6 for R2 (Fig. 25 Bii) and between 1 and 0.55 for R3 (Fig. 25 Biii), with decreasing values when the speed increased. For the stump of R1 the duty factor (time between DEP and subsequent VEP divided by stump oscillation period) ranged from 0.8 to 0.19 (Fig. 25 Bi), with values that became more concentrated around approx. 0.4 when speed increased.

For walking speeds between 1.5 and 5 BL/s the phase relation between the R1 stump and R3 was more variable than the relation between R1 and R3 in intact animals. However, average phase also approached 0 between 5 and 8 BL/s (Fig. 21 Bi). An analysis of the mean resultant vector further substantiated this speed-dependent change in inter-leg coordination as it had a value of almost 0 at very low walking speeds of approx. 1.5 BL/s, reached values of 0.5 at around 5 BL/s and then increased rapidly to high values of almost 1 at approx. 8 BL/s. Interestingly, the phase relation between the intact leg R2 and the R1 stump did not show major differences when compared to that between R2 and R1 in intact animals. The mean resultant vector length of the phase values increased over the whole speed range from about 0.3 to almost 1, with a sharp drop from approx. 0.8 to approx. 0.4 between 4 and 6 BL/s (Fig. 22 Bi and Biii). In contrast, the phase relation between the intact legs R3 and R2 at walking speeds between 0 and 5 BL/s was much more variable than in intact animals, with mean values ranging from -0.5 to 0.4. For the speed range above 5 BL/s the phase relation approached 0 and showed a much lower variability (Fig. 21 Biii). Calculations of the mean resultant

vector length showed increasing values from 2 to 6 BL/s with a slight decrease above 6 BL/s (Fig. 22 Biii).

Analysis of the temporal delay between intact legs (R2 and R3) and the stump (R1) showed a preferred time interval between PEPs in the intact legs and subsequent events in the stump (Fig. 23 A, red dots) during fast walking. This time interval was either approx. 0 or 100 ms, respectively (R2>VEP and R3>DEP), or approx. 50 ms (R2>DEP and R3>VEP). Given a cycle-to-cycle coupling and a stepping frequency of approx. 10 Hz a strong temporal preference seemed likely during fast walking. During slow walking (Fig. 23 A, green dots), most of this strict temporal coordination vanished (R2>VEP, R3>VEP, and R3>DEP); this was consistent with the finding that during slow walking there was no cycle-to-cycle coupling between the intact legs and the stump. However, a preferred temporal delay of approx. 50 ms between PEP events in the middle leg and the first subsequent DEP events in the front leg stump (R2>DEP, green dots) was found even in slow walking animals. This suggests a coordinating influence between the middle leg and the front leg stump, even in the absence of strict cycle-to-cycle coupling. It is important to note that multiple stump oscillations were neglected for this analysis as it only covered the time delay between a PEP event in an intact leg and the first subsequent VEP or DEP event in the stump.

In order to visualize possible influences of the steps in intact legs on movements of the stump, levation and depression of the stump was superimposed for a time window of 100ms before and after a PEP event in an intact reference leg (Fig. 26). This analysis showed that a PEP in the intact leg R3 is followed, in most cases, by a VEP in the R1 stump with a delay of 50 ms on average. This holds for a walking speed below (Fig. 24 Aiii) and above 5 BL/s (Fig. 24 Aiv). However, the situation was different for PEP events in the intact leg R2, where the next subsequent event was a DEP with a latency of 50 ms on average during fast walking (Fig. 24 Aiii) and a VEP with a latency of approx 20 ms on average during slow walking (Fig. 24 Aiv). However, the stump movement showed a lot of variability during slow walking (Fig. 24 Aiv), and it appeared to be much more coordinated during fast walking (Fig. 24 Aiii). These findings were in agreement with the values in Fig. 23.

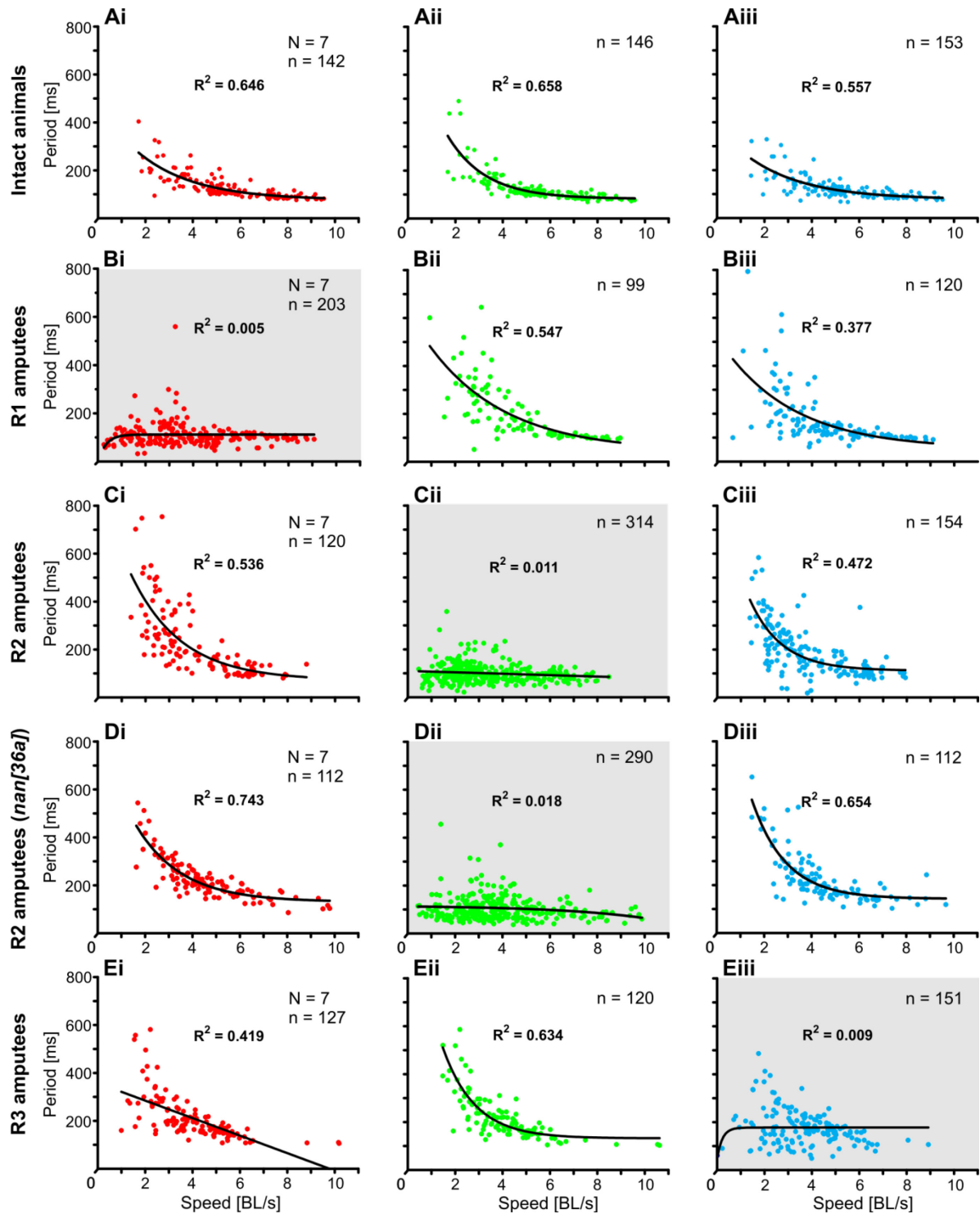


Fig. 19: Periods of leg movement vs. walking speed (in body lengths per second, BL/s) for the legs ipsilateral to the camera ( $N$  = number of animals;  $n$  = number of steps). Values are shown for intact animals and flies whose front (panels B), middle (panels C and D), or hind leg (panels E) was amputated. Panels D show data obtained for middle leg amputees of *nan/36a* mutant flies that have defective chordotonal organs. All other panels in this figure show data derived from *Canton-S* wild type flies. Each dot represents the period of one step (PEP to the following PEP for intact legs) or one oscillation (from DEP to DEP for stumps), respectively. Red dots correspond to front leg or stump (Bi) data, green dots indicate middle leg or stump (Cii) data and blue dots indicate hind leg or stump data (Eiii). An exponential fit was performed on the values in each plot. All intact legs show an exponential decrease of period with increasing walking speed. The stumps of the leg amputees (plots are highlighted in grey) do not show such an exponential dependence. For R1 and R2 amputated flies the values are almost independent of walking speed (Bi and Cii).

## R2 amputees

In another series of experiments the right middle leg was amputated. Again, data from 7 animals were obtained in 12 trials. Typical trajectories of the intact legs R1 and R3 and the R2 stump from a single trial are shown in Fig. 16 C. The average speed of the recorded walking sequences differed between 1.8 and 6.1 BL/s. This corresponded to an absolute speed range of 3.7 to 13.8 mm/s. The number of recorded steps ranged between 4 and 26 steps of R1, between 18 and 38 oscillations of the R2 stump and between 6 and 26 steps of R3. In total, 120 steps of the right front leg (R1), 314 oscillations of the right middle leg stump (R2), and 154 steps of the right hind leg (R3) were recorded. Average step periods were 227 ms (SD = 145 ms) for R1 and 192 ms (SD = 105 ms) for R3. The R2 stump oscillated with an average period of 99 ms (SD = 40 ms).

The step period of the intact legs R1 and R3 decreased with increasing speed (see Fig. 19 Ci and Cii,  $R^2 = 0.54$  and  $R^2 = 0.47$ , respectively), whereas the oscillation period of the R2 stump did not show a similar decrease (Fig. 19 Cii,  $R^2 = 0.01$ ). Comparable to the findings for the R1 stump, the oscillation periods of the R2 stump were independent of walking speed, with periods that varied around 100 ms. At low walking speed multiple stump oscillations were regularly observed during single steps of the intact legs (example in Fig. 18 C). In some cases before or after a very slow walk, the stump oscillated even if the intact legs did not start or just stopped stepping (Fig. 20). In fast walking animals the number of stump oscillations was comparable to the number of steps in intact legs (for an example see Fig. 18 D).

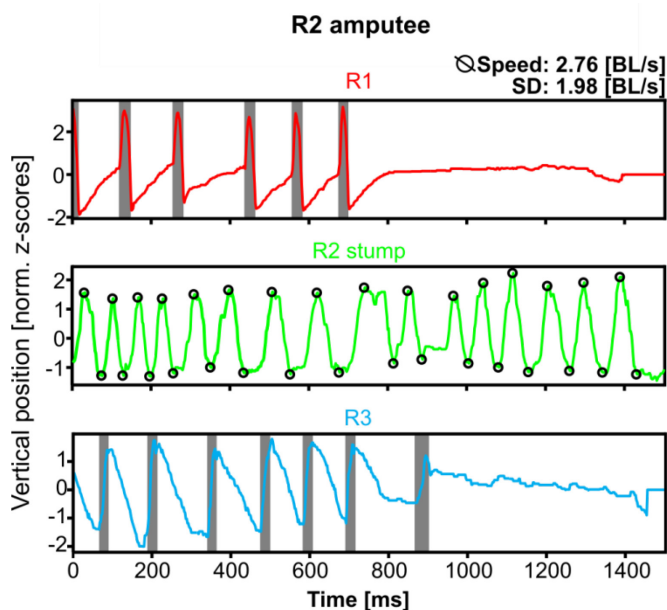


Fig. 20: Example trial of a CS R2 amputee during which the animal stopped stepping with the intact legs whereas the stump was still continuously active. Trajectories are color coded (red: front leg, green: middle leg and stumps, blue: hind leg) and show the movements (vertical component only) of intact leg tarsi and the tip of the R2 stump, respectively, over time. Grey bars indicate swing phases in traces of intact legs. Black circles indicate ventral extreme positions (VEPs) and dorsal extreme positions (DEPs) in the stump traces. Trajectories have been normalized to their z-scores.

The duty factor ranged between almost 1 and 0.6 for R1 (Fig. 25 Ci) and between 1 and 0.2 for R3 (only three outliers below 0.6, Fig. 25 Ciii), with decreasing values when the speed increased. For the stump of R2 the duty factor ranged from 0.8 to almost 0 (Fig. 25 Cii), with a trend for values to become more concentrated around 0.5 when walking speed increased.

An analysis of the phase relations revealed a much higher variability than in intact animals, R1 amputees or R3 amputees, as indicated by the distribution of the average phases that cover a range of more than 0.4 in all legs (Fig. 21 A, B and D). The mean phase value between R1 and R3 varied around 0.5 in a speed range of approx. 1.5 to 5 BL/s. For speeds above 5 BL/s the mean phase value quickly approached 0. Interestingly, mean resultant vector length did not rise above a value of 0.7 and was even slightly lower for steps at the highest speeds (Fig. 22 Ci). Phase relations between the R2 stump and R1 were even more variable with no preferred value at walking speeds between 1.5 and 5 BL/s. For speeds above 5 BL/s the variability decreased markedly and average phase values reached approx. 0.6 (Fig. 21 Cii); the resultant vector length increased from 0.2 to 0.7 for speeds above 5 BL/s (Fig. 22 Cii). The phase relation analysis between R3 and the R2 stump showed average phase relation values between 0.25 and 0.75 at walking speeds ranging from 1.5 to 5 BL/s (Fig. 21 Ciii). Again, the situation changed at walking speeds above 5 BL/s where the values approached approx. 0.4. However, the mean resultant vector length did not show a constant increase with speed but it varied between 0.6 and 0.7 (Fig. 22 Ciii).

An analysis of the temporal delay (Fig. 23 B, red dots) between the intact legs (R1 and R3) and the stump (R2) showed that, during fast walking, the situation was very similar to the front leg amputees. Preferred temporal intervals between PEPs in intact legs and the first subsequent VEPs or DEPs in the stump of either 0 and 100 ms (R1>VEP and R3>VEP), respectively, or approx. 50 ms (R1>DEP and R3>DEP) were found. In slowly walking animals (green dots) the variance of these intervals was higher but they still clustered around the values observed during fast walking. The superimposed stump traces in Fig. 24 visualize the aforementioned findings (Fig. 24 panels B). Taken together the results indicate that the middle leg receives coordinating influences from both the front and the hind leg; these influences persist even during slow walking when the relatively strict cycle-to-cycle coupling observed during fast walking was absent.

### **R2 amputees of the genotype *nan[36a]***

As an example for sensory feedback mutants flies of the genotype *nan[36a]* (Kim et al., 2003), were included in the analysis. 7 R2 amputated animals of this genotype were analyzed in 16 trials. The average speed during walking ranged from 1.9 to 6.8 BL/s. This corresponded to an absolute speed range of 4.3 to 15.4 mm/s. The trials contained between 2 and 13 steps of R1, between 7 and 29 oscillations of the R2 stump and between 2 and 14 steps of R3. In total, 112 steps of the right front leg

(R1), 290 oscillations of the right middle leg stump (R2), and 112 steps of the right hind leg (R3) were recorded. Mean steps periods were 231 ms (SD = 84 ms) for R1, 104 ms (SD = 51 ms) for oscillations of the R2 stump and 231 ms (SD = 102 ms) for R3.

The step periods of the intact legs R1 and R3 decreased with increasing walking speed (see Fig. 19 Di and Diii,  $R^2 = 0.74$  and  $R^2 = 0.65$ , respectively) comparable to observations in R2 amputees of the wild type *CS*. Again the stump oscillation period did not show a similar decrease (Fig. 19 Dii,  $R^2 = 0.02$ ). Like in R2 amputees of the *CS* wild type the stump oscillations were almost constant at an average frequency of 10 Hz for the whole speed range, which means that during slow walking multiple oscillations of the stump occurred during single steps of the intact legs.

The duty factor ranged between almost 1 and 0.55 for R1 (Fig. 25 Di) and between almost 1 and 0.5 for R2 (Fig. 25 Dii), with decreasing values when the speed increased. For the stump of R3 the duty factor ranged from 0.8 to 0.15 (Fig. 25 Diii), with a trend for the values to become more concentrated around 0.6 for speeds above 5 BL/s.

Differences between R2 amputees of the *CS* wild type and R2 amputees of the genotype *nan[36a]* were uncovered when the temporal coordination between the legs and stump was analyzed. The average phase relation between R1 and R3 was almost constant at values of about 0.5 for the whole range of walking speeds (Fig. 21 Di). A change to 0 for speed values above 5 BL/s, that was observed for the R2 amputees of *CS* flies (Fig. 21 Ci), was absent in the *nan[36a]* mutant. Average phase relations between the R2 stump and R1 (Fig. 21 Dii) were even more variable than in *CS* flies (Fig. 21 Cii). Similar to *CS* flies the variability decreased markedly for speeds above 6 BL/s where it reached values between 0.5 and 0.7. The mean resultant vector length ranged from 0 to 0.3 for speeds between 2 and 5 BL/s with a slight decrease from 0.3 - 0.1 for 5-6 BL/s, but it never increased to values above 0.4 for the whole speed range (Fig. 22 Dii).

Phase relations between R3 and the R2 stump (Fig. 21 Diii) showed once more an increase in variability when compared to the same situation in the wild type (Fig. 21 Ciii). However, the values still reached an average of 0.4 for walking speeds above 6 BL/s (Fig. 21 Diii). The mean resultant vector length was quite variable ranging between 0.1 and 0.6. A constant increase in speed was absent and between 5 and 7 BL/s there was even a decrease from 0.5 to below 0.1 (Fig. 22 Diii). This decrease was not found for wild type animals (Fig. 22 Ciii), which showed almost constant values of 0.6 between 5 and 8 BL/s.

An analysis of the temporal delay between PEPs in the intact legs (R1 and R3) and the first subsequent VEPs or DEPs in the stump (R2) revealed a broader distribution of the values (Fig. 23 C) when compared to R2 amputees of wild type *CS* flies (Fig. 23 B). This holds especially for fast walking (Fig. 23 C, red dots).



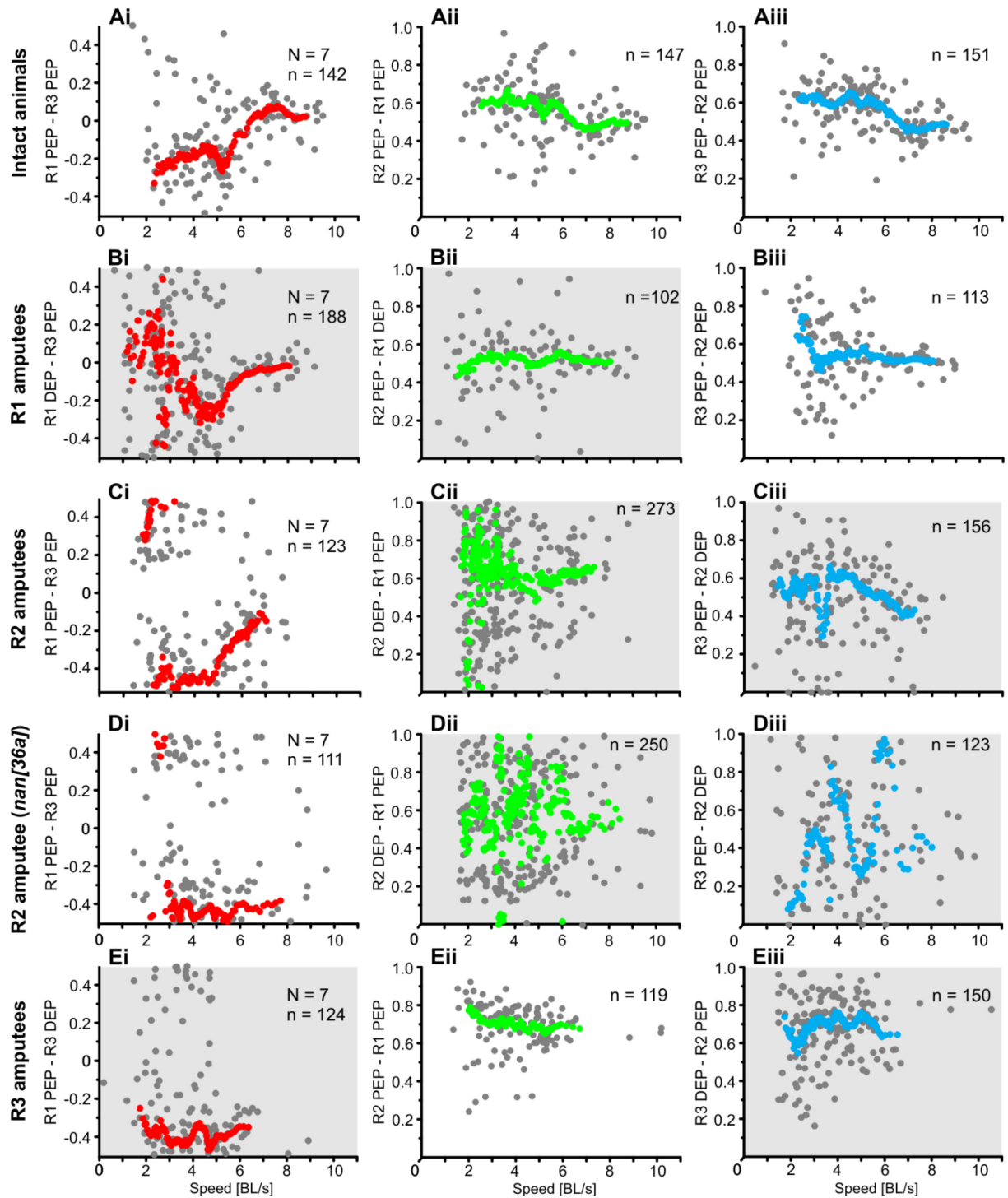


**Fig. 21:** Relative phase relation of an event in one leg (PEP) or stump (DEP) versus a reference event in another leg or stump ( $N$  = number of animals;  $n$  = number of steps). The y axis label depicts the dependent leg and event first and the reference leg and event last. For instance, R2PEP-R1DEP (Bii) indicates a PEP in the right middle leg as the dependent event and a DEP in the stump of the right front leg as the reference event. Grey dots show the phase relation values calculated for each event plotted versus the walking speed [BL/s] of the animal during the period of the reference leg. Colored dots indicate mean values (circular means for the phase relation versus arithmetic means for the speed) calculated for a sliding window of 15 values that has been applied on the speed sorted data. The color of the dots represents the first leg in the plot titles, the dependent leg during phase relation calculation (front leg: red, middle leg: green, hind leg: blue). Panels that include stump data as reference or dependent values are highlighted with a grey background.

Most values for the temporal intervals between PEPs in intact legs and the stump were distributed between 0 and 50 ms ( $R1 > VEP$  and  $R3 > VEP$ ), or 50 - 100 ms ( $R1 > DEP$  and  $R3 > DEP$ ).

The increase in variability of stump movements becomes obvious when comparing panels B and D of Fig. 24.

### R3 amputees

In hind leg amputees walking sequences of 7 animals were recorded in 13 trials. Exemplary trajectories for the intact legs R1 and R2 and the stump of R3 are shown in Fig. 16 D. The average speed of the recorded trials ranged from 2.0 to 8.7 BL/s, which was equivalent to absolute speeds between 4.6 and 20.5 mm /s. Individual trials consisted of 4 to 16 steps of R1, 3 to 16 steps of R2, and between 2 to 19 oscillations of the R3 stump. A total number of 127 steps of the right front leg (R1), 120 steps of the right middle leg (R2), and 151 oscillations of the right hind leg stump (R3) were recorded.

The average step periods were 210 ms (SD = 90 ms) for R1 and 224 ms (SD = 107 ms) for R2, while the R3 stump oscillated with an average period of 175 ms (SD = 75 ms). Fig. 19 shows that the step period for both intact legs R1 (Fig. 19 Ei,  $R^2 = 0.42$ ) and R2 (Fig. 19 Eii,  $R^2 = 0.63$ ) decreased with increasing speed. The stump oscillation periods of the hind leg stump did not depend on speed in the same way as intact hind legs did in the other experiments. However, they did not show the same clear independence of walking speed like the front and middle leg stumps either (Fig. 19 Eiii,  $R^2 = 0.009$ ). Also in the R3 amputees multiple oscillation of the stump during single steps of the intact legs were regularly observed during slow walking.

The duty factor (stance duration divided by leg period) ranged between almost 1 and 0.6 for R1 (Fig. 25 Ei) and between 1 and 0.8 for R2 (Fig. 25 Eii), with decreasing values when the speed increased. For the stump of R3 the duty factor (time between DEP and subsequent VEP divided by stump oscillation period) ranged from 0.8 to 0.15, with a trend for values to become more concentrated around 0.5 for speeds above 5 BL/s (Fig. 25 Eiii).

The phase relations between the analyzed legs were less variable than during experiments with R1 and R2 amputees as indicated by the distribution of the mean phase relation, which did not vary for more than 0.2 in all 3 legs (Fig. 21 E). Between R1 and R3 the average phase relation values ranged from -0.5 to -0.25 (Fig. 21 Ei). For the relation between R2 and R1 the average phase relation values were almost constant at approx. 0.75 for the whole range of walking speeds (Fig. 21 Eii). In both cases the mean resultant vector length generally increased with speed but displayed a drop to lower values for speeds between 4 and 5 BL/s. For walking speeds above 5 BL/s the values increased again (Fig. 22 Ei and Eii). The average values that were obtained for the phase relation between the R3 stump and R2

ranged from 0.5 to 0.75 (Fig. 21 Eiii). In this case mean resultant vector length increased up to a speed of 5 BL/s and dropped to slightly lower values for the highest recorded speeds (Fig. 22 Eiii).

Compared to the findings for front and middle leg amputees, an analysis of the temporal delay between intact legs (R1 and R2) and the hind leg stump revealed a different picture (Fig. 23 C). Even in fast walking animals (Fig. 23 C, red dots) the time intervals between PEPs in the intact legs and subsequent events in the stump were much more variable, even though the tendency to cluster at approx. 0 and 100 ms ( $R1 > VEP$ ,  $R2 > VEP$ ,  $R2 > DEP$ ) or 50 ms ( $R1 > DEP$ ), respectively, persisted. In slowly walking hind leg amputees this increase in variability was even more pronounced (Fig. 23 C, green dots) and there was almost no preferred time interval between PEPs in intact legs and the first subsequent VEPs or DEPs in the stump. The superimposed traces of stump movement in Fig. 26 further substantiated these findings (Fig. 24 panels D). The results suggest that there are only weak influences originating in the front and middle leg that affect movement in the hind leg.

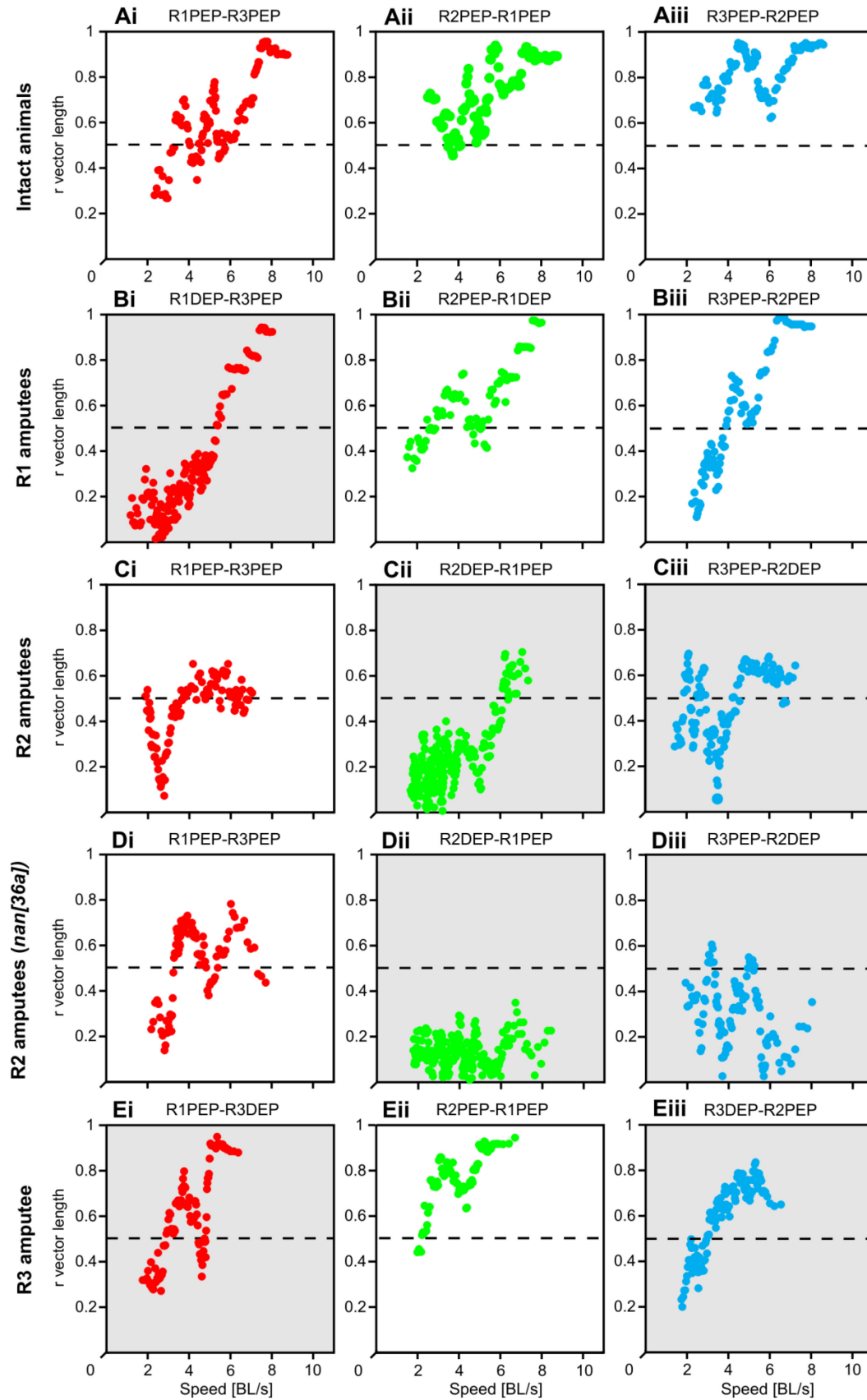
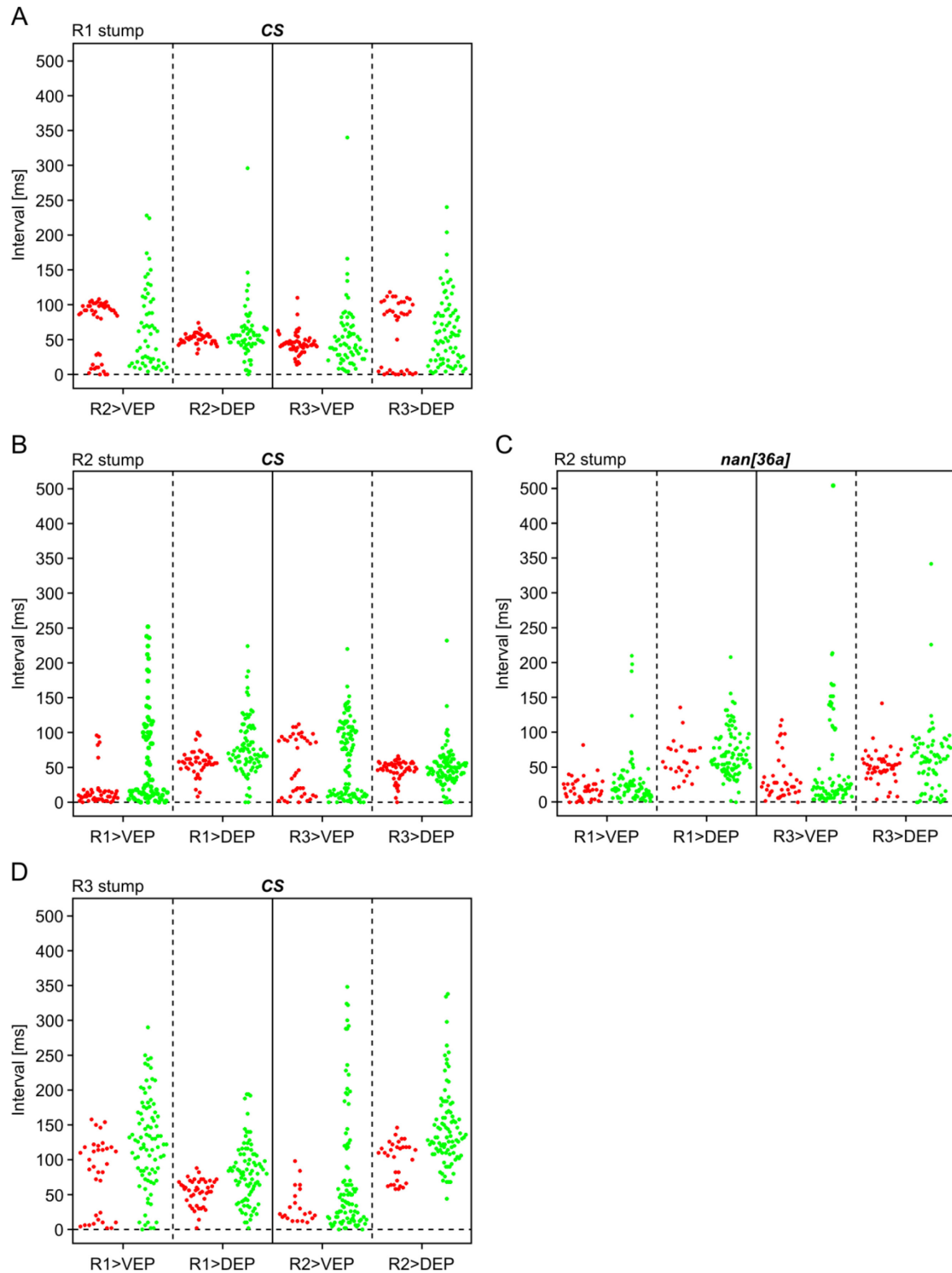
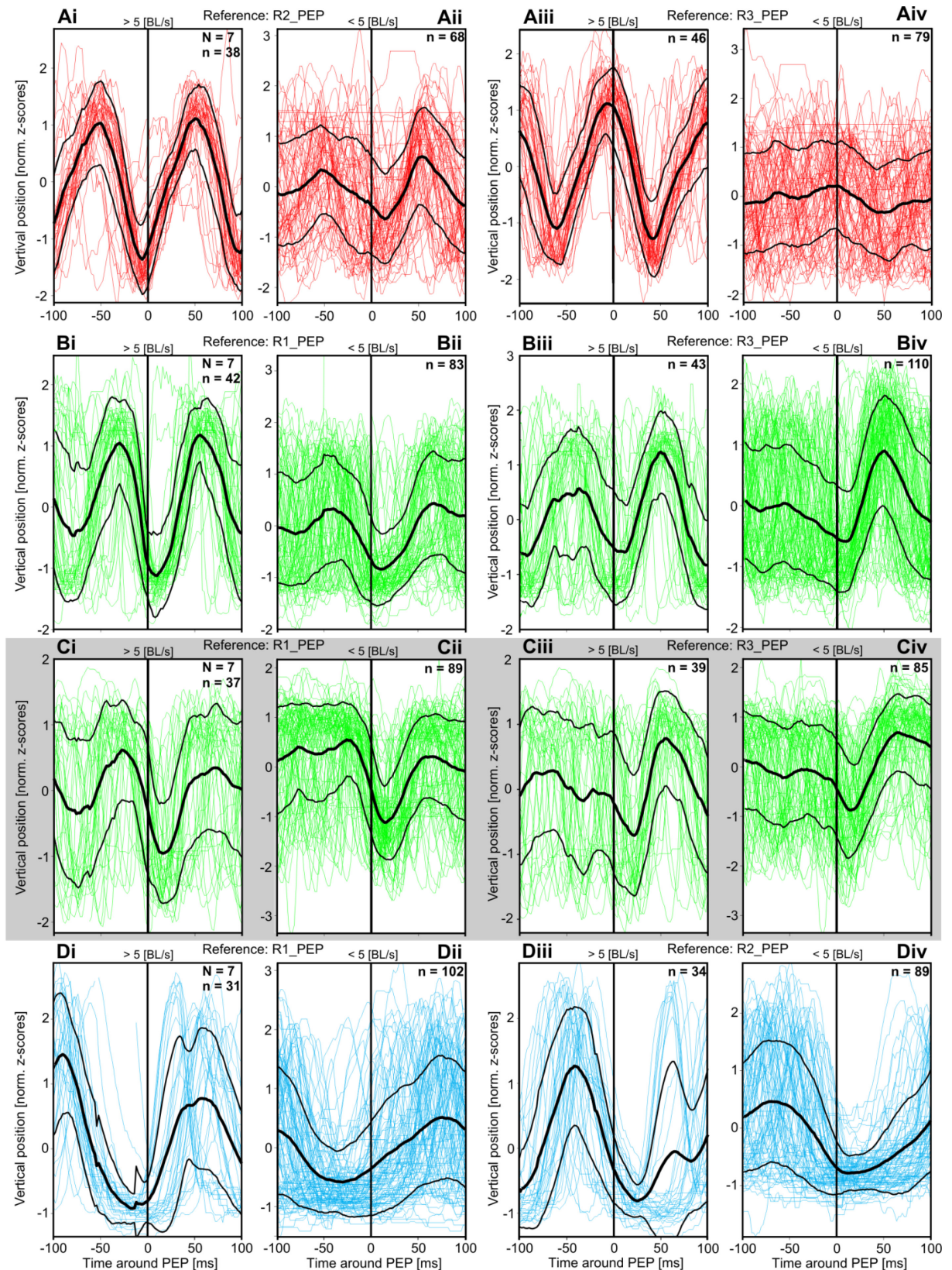


Fig. 22: Length of the mean resultant vector plotted versus walking speed [BL/s]. The values were calculated for a sliding window of 15 values that has been applied on the speed sorted phase relation values plotted in figure 6. The color of the dots represents the dependent leg (red: front leg or stump; green: middle leg or stump; blue: hind leg or stump). The first leg and event mentioned in the plot titles is always the dependent leg the second leg and event mentioned is always the reference. Panels that include stump data as reference or dependent values are highlighted with a grey background.



**Fig. 23:** Time intervals between PEPs in intact legs and stump VEPs and DEPs, respectively. Panel A shows data for front leg amputees, panel B shows data for middle leg amputees, and panel D shows data for hind leg amputees. Panel C shows data for middle leg amputees of the chordotonal organ defective *nan[36a]* mutant. Each data point refers to the first VEP or DEP event in a stump following a PEP in an intact leg; for instance, R2>VEP in Panel A refers to the time that elapsed between a PEP in the middle leg (R2) and the next VEP in the front leg stump. Data has been subdivided into those associated with a walking speed equal to or above 5 BL/s (red dots) and those associated with walking speeds below 5 BL/s. If multiple stump movements occurred during the step period of an intact leg only the first DEP or VEP of the stump after the PEP in the reference leg was taken in consideration.





**Fig. 24:** Stump levation and depression movements 100ms before and after a PEP event in intact legs ( $N$  = number of animals;  $n$  = number of steps). Stump traces are color coded (Red: stump of R1, green: stump of R2, blue: stump of R3). Trajectories were normalized to their z-scores to improve comparability. Average traces (thick black traces)  $\pm$  SD (thin black traces) are given for each plot.  $N$  depicts number of animals;  $n$  depicts number of traces in the corresponding plot. Plot titles indicate the intact leg that served as a reference. Stump traces recorded during walking speeds above 5 BL/s (panels i and iii) and below 5 BL/s (ii and iv) are displayed in separate plots for each reference leg. The plots highlighted with a gray background show data obtained for R2 amputees of the *nan[36a]* mutant. Stump movements that occurred independent of a PEP in an intact leg are not shown in this figure.

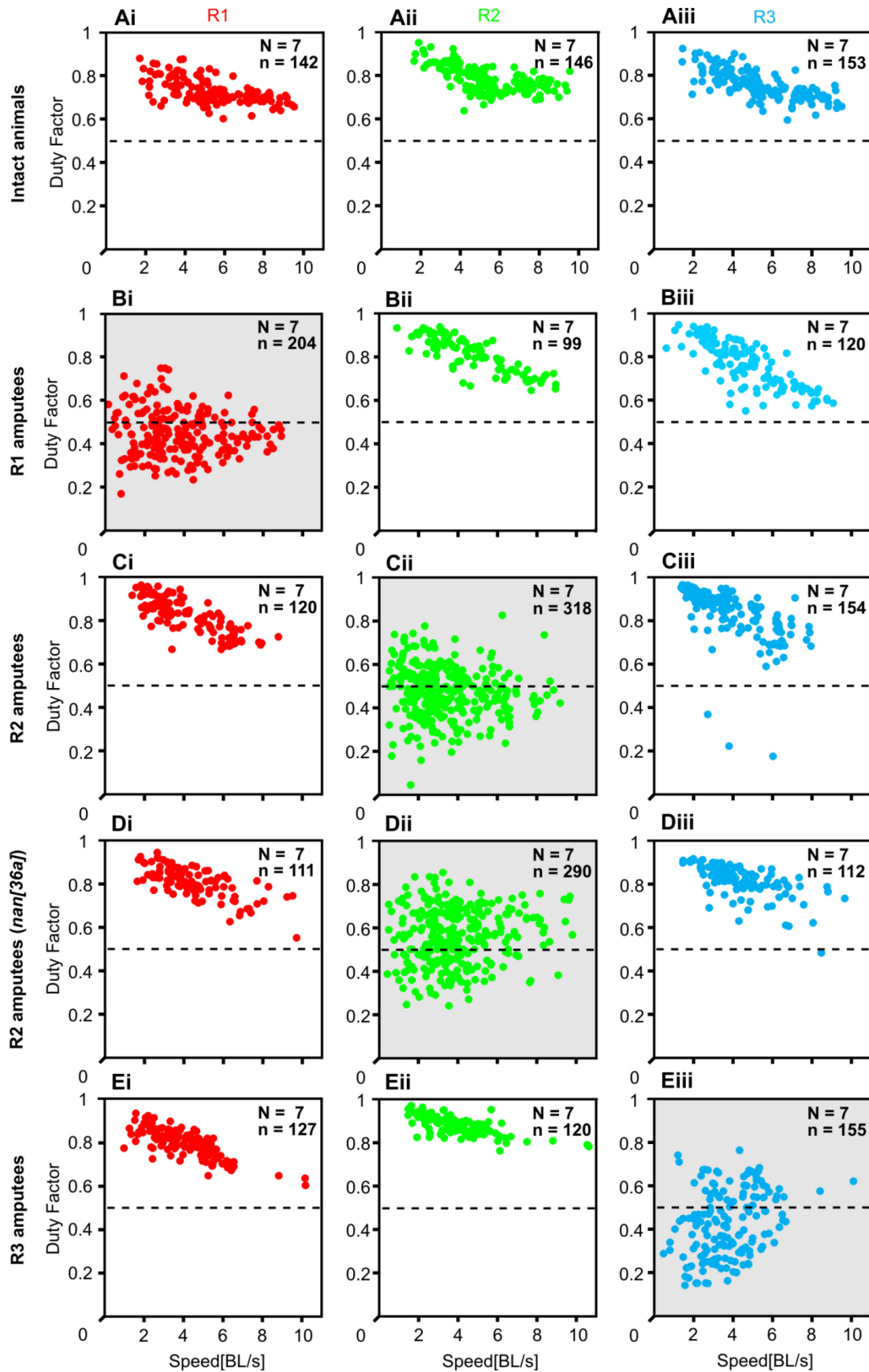
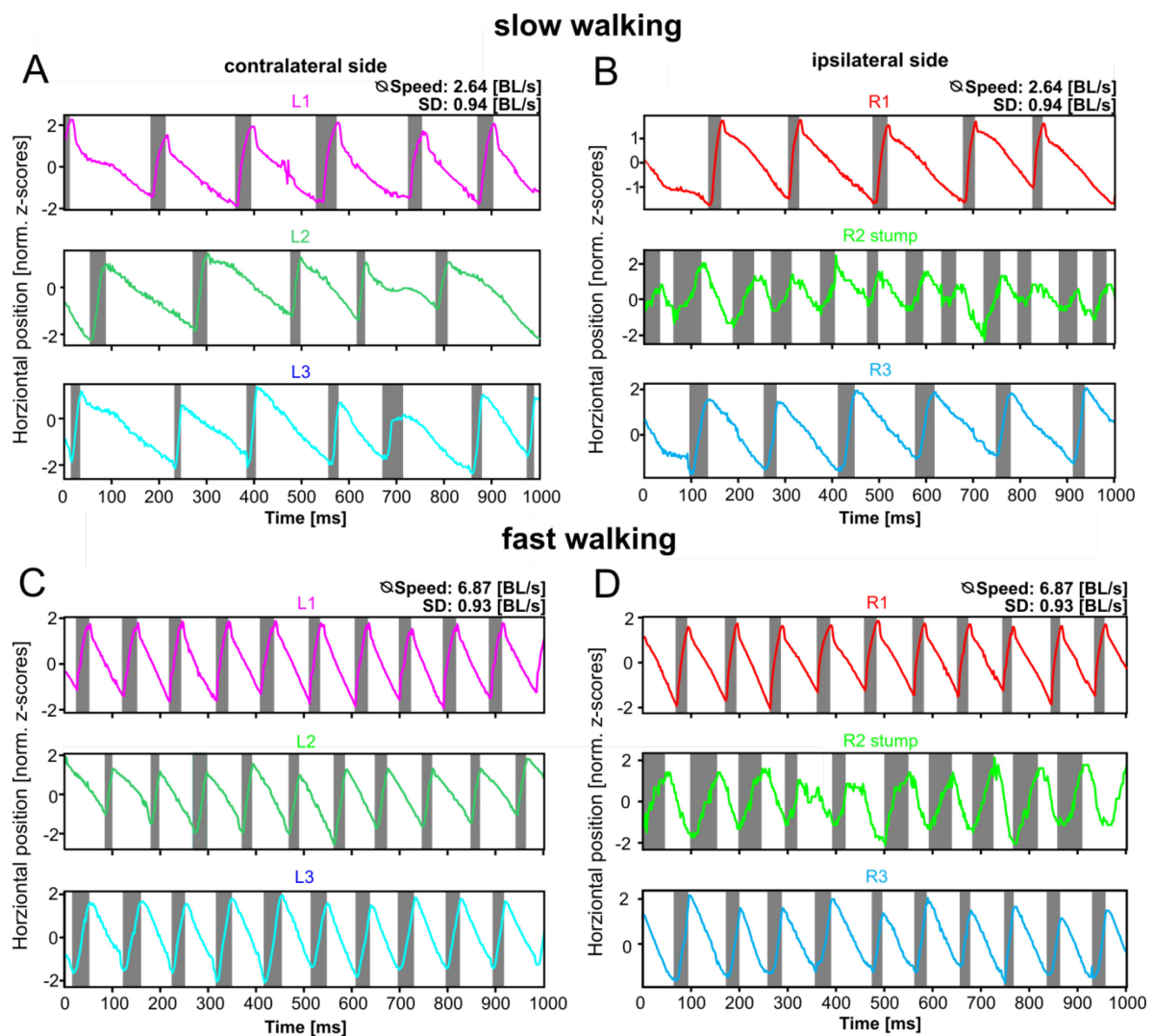


Fig. 25: Duty factor as a function of walking speed [BL/s] ( $N$  = number of animals;  $n$  = number of steps). Values are shown for intact animals (A), front leg amputees (B), middle leg amputees (C) and hind leg amputees (D). Red dots correspond to front leg or stump (Bi) data, green dots indicate middle leg or stump (Cii and Dii) data and blue dots indicate hind leg or stump data (Eiii). Panels containing stump data are highlighted with a gray background.



### 3.1.2 Experiments on the top-view setup

In order to gain insights on the behavior of all six legs of the fly during tethered walking on the ball a series of experiments were performed on the top-view setup (Fig. 7). In this setup the high-speed camera provided a dorsal view of the animal (Fig. 9) that allowed an automated detection of the legs protraction and retraction movements. Protraction and retraction movements of the stump could only be tracked for R2 amputees, in most cases manually. It was not possible to track front and hind leg stumps because they were partly occluded during their movements by either the animal's head or the abdomen (Fig. 27).



**Fig. 26:** Movements (horizontal component only) of intact leg tarsi or the tip of stumps, respectively, over time for typical slow (A and B) and fast walks (C and D) of a middle leg amputee. Grey bars indicate swing phases in traces of intact legs and duration of protraction in stump traces. Trajectories have been normalized to their z-scores. Legs and stumps are color coded (red: right front leg, green: right middle leg and stumps, blue: right hind leg, magenta: left front leg, dark green: left middle leg, cyan: left hind leg). (A and C) All intact legs on the left body side (contralateral to the lesion) performed approx. the same number of steps over time. This was true for slow (A) and fast walking (C). (B and D) the stump of R2 performs oscillations with a relatively high frequency. This frequency was independent of walking speed, thus in slow walking animals the stump performed several oscillations during single steps of the intact legs (B).



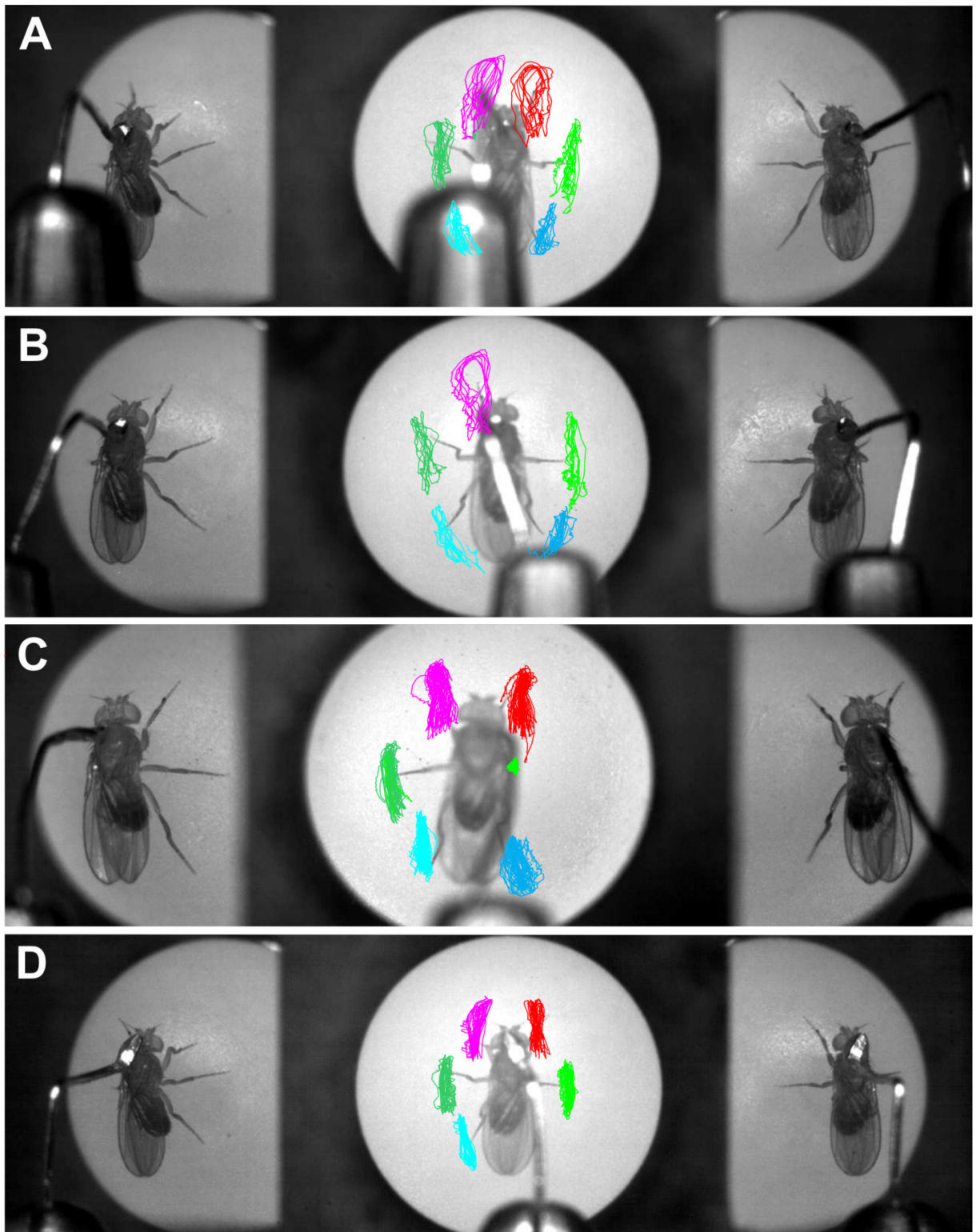


**Fig. 27:** (A) Trajectories of all legs derived from a single walk of an intact animal. (B) Trajectories for intact legs and leg stump of an animal with an amputation of the right front leg. (C) Trajectories for intact legs and leg stump of an animal with an amputation of the right middle leg. (D) Trajectories for intact legs and leg stump of an animal with an amputation of the right hind leg. The trajectories were derived from a single walk and superimposed on a single frame of the corresponding video. (red: front leg or stump trajectory (B), (red: right front leg, green: right middle leg and stump (C), blue: right hind leg, magenta: left front leg, dark green: left middle leg, cyan: left hind leg)

## Intact flies

Straight walking of 7 animals was recorded during 12 trials. The average walking speeds ranged between 1.4 and 6.5 BL/s (equivalent to 3.3 to 13.6 mm/s). The number of steps recorded during each trial varied from 5 to 38 steps of R1, 3 to 37 steps of R2, 5 to 37 steps of R3 and L3 and 4 to 37 steps of L1 and L2. The total number of steps analyzed was 147 (R1), 143 (R2), 151 (R3), 152 (L1), 150 (L2) and 158 (L3).

Average step periods were 148 ms (SD = 82 ms) for R1, 150 (SD = 100 ms) for R2, 142 (SD = 72 ms) for R3, 148 ms (SD = 71 ms) for L1, 150 ms (SD = 84 ms) for L2 and 144 ms (SD = 59 ms) for L3. All legs showed a decrease of step period with increasing speed (Fig. 28). An exponential fit that was applied on the data in each panel showed fairly high  $R^2$  values ( $R^2=0.807$  for R1 (Fig. 28 Ai),  $R^2=0.718$  for R2 (Aii),  $R^2=0.585$  for R3 (Aiii),  $R^2=0.828$  for L1 (Fig. 28 Bi),  $R^2=0.662$  for L2 (Bii) and  $R^2=0.669$  for L3 (Biii)).

Phase relations were calculated for the legs on each body side separately (left legs: Fig. 31; right legs: Fig. 32) according to the analysis performed in section 3.1 (Fig. 21). The phase relation between L1 and L3 (Fig. 31 Ai) and between R1 and R3 (Fig. 32 Ai) developed very similar with increasing walking speed with mean values ranging from approx. -0.5 at a speed of 2 BL/s to -0.1 at a speed of 7 BL/s. This indicates that R1 and R3 as well as L1 and L3 are mostly in-phase at high walking speeds.

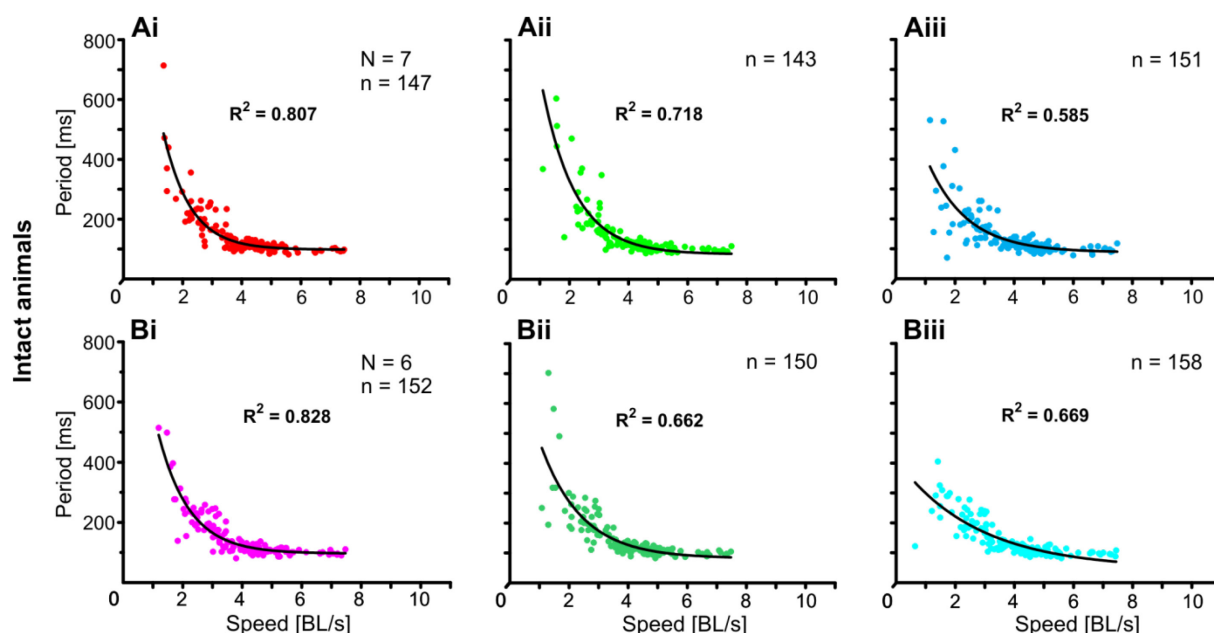


**Fig. 28:** Leg periods (in ms) as a function of walking speed (in body length per second, BLs) for all legs on the right (panels A) and left (panels B) body side of an intact animal (N = number of animals; n = number of steps). Values are color coded (red: right front leg (Ai), green: right middle leg (Aii), blue: right hind leg (Aiii), magenta: left front leg (Bi), dark green: left middle leg (Bii), cyan: left hind leg (Biii)). An exponential fit was performed on the values in each plot. All legs of the intact animal showed an exponential decrease of period with increasing walking speed.

The phase relation between R1 and R3 showed a higher variability in the speed range between 2 and 4 BL/s with a mean resultant vector length between 0.2 and 0.5 (Fig. 37 Ai) compared to 0.55 to 0.7 for L1 and L3 (Fig. 36 Ai) in the same speed range. The mean resultant vector length increased to approx. 0.9 at 7 BL/s in both cases (Fig. 36 Ai and Fig. 37 Ai). The average phase relation between L2 and L1 (Fig. 31 Aii) stayed almost constant for the entire speed range with values ranging from 0.7 at 2 BL/s to 0.6 at approx. 7 BL/s, with an intermediate excursion to 0.5 at 4 BL/s. The corresponding mean resultant vector length increased from 0.5 at 2 BL/s to 0.9 at 7 BL/s, with a dip to 0.7 at 4 BL/s (Fig. 36 Aii). Phase relation between R2 and R1 was quite similar to the data found for L2 and L1 with mean values of approx. 0.7 at 2 BL/s and approx. 0.5 between 4 and 7 BL/s (Fig. 32 Aii). Mean resultant vector length increased from 0.7 at 2 BL/s to almost 1 at 7 BL/s, with an intermediate drop to approx. 0.6 at 3.5 BL/s (Fig. 37 Aii). The average phase relation between L3 and L2 (Fig. 31 Aiii) developed from approx. 0.7 at 2 BL/s to approx. 0.5 at 7 BL/s. For the relation between R3 and R2 (Fig. 32 Aiii) average phase relation values varied around 0.5 for the entire speed range. This indicates that hind and middle leg on either body sides were active in anti-phase during fast walking.

To investigate leg coordination in between both body sides, the phase relation between ipsi- and contralateral legs was calculated (Fig. 33). The average phase relations between R1 and L1 (Fig. 33 Ai), R2 and L2 (Aii) and R3 and L3 (Aiii) all varied between 0.4 and 0.6 for the whole range of recorded walking speeds. This indicates roughly anti-phase activity of intrasegmental legs, even though the phase relation values showed quite some variability, especially in the speed range below 5 BL/s. An analysis of the mean resultant vector length (Fig. 34) revealed increasing values for all phase relations with increasing speed. The mean resultant vector length of the phase relation between R1 and L1 increased from approx. 0.6 at a speed of 2 BL/s to 1 at a speed of 7 BL/s. Between R2 and L2 the phase relation was more variable as judged by the mean resultant vector length (Fig. 34 Aii) that had a value of approx. 0.3 at speed of 2 BL/s and increased to almost 1 at a speed of 4 BL/s then it decreased again to reach 0.8 at a speed of about 7 BL/s. The mean resultant vector length of the phase relation between R3 and L3 increased from approx. 0.5 at a speed of 2 BL/s to 0.9 at 7 BL/s.

Wosnitza and colleagues (2013) studied the behavior of intact 5 day old male *Canton-S* flies during untethered walking in a tunnel. During their study they calculated the phase relation of swing onset for each leg with regard to L1 as a reference leg (Wosnitza et al., 2013 Fig. 2 C). In order to compare tethered walking of intact animals on the ball and untethered walking in the tunnel the same values were calculated for the current dataset (Fig. 29 B) and compared to the already published values (Fig. 29 A).

This comparison (Fig. 29) revealed almost identical circular means in between both datasets, albeit the variability of the values was higher in the data obtained during tethered walking on the top-view setup, where the values sometimes spread around more than half of a circle. This variability was also

reflected in shorter mean resultant vectors for the phase relations during tethered walking on the top-view setup.

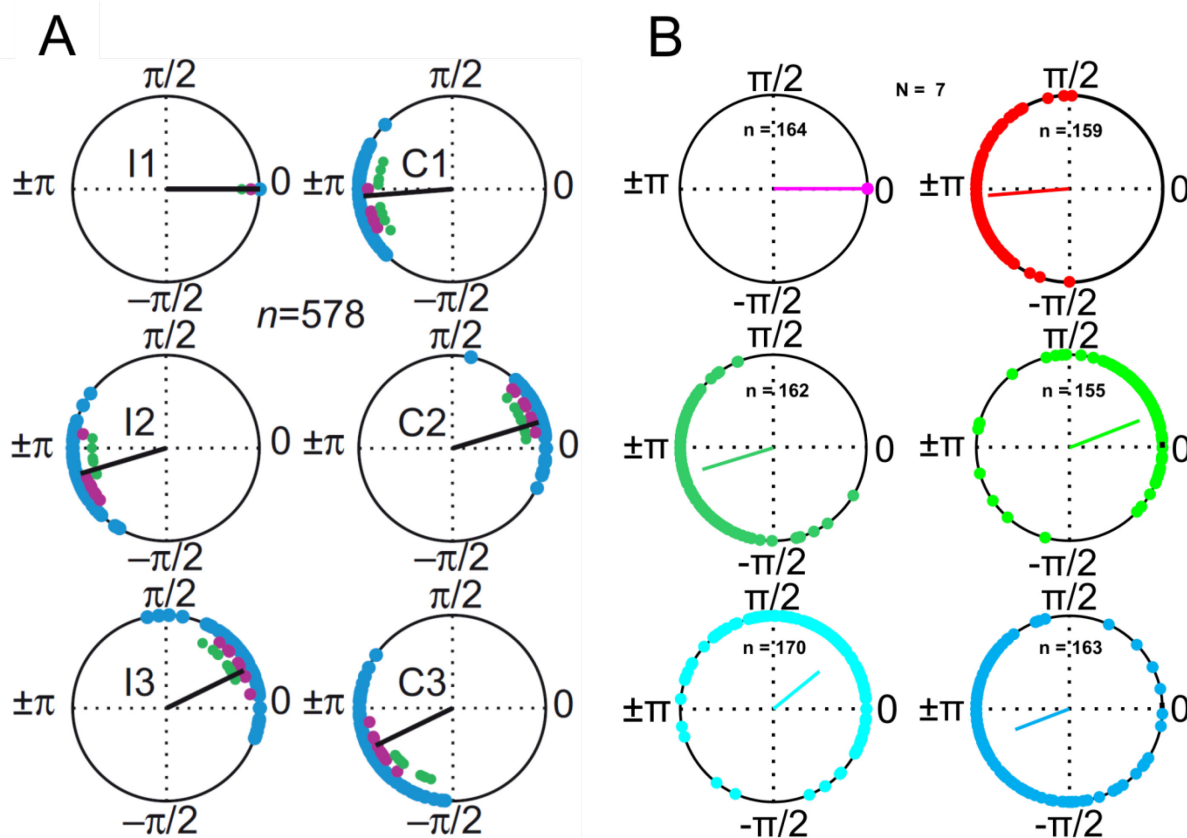


**Fig. 29: Phase relations of swing onset for all legs of intact animals (N = number of animals; n = number of steps).** Swing onset (PEP) in L1 served as a reference in all plots. (A) Published data of intact animals walking untethered in a tunnel (Wosnitza et al., 2013 Fig. 2 C). The phase relations are shown in circular plots with a mean resultant vector pointing to the circular mean of the data. The length of the vector is a measure for circular spread of the data. The blue dots represent data from all animals. Magenta and green dots show data that is used as an example in other panels of Fig. 2 in Wosnitza et al., 2013. (B) Data obtained during the current study for tethered walking of R3 amputees on the top-view setup. Phase relations of different legs are color coded (magenta: L1, dark green: L2, L3: cyan, red: R1, green: R2, blue: R3)

### R1 amputees

Walking sequences of 6 R1 amputees were recorded in 10 trials. Average walking speeds ranged from 0.8 to 2.9 BL/s (equivalent to 1.7 and 6.7 mm/s). During each trial the number of recorded steps varied from 2 to 11 for R2, 4 to 11 for R3, 3 to 7 for L1, 3 to 8 for L2 and 4 to 10 for L3. The stump of R1 could not be tracked because it was occluded by the head during parts of its movement trajectory.

In total 51 steps of R2, 74 steps of R3, 50 steps of L1, 51 steps of L2 and 66 steps of L3 were analyzed.

Average step periods were 383 ms (SD = 176 ms) for R2, 278 ms (SD = 103 ms) for R3, 380 ms (SD = 109 ms) for L1, 382 ms (SD = 134 ms) for L2 and 296 ms (SD = 116 ms) for L3. Step periods of all

intact legs decreased with increasing speed, but an exponential fit, that was applied to the data, showed lower  $R^2$  values compared to R2 or R3 amputees ( $R^2=0.213$  for R2 (see Fig. 30 Aii),  $R^2=0.426$  for R3 (Fig. 30 Aiii),  $R^2=0.291$  for L1 (Fig. 30 Bi),  $R^2=0.240$  for L2 (Fig. 30 Bii) and  $R^2=0.376$  for L3 (Fig. 30 Biii)). However, the absolute range of recorded walking speeds was limited in R1 amputees as it varied between 1 and 4 BL/s (Fig. 30 panels A and B), whereas R2 and R3 amputees had an absolute speed range between 2 and 8 BL/s (Fig. 30 panels C,D and E,F). It was generally observed throughout the experiments that an amputation of the right front leg decreased the activity level of the animal and made it hard to record episodes of fast walking.

An analysis of the temporal coordination in between intact ipsilateral legs (Fig. 31 and Fig. 32) revealed a high degree of variability, similar to values found in intact animals or other amputees for this slow speed range. The average phase relation of L1 and L3 (Fig. 31 Bi) ranged between -0.5 at a walking speed of 2 BL/s and around 0 at a speed of 3 BL/s. This was different from intact animals (Fig. 31 Ai) which showed a constant increase from -0.4 to -0.2 for the phase relation between L1 and L3 in the same speed range, albeit the trend was the same. The phase relation between L2 and L1 (Fig. 31 Bii) showed average values that ranged between 0.6 and 0.7, which was consistent to findings in intact animals at the same speed range. The corresponding mean resultant vector varied around 0.5.

The average phase relation between L3 and L2 (Fig. 31 Biii) changed from 0.9 to 0.5 in a speed range between 1.5 and 3 BL/s and it was again more variable than the relation between L3 and L2 in intact animals. This was also reflected in the mean resultant vector length (Fig. 36 Biii) that increased from 0.1 at 1.5 BL/s to approx. 0.7 at 2 BL/s and decreased again to reach about 0.3 at 3 BL/s.

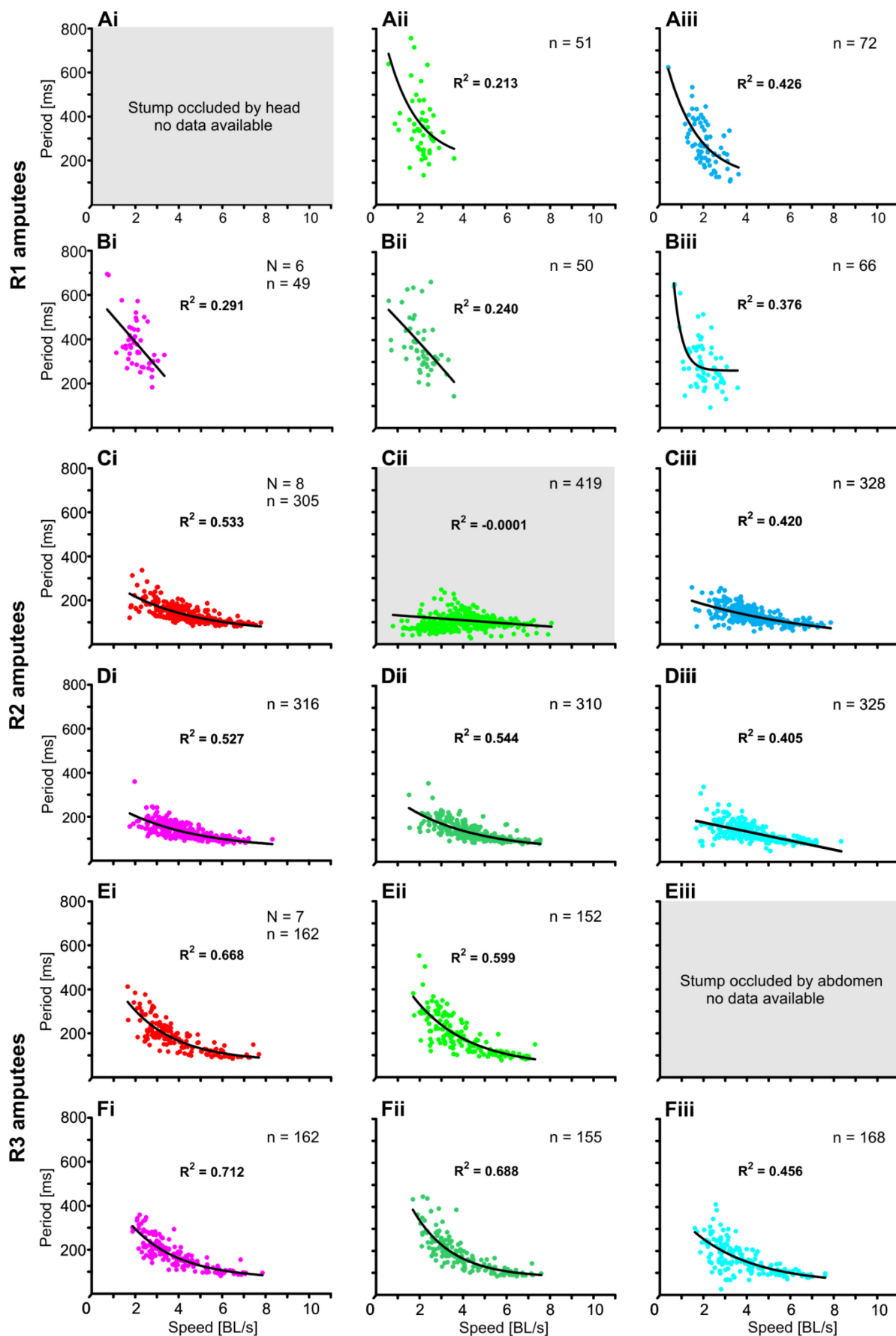
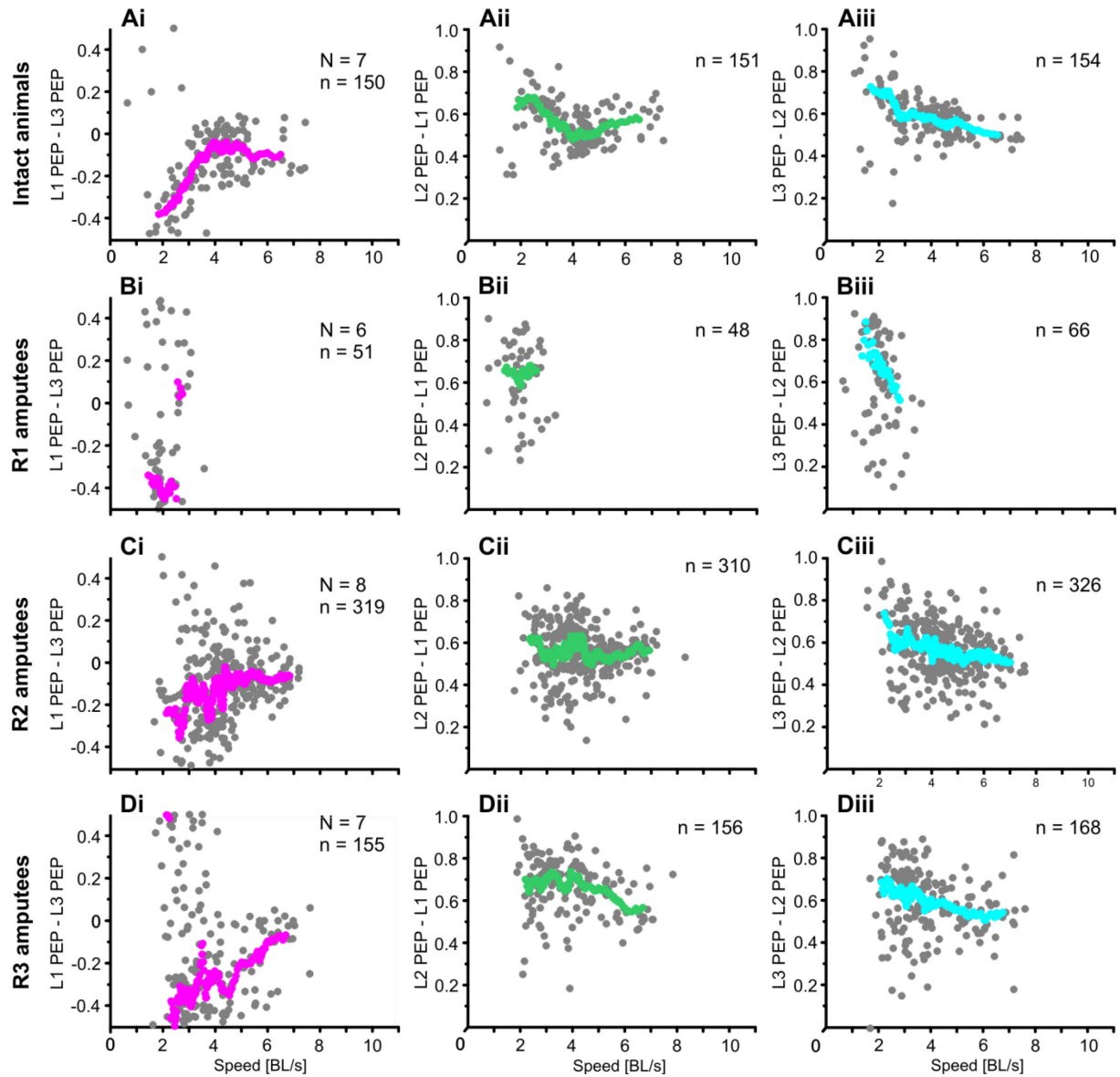


Fig. 30: Periods of leg movement as a function of walking speed (specified as body length per second, BL/s) displayed for R1 amputees (panels A and B), R2 amputees (panels C and D) and R3 amputees (panels E and F). Each dot corresponds to a step period (PEP to PEP) in intact legs or an oscillation period of the stump (panel Cii). The dots are



color coded (red: right front leg (Ai, Ci, Ei), green: right middle leg (Aii, Cii, Eii); blue: right hind leg (Aiii, Ciii, Eiii); magenta: left front leg (Bi,Di,Fi), dark green: left middle leg (Bii,Dii,Fii); cyan: left hindleg (Biii, Diii, Fiii)). All panels that should include stump data are highlighted with a gray background. For the stump of the right front and hind leg there is no available data because they are occluded by either the head or the abdomen. An exponential fit was applied to the data of each leg. All intact showed an exponential decrease of period with increasing walking speed ( $N$  = number of animals;  $n$  = number of steps).



**Fig. 31:** Phase relations between reference legs and dependent legs on the left body side of the animal, contralateral to possible leg amputations on the right body side ( $N$  = number of animals;  $n$  = number of steps). The panels are labeled analogous to Fig. 21. The y axis label depicts the dependent leg and event first and the reference leg and event last. The y axis of panels i, that show the values for the frontlegs, are scaled from  $-0.5$  to  $0.5$ , whereas the y axis of all other plots (ii and iii) ranges from  $0$  to  $1$ . Grey dots show the phase relation values calculated for each event plotted versus the walking speed [BL/s] of the animal during the period of the reference leg. Colored dots indicate mean values (circular means for the phase relation versus arithmetic means for the speed) calculated for a sliding window of 15 values that has been applied on the speed sorted data. The color of the dots represents the first leg in the plot titles, the dependent leg during phase relation calculation (left front leg: magenta, left middle leg: dark green, left hind leg: cyan).

Average phase relations between R3 and R2 (Fig. 32 Biii), ipsilateral to the amputation in R1, developed from  $0.8$  at a speed of  $1.5$  BL/s to approx.  $0.6$  at a speed of  $3$  BL/s. The absolute phase

relation values were distributed between 0.1 and 1. The corresponding mean resultant vector (Fig. 37 Biii) varied in its length from approx. 0.1 at a speed of 2 BL/s to 0.5 at 3 BL/s.

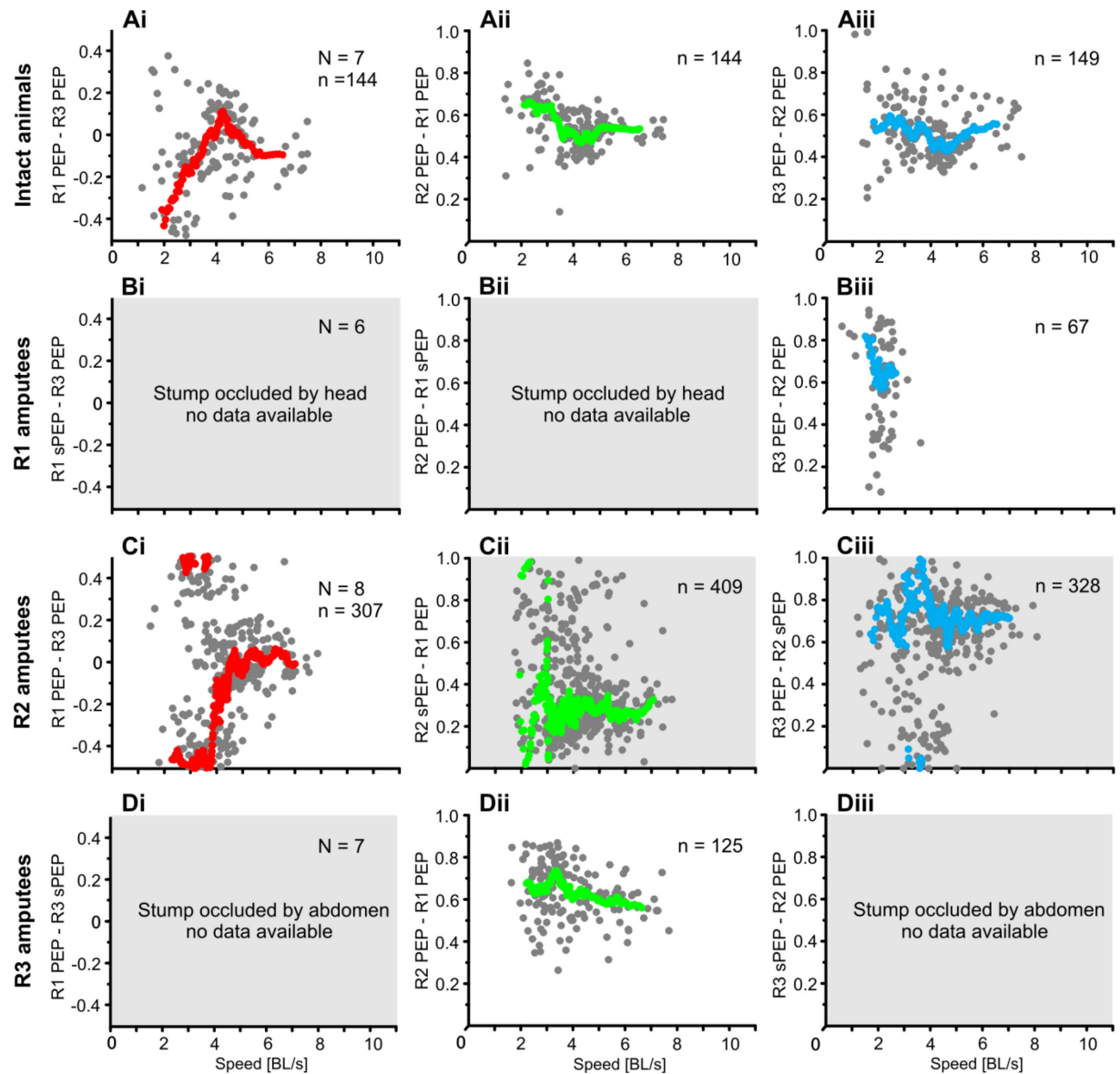


**Fig. 32:** Phase relations between reference legs and dependent legs on the right body side of the animal ( $N$  = number of animals;  $n$  = number of steps). All panels that include stump data are highlighted with a gray background. For the stump of the right front (panels Bi and Bii) and the right hindleg (panels Di and Diii) there is no data available because they were occluded by either the head or the abdomen during parts of their movement.



## R2 amputees

For amputees of the right middle leg data of 8 animals were collected during 17 trials. The recorded mean walking speeds ranged between 2.7 and 6.4 BL/s, which was equivalent to 5.8 and 13.2 mm/s.

Compared to R1 and R3 stumps the stump of R2 was not blocked from view, which made it possible to record protraction and retraction movements of the stump during all trials. The point in time at which the stump switched from retraction to protraction will be called sPEP in the figures.

The number of steps recorded during each trial varied from 7 to 42 steps of R1, from 6 to 42 steps of R3, from 6 to 42 steps of L1, from 7 to 43 steps of L2 and from 7 to 47 steps of L3. For the R2 stump between 10 and 61 oscillations were recorded during each trial. In total 305 steps of R1, 419 oscillations of the R2 stump, 328 steps of R3, 316 steps of L1, 311 steps of L2 and 325 steps of L3 were recorded. The average step periods were 136 ms (SD = 41 ms) for R1, 127 ms (SD = 36 ms) for R3, 132 ms (SD = 36 ms) for L1, 135 ms (SD = 40 ms) for L2 and 128 ms (SD = 38 ms) for L3. The R2 stump oscillated with a period of 108 ms (SD = 143 ms). Similar to the results presented for levation and depression movements in section 3.1 (Fig. 18 D) multiple oscillations during single steps of the intact legs were also found for protraction and retraction movements (Fig. 26 B) recorded on the top-view setup. Accordingly during fast walking the number of stump oscillations converged to the number of steps in the intact legs (Fig. 26 D).

The phase relation between L1 and L3 (Fig. 31 Ci) varied from approx. -0.3 at a speed of around 3 BL/s to -0.1 at a speed of 7 BL/s. For the whole speed range it showed a higher variability than the same values in intact animals (Fig. 31 Ai). This is also reflected in the mean resultant vector length (Fig. 36 Ci) which had a minimum value of 0.2 at a speed of approx. 2 BL/s, whereas the corresponding value in intact animals was approx. 0.55 (Fig. 36 Ai). Nevertheless the mean resultant vector length for the phase relation between L1 and L3 in R2 amputees (Fig. 36 Ci) showed a constant increase throughout the speed range from 0.2 up to values of almost 1 at a walking speed of 7 BL/s. The average phase relation between L2 and L1 (Fig. 31 Cii) and between L3 and L2 (Fig. 31 Ciii) ranged from 0.7 to 0.5 and were thereby in agreement to the values found for intact animals (Fig. 31 Aii and Aiii) and R3 amputees (Fig. 31 Dii and Diii). The values were again more variable than those found in intact animals, which was reflected in the mean resultant vector length (Fig. 36 Cii and Ciii) that showed more fluctuations for the whole speed range compared to the values of intact animals (Fig. 36 Aii and Aiii).

The phase relation between the intact legs R1 and R3 (Fig. 32 Ci), ipsilateral to the lesion, developed from mean values of 0.5 or -0.5 at a speed of 2 BL/s to values of about 0 at a speed of 7 BL/s, thus front and hindleg on the right body side changed their coordination from almost exact anti-phase to in-phase activity. The mean resultant vector of the relation between R1 and R3 (Fig. 37 Ci) increased

from 0.5 at a speed of 2 BL/s to 0.9 at a speed of 7 BL/s, with two intermittent drops to lower values at 4 and approx. 6.5 BL/s. A lot of variability was found, for the phase relation between the stump of R2 and the intact ipsilateral legs R1 (Fig. 32 Cii) and R3 (Fig. 32 Ciii), especially in the speed range from 2 to 5 BL/s were the absolute phase relation values ranged between 0 and 1, but the values became less variable with increasing walking speed. Average phase relations between the R2 stump and R1 (Fig. 32 Cii) varied in the entire range from 0 to 1 for speeds between 2 and 3 BL/s and became less variable for the speed range from 3 to 7 BL/s, where they fluctuated around 0.25. The corresponding mean resultant vector length (Fig. 37 Cii) increased from around 0 at a speed of 2 BL/s to almost 1 at 5 BL/s and then decreased again to reach approx. 0.7 at a speed of 7 BL/s. Average phase relations between the intact leg R3 and the stump of R2 (Fig. 32 Ciii) varied between 0.6 and 1 in the speed range from 2 to 5 BL/s and became less variable with fluctuations around 0.7 between 5 and 7 BL/s. In this case the mean resultant vector length increased from approx. 0.3 to 0.9 (Fig. 37 Ciii) in a speed range between 2 and 7 BL/s and it showed 1 intermittent drop to 0 at a walking speed of 3 BL/s and a drop to 0.7 at 6 BL/s.

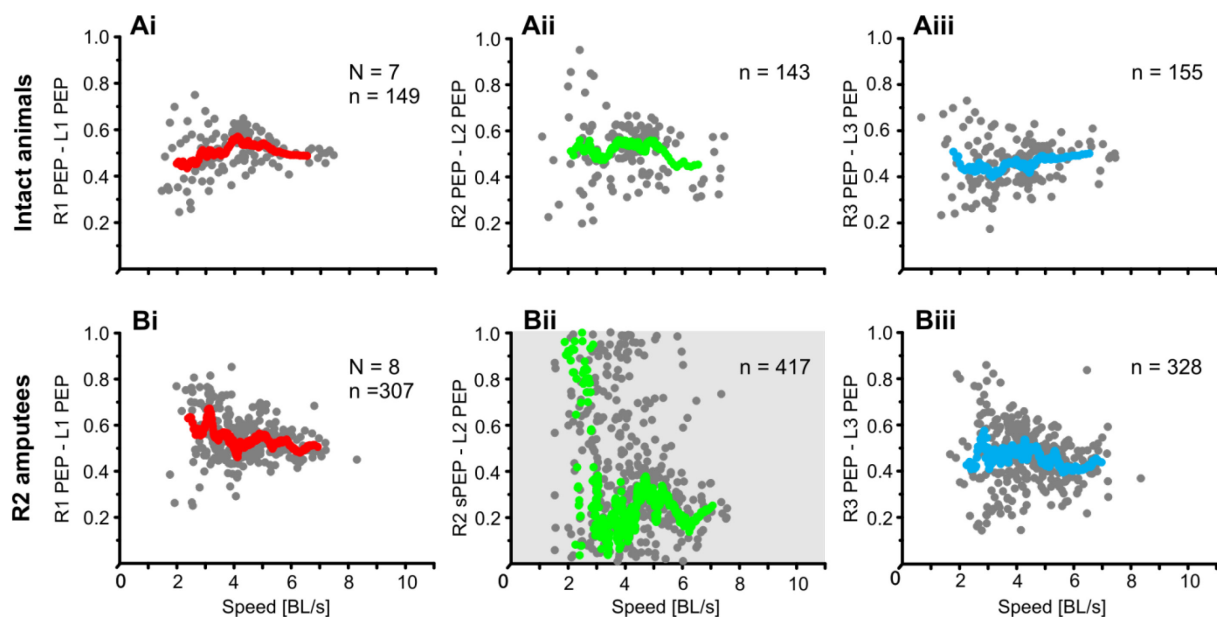


**Fig. 33:** Relative phase of a PEP event in a leg or stump on the right body side versus a reference PEP in a leg on the left body side ( $N$  = number of animals;  $n$  = number of steps). Data in panels A are derived from intact animals, the data in panels B are derived from animals with an amputation of the right middle leg. Panel Bii contains stump data and is therefore highlighted with a gray background. The y axis label depicts the dependent leg and event first and the reference leg and event last. The y axis of the plots that show the values for the front legs are scaled from -0.5 to 0.5, whereas the y axis of all other plots ranges from 0 to 1. Grey dots show the phase relation values calculated for each event plotted versus the walking speed [BL/s] of the animal during the period of the reference leg. Colored dots indicate mean values (circular means for the phase relation versus arithmetic means for the speed) calculated for a sliding window of 15 values that has been applied on the speed sorted data. The color of the dots represents the first leg in the plot titles, the dependent leg during phase relation calculation (front leg: red, middle leg: green, hind leg: blue).

To investigate the coordination in between both body sides, the phase relation between ipsi- and contralateral legs was calculated (Fig. 33). In general a decrease in variability was found for all phase relations with increasing speed. The relation between the intact legs R1 and L1 (Fig. 33 Bi) showed an

average phase relation that fluctuates between 0.7 and 0.4. For walking speeds above 5 BL/s, values of about 0.5 were found, which indicates that, during fast walking, the front legs showed almost perfect anti-phase swing activity. The length of the mean resultant vector for the phase relation between R1 and L1 increased from 0.4 at a speed of 2 BL/s to almost 1 at a speed of 7 BL/s. For R3 and L3 (Fig. 33 Biii) the phase relation showed fluctuations between 0.4 and 0.6 in the entire range of recorded walking speeds. For slow speeds the values were more variable than those found in intact animals (Fig. 33 Aiii). This was also reflected in the length of the mean resultant vector that showed values between 0.2 and 0.5 (Fig. 34 Biii) in the speed range from 2 to 4 BL/s, whereas intact animals showed increasing values from 0.5 to almost 0.8 (Fig. 34 Aiii) for the relation between R3 and L3 in the same speed range. However, the mean resultant vector length for the relation between R3 and L3 (Fig. 34 Biii) increased to almost 0.9 at a walking speed of 7 BL/s. The variability of the phase relation between the stump of R2 and the intact leg L2 (Fig. 33 Bii) showed a lot more variability when compared to R2 and L2 (Fig. 33 Aii) in intact animals, especially for walking speeds below 5 BL/s. The mean resultant vector length for the relation between the R2 stump and L2 (Fig. 34 Bii) increased from 0 at a walking speed of 2 BL/s to approx. 0.8 at a speed of 7 BL/s, with an intermittent dip to 0.4 at a speed of 6 BL/s.

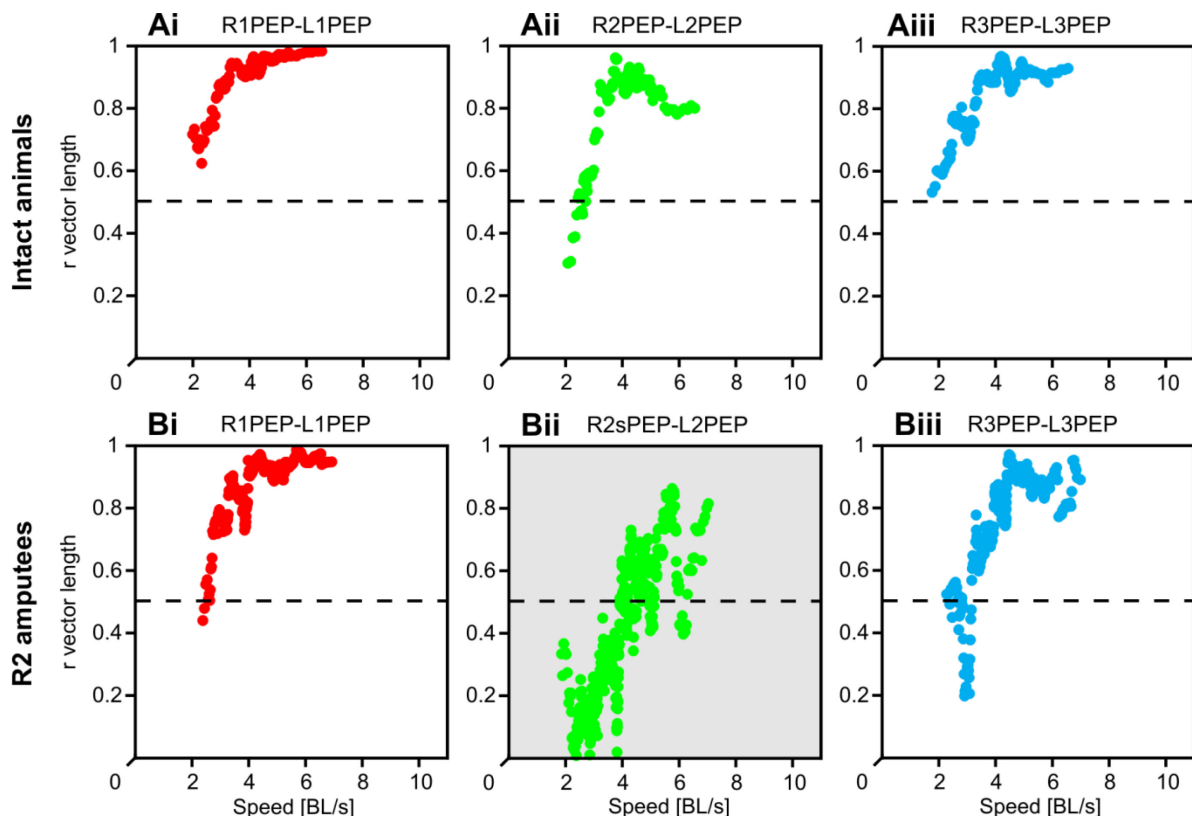


**Fig. 34:** Length of the mean resultant vector plotted versus walking speed [BL/s]. The values were calculated for a sliding window of 15 values that has been applied on the speed sorted phase relation values plotted in Fig. 33. Data in panels A are derived from intact animals, the data in panels B are derived from animals with an amputation of the right middle leg. Panel Bii contains stump data and is therefore highlighted with a gray background. The color of the dots represents the dependent leg or stump during phase relation calculation (red: R1, green: R2, blue: R3).

### R3 amputees

Data of 7 animals with an amputation of the right hind leg were obtained in 15 trials.

The average walking speed of the animals ranged from 1.7 and 6.1 BL/s, which corresponds to absolute values of 3.8 and 13.2 mm/s.

During each trial between 5 and 16 steps of R1, R2 and L1 were recorded. For L2 the number of recorded steps ranged from 5 to 15 and for L3 it ranged from 5 to 20 steps. Data for the stump could not be obtained, because its movements were partly occluded by the abdomen during the time course of the recording.

In total 162 steps were recorded for R1, 152 for R2, 162 for L1, 155 for L2 and 168 for L3.

The step period was on average 183 ms (SD = 70 ms) for R1, 196 ms (SD = 89 ms) for R2, 180 ms (SD = 66 ms) for L1, 188 ms (SD = 79 ms) for L2 and 168 ms (SD = 71 ms) for L3. Similar to findings in intact animals all intact legs of the R3 amputees showed a decreasing step period with increasing walking speed (Fig. 30). This was also reflected in the  $R^2$  values of the exponential fit applied to the data ( $R^2=0.668$  for R1 (Fig. 30Ei),  $R^2=0.599$  for R2 (Eii),  $R^2=0.712$  for L1 (Fi),  $R^2=0.668$  for L2 (Fii),  $R^2=0.456$  for L3 (Fiii)).

The phase relation between L1 and L3 ranged from -0.5 at a speed of 2 BL/s to approx. 0 at a speed of 7BL/s (Fig. 31 Di). In the speed range between 2 and 3.5 BL/s it was more variable than the relation found between L1 and L2 in intact animals. This higher variability was also reflected in the mean resultant vector length that had a value of about 0.2 at a walking speed of 2 BL/s, compared to 0.55 in intact animals. However, the mean resultant vector length increased to approx. 0.8 at a speed of 7 BL/s, with an intermittent dip to 0.1 at about 4 BL/s. The phase relation between L2 and L1 (Fig. 31 Dii) and the phase relation between L3 and L2 (Fig. 31 Diii) were very similar to each other with values ranging from approx. 0.7 at a speed of 2 BL/s to 0.55 at a speed of about 7 BL/s. This indicates anti-phase activity of L2 and L1, and L3 and L2 during fast walking, very similar to what was found in intact animals (Fig. 31 Aii and Aiii). This similarity also holds for the mean resultant vector length of the phase relation between L2 and L1 (Fig. 36 Dii) that increased from approx. 0.45 to almost 0.9 in a speed range between 2 and 7 BL/s, with an intermittent dip at a speed of 4 BL/s. For the phase relation between L3 and L2 (Fig. 36 Diii) the values were approx. 0.3 at a walking speed of about 2 BL/s and approx. 0.7 at a speed of 7 BL/s, an intermittent dip to lower values at a speed of 4 BL/s was also present. The mean phase relation between R2 and R1 (Fig. 32 Dii) ranged between 0.8 and 0.5, with a value of 0.7 at a speed of 2 BL/s and approx. 0.6 at 7 BL/s. The corresponding mean resultant vector length (Fig. 37 Dii) increased from values of approx. 0.55 to 0.85 in the speed range between 2 and 7 BL/s.

R3 amputees of 5 day old male *Canton-S* flies were also investigated in the study of Wosnitza and colleagues (2013), who studied untethered walking of the flies in a tunnel setup. In their study they show circular plots of the phase relations between each leg of the animal and L1 as a reference leg (Wosnitza et al., 2013 Fig. 8 C). The same plots were created for the dataset of the current study obtained during tethered walking of R3 amputees on the top-view setup. A comparison (Fig. 35) revealed a high degree of similarity in between both datasets. However, the circular mean values calculated for the top-view data (Fig. 35 B) were slightly increased in phase relation and they showed a broader distribution than the values published for untethered walking in a tunnel (Fig. 35 B).

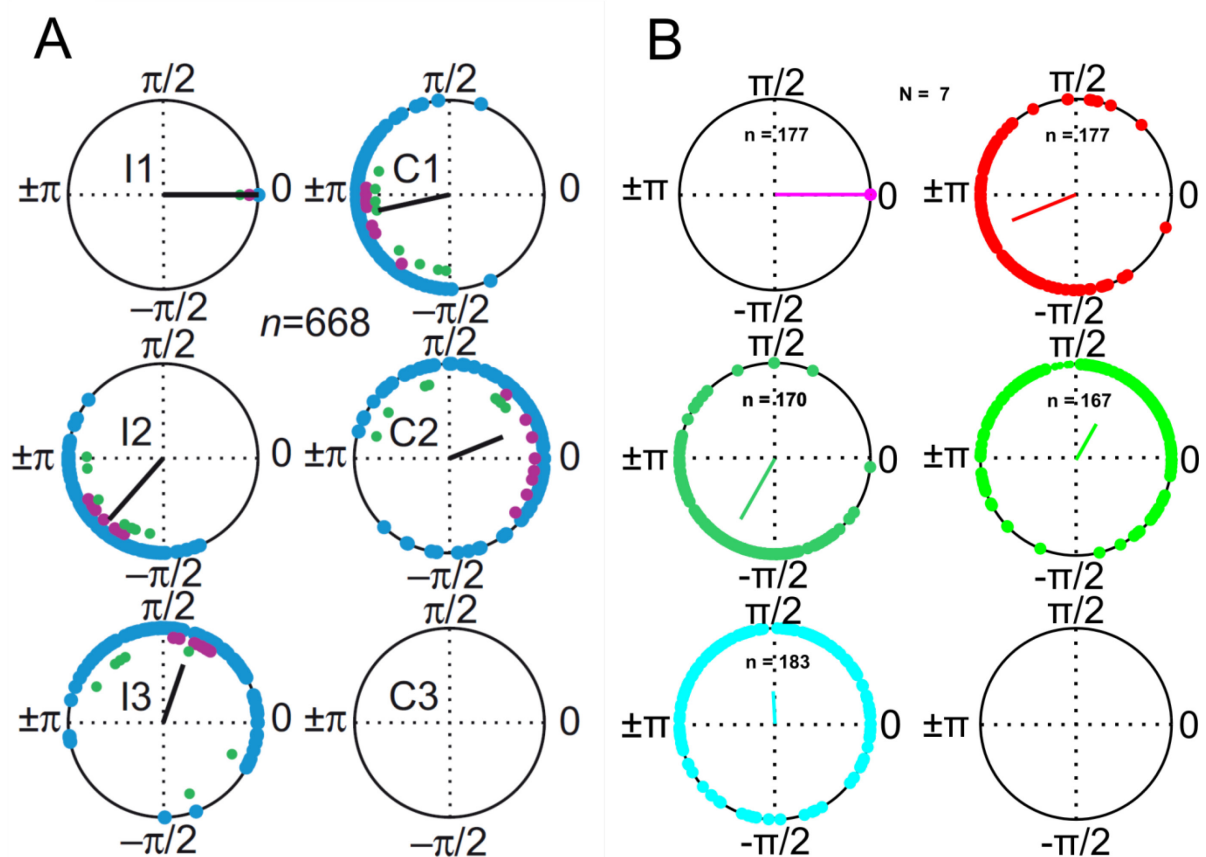


Fig. 35: Phase relations of swing onset for the five intact legs of R3 amputees ( $N$  = number of animals;  $n$  = number of steps). Swing onset (PEP) in L1 served as a reference in all plots. (A) Published data of R3 amputees walking untethered in a tunnel (Wosnitza et al., 2013 Fig. 8 C). Phase relation values are shown in circular plots with a mean resultant vector pointing to the circular mean of the data. The length of the vector is a measure for circular spread. The blue dots represent pooled values from all animals. Magenta and green dots show data that are used as an example in other panels of Fig. 8 in Wosnitza et al., 2013. (B) Data obtained during the current study for tethered walking of R3 amputees on the top-view setup. Phase relations of different legs are color coded (magenta: L1, dark green: L2, L3: cyan, red: R1, green: R2).

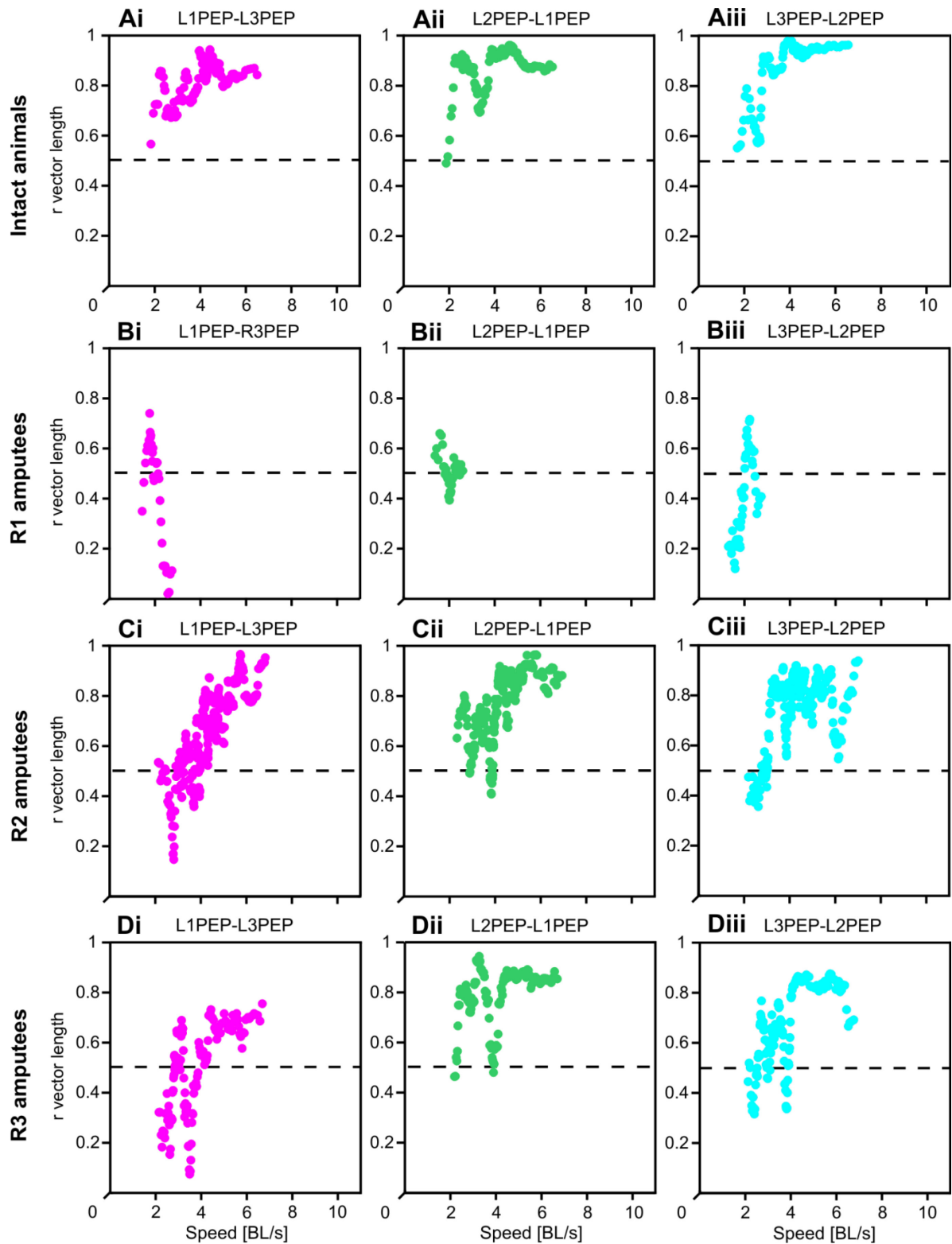


Fig. 36: Length of the mean resultant vector plotted versus walking speed [BL/s], for the legs on the left body side, contralateral to possible leg amputations on the right body side. The values were calculated for a gliding window of 15 values that has been applied on the speed sorted phase relation values plotted in Fig. 32. The color of the dots represents the dependent leg (red: right front leg or stump; green: right middle leg or stump; blue: right hind leg or stump). The first leg and event mentioned in the plot titles is always the dependent leg the second leg and event mentioned is always the reference.

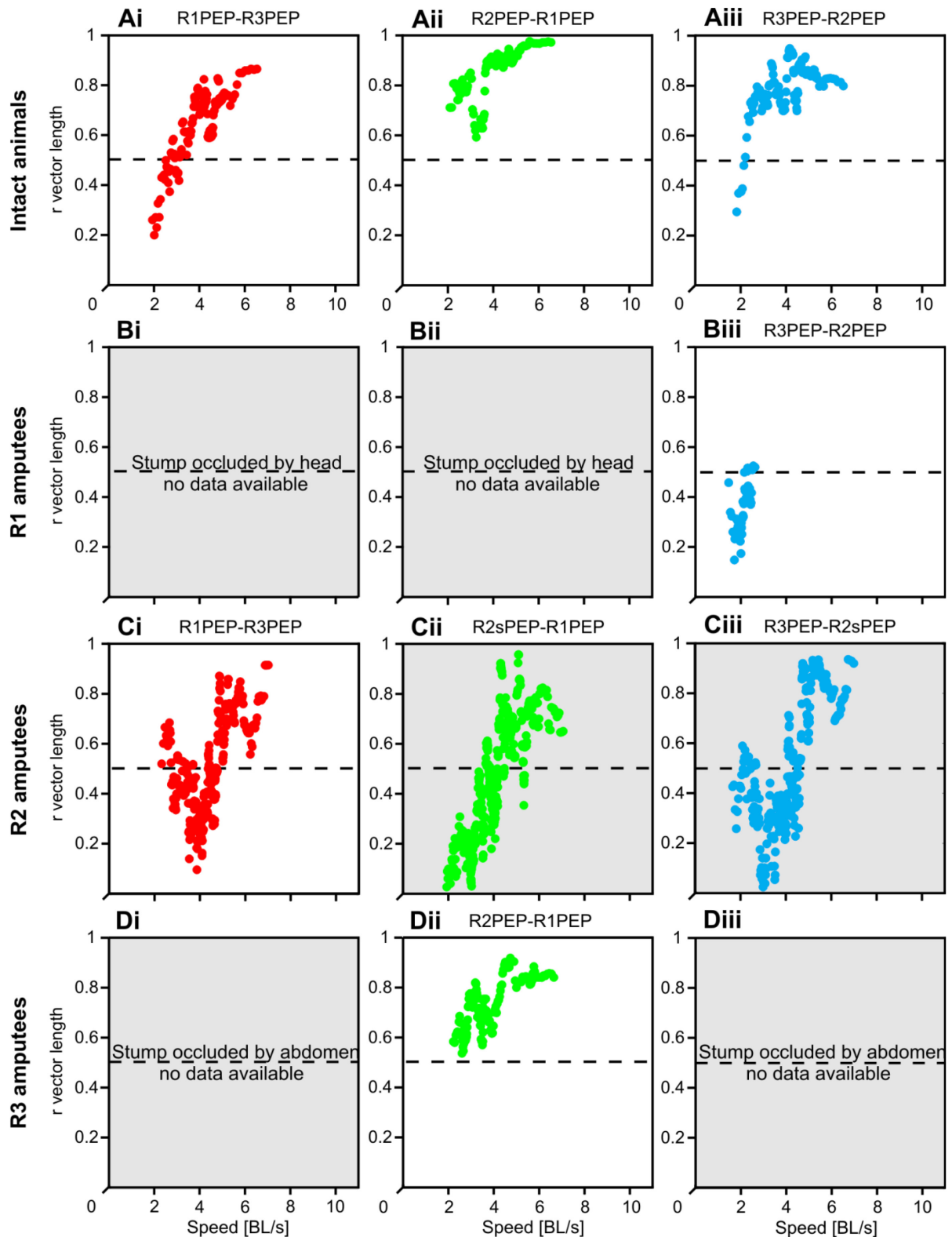


Fig. 37: Length of the mean resultant vector plotted versus walking speed [BL/s], for the legs on the right body side. The values were calculated for a gliding window of 15 values that has been applied on the speed sorted phase relation values plotted in Fig. 32. The color of the dots represents the dependent leg (red: right front leg or stump; green: right middle leg or stump; blue: right hind leg or stump). The first leg and event mentioned in the plot titles is always the dependent leg the second leg and event mentioned is always the reference. Panels that include stump data as reference or dependent values are highlighted with a grey background. There is no data available for the stump of the right front (Bi and Bii) and the right hind leg (Di and Diii) because they were occluded by either the head or the abdomen during parts of their movement.



### 3.2 Animal Speed and Activity Assay

All new data presented so far were obtained from short term videos of flies during tethered walking on top of an air-cushioned ball.

To investigate general parameters such as the range of walking speeds, the probability of walking activity and the duration of single walking bouts in both intact flies and amputees a special behavioral paradigm was developed (for detail on the methods see section 2.2). This paradigm allowed capturing the walking behavior of up to 9 flies during untethered voluntary walking in separate enclosures.

15 videos have been recorded including the walking behavior of in total 64 flies. The videos had an average length of 31.5 min (shortest trial: 30 min, longest trial: 39.6 min). For most of the experiments flies in a different amputation situation (e.g. intact animals, R1 amputees, R2 amputees or R3 amputees) were recorded simultaneously. Walking speeds below 2 mm/s were discarded from the analysis to remove tracking inaccuracies.

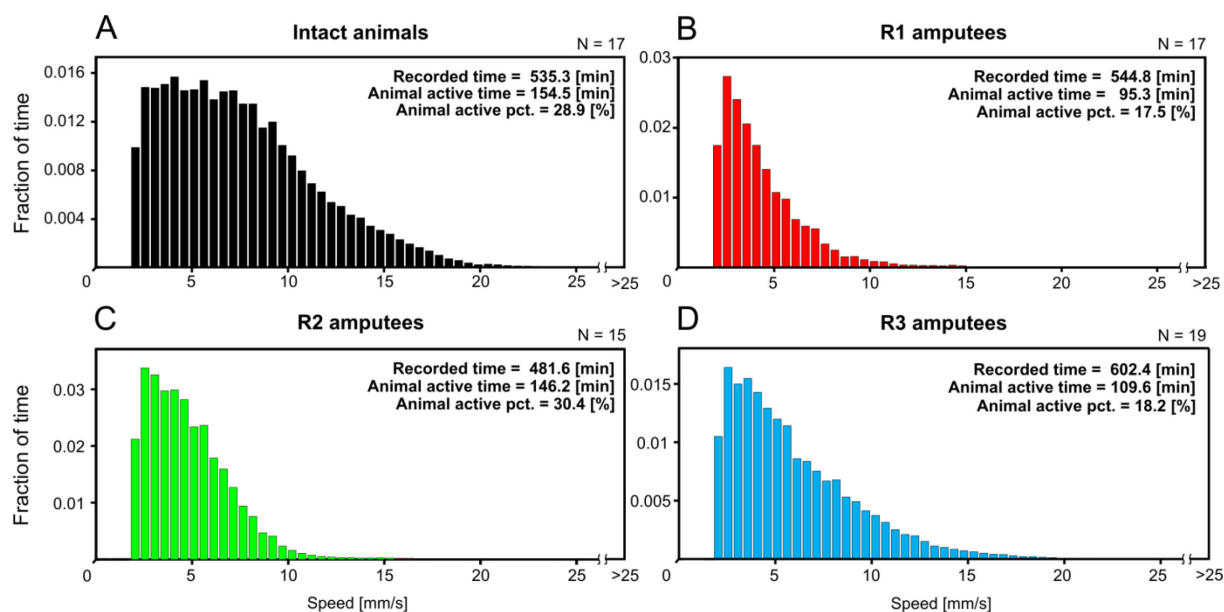


**Fig. 38:** Histograms showing the probability with which the animals walked at a certain speed ( $N$  = number of animals). The panels contain pooled data for all animals and all recorded videos in each experimental situation respectively. The histogram bins are color coded according to the experimental situation (black: intact animals (A), red: R1 amputees (B), green: R2 amputees (C), blue: R3 amputees (D)).



## Intact animals

Data from 17 intact animals were collected in 8 videos.

The behavior of every fly was recorded for at least 30 min, that results in a total recording time of 535.3 min for the 17 recorded individuals. Flies were classified to show walking activity for 28.9 % (154.5 min) of the recorded time (Fig. 38 A). They spend 6.9 % (37.2 min of the total recorded time) for walks in the center of the arena (Fig. 39 Ai) and 21.8 % (116.7 min of the total recorded time) for walks close to the rim (Fig. 39 Aii). This indicates a clear preference of the flies to walk close to the rim of the enclosures. The animals walked in bouts that had a length of less than 2 s, regardless if the data were pooled (Fig. 34 A) or separated for the area in the center of the arena (Fig. 35 Ai) and the rim (Fig. 35 Aii). Most of the walking activity was in a speed range below 10 mm/s. Walking speeds above 10 mm/s were found with a decreasing probability. The frequency with which certain walking speeds occurred differed between the area close to the rim of the arena and the center. At the center of the arena (Fig. 39 Ai) the animals showed a preference for higher walking speeds (the probability for walking speeds up to 15 mm/s is almost constant), whereas the flies walked preferentially slower (Fig. 39 Aii) at the rim (the probability of walking speeds above 10 mm/s decreased drastically). The accumulated activity of all animals showed fluctuations for the first 30 min of the recorded videos (Fig. 42 A), but there was no evidence for the majority of animals to be active only at a preferred time period throughout the recording (e.g. only exploratory behavior in the first minutes followed by complete inactivity). Additionally, there was no point in time where the majority of animals was exclusively active in the center (Fig. 43 Bi) or at the rim of the arena (Fig. 43 Bii).

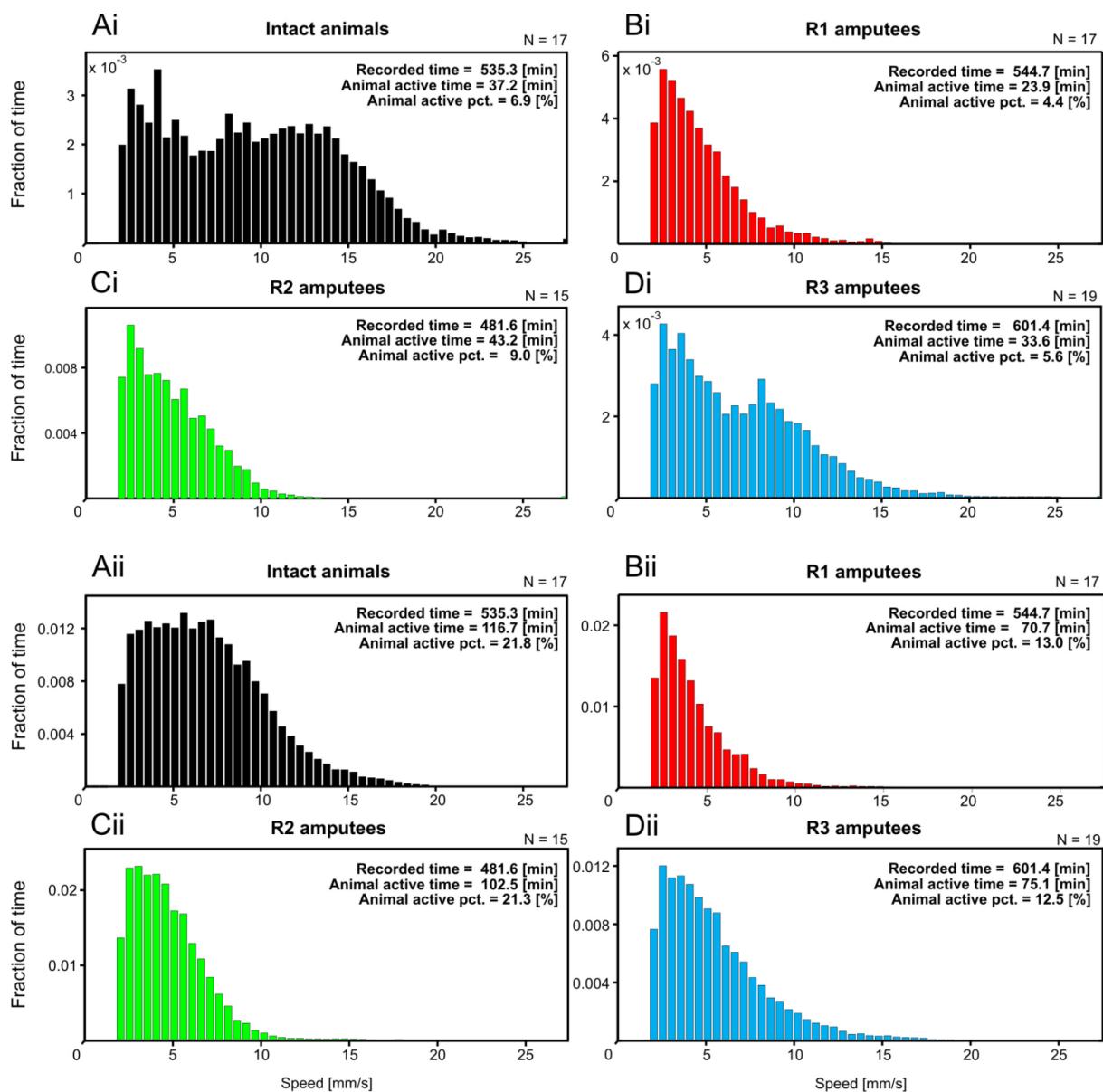


**Fig. 39: Histograms showing the probability with which the animals walked at a certain speed (N = number of animals). In contrast to (Fig. 38) this figure shows the data separated for the center of the arena (panels i) and the rim area (panels ii). The panels contain pooled data for all animals and all recorded videos in each experimental situation, respectively. The histogram bins are color coded according to the experimental situation (black: intact animals (panels A), red: R1 amputees (panels B), green: R2 amputees (panels C), blue: R3 amputees (panels D)).**

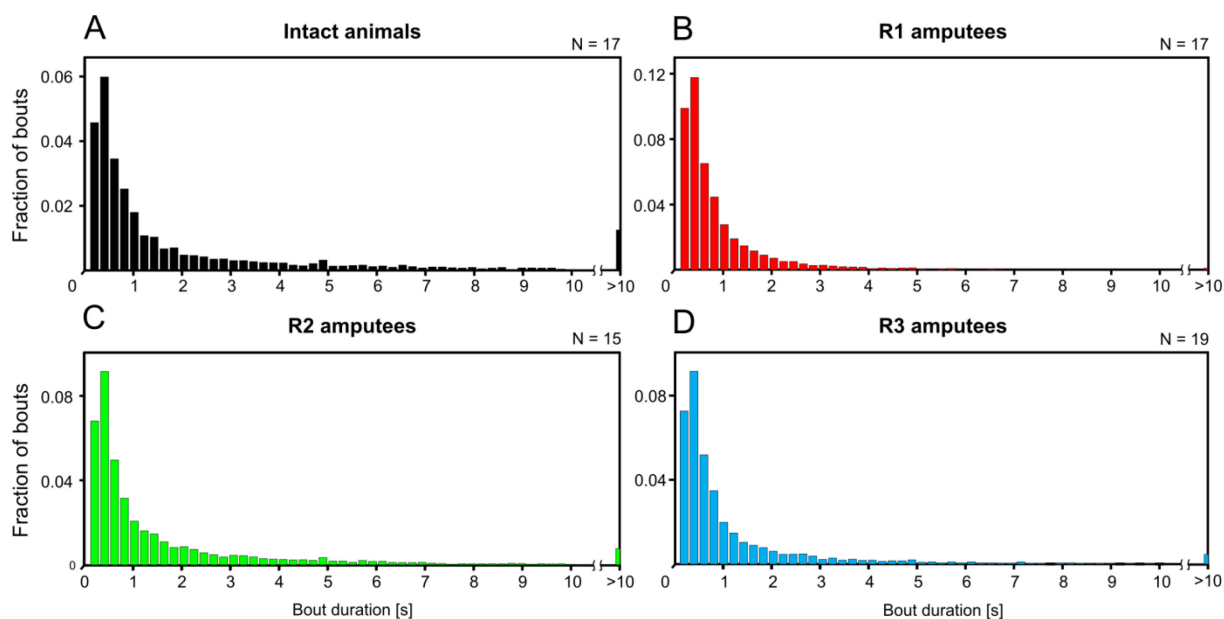


**Fig. 40: Bouts of walking activity [specified as fraction of bouts =  $n$  bouts/total  $n$  bouts] that showed a certain length (specified in s). The panels contain pooled data for all animals and all recorded videos in each experimental situation respectively. Histogram bins are color coded according to the experimental situation (black: intact animals (A), red: R1 amputees (B), green: R2 amputees (C), blue: R3 amputees (D)). The last histogram bin  $> 10$  includes all bouts that lasted longer than 10 s.**

### R1 amputees

Data from 17 flies were collected in 9 videos with a total recording time of 544.7 min. The flies were classified to show walking activity for 17.5 % (95.3 min) of the recorded time (Fig. 38 B). They spend 4.4 % (23.9 min of the total recorded time) for walks in the center of the arena (Fig. 39 Bi) and 13.0 % (70.7 min of the total recorded time) for walks close to the rim (Fig. 39 Bii). Similar to intact animals the R1 amputees showed a clear preference to walk close to the rim of the enclosures (Fig. 39 Bi and Bii). However, the probability distribution of recorded walking speeds was quite different from what was found in intact animals, as most of the recorded speeds were below 5 mm/s (Fig. 38). Walking speeds between 5 mm/s and 15 mm/s were found with a rapidly decreasing probability. At the center of the arena the preference for walking speeds above 5 BL/s was slightly higher (Fig. 39 Bi), whereas the flies walked preferentially slower at the rim (Fig. 39 Bii). Compared to intact animals this difference was rather small. Consistent to intact animals the majority of walking bouts in R1 amputees was shorter than 2 s, this holds for all values (Fig. 40 B) and values separated for the center (Fig. 41 Bi) and at the rim of the arena (Fig. 41 Bii). The accumulated walking activity of all animals showed a lot of variability throughout the first 30 min of all recorded videos (Fig. 42 B) but as in intact animals the activity of the animals was not restricted to a certain timepoint of the recording. This also holds if the data for the center of the arena (Fig. 43 Bi) and the rim area (Fig. 43 Bii) were separated.

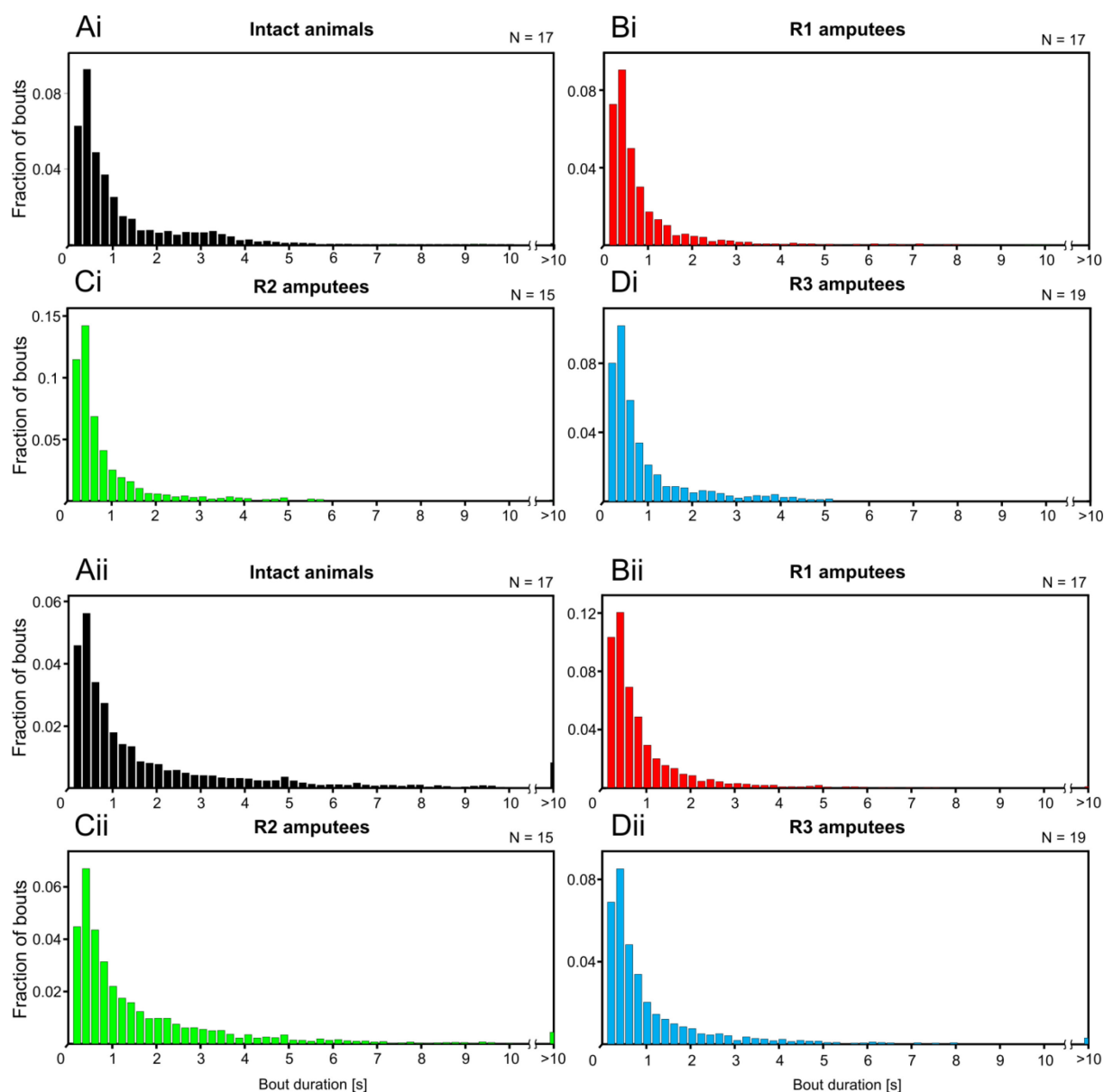


**Fig. 41:** Bouts of walking activity (specified as fraction of bouts =  $n$  bouts/total  $n$  bouts) that showed a certain duration (specified in s). In contrast to (Fig. 40) this figure shows the data separated for the center of the arena (panels i) and the rim area (panels ii). The panels contain pooled data for all animals and all recorded videos in each experimental situation respectively. Histogram bins are color coded according to the experimental situation (black: intact animals (A), red: R1 amputees (B), green: R2 amputees (C), blue: R3 amputees (D)). The last histogram bin  $> 10$  includes all bouts that lasted longer than 10 s.

## R2 amputees

Data from 15 animals were collected in 10 videos.

The total recording time for all individuals was 481.6 min, for 30.4 % (146.2 min) of this time the flies showed an activity that was classified as walking (Fig. 38 C). They spend 9.0 % (43.2 min of the total recorded time) for walks in the center of the arena (Fig. 39 Ci) and 21.3 % (102.5 min of the total recorded time) for walks close to the rim (Fig. 39 Cii). With this values R2 amputees showed the highest level of walking activity of either amputees and intact animals (intact animals were only active

in 28.9 % of the recorded time). Consistent to what was found in intact animals the R2 amputees showed a higher preference to walk close to the rim of the enclosure. The walking activity occurred in bouts that were mostly shorter than 2s, this was true for pooled data (Fig. 34 C) and data separated between the center (Fig. 35 Ci) and the rim of the arena (Fig. 35 Cii).

However, the speed range (Fig. 38 C) was much reduced compared to intact animals (Fig. 38 A) and R3 amputees (Fig. 38 D). Most of the recorded speeds were in a range up to approximately 7 mm/s, the probability for speeds above 7 mm/s showed a rapid decrease (Fig. 38 C). This decrease was less distinct for walks in the center of the arena (Fig. 39 Ci) compared to the rim area (Fig. 39 Cii). A preference for higher walking speeds in the center of the arena was also found in intact animals and all other amputees tested. The number of animals that showed walking activity was slightly increased during the second half of the first 30 min of all recorded videos (Fig. 42 C). A separation between the walking activity recorded for the center of the arena and the rim area revealed that the activity in the center was evenly distributed throughout time (Fig. 43 Ci) but the R2 amputees preferentially walked close to the rim of the enclosures in the second half of the recorded videos (Fig. 43 Cii).

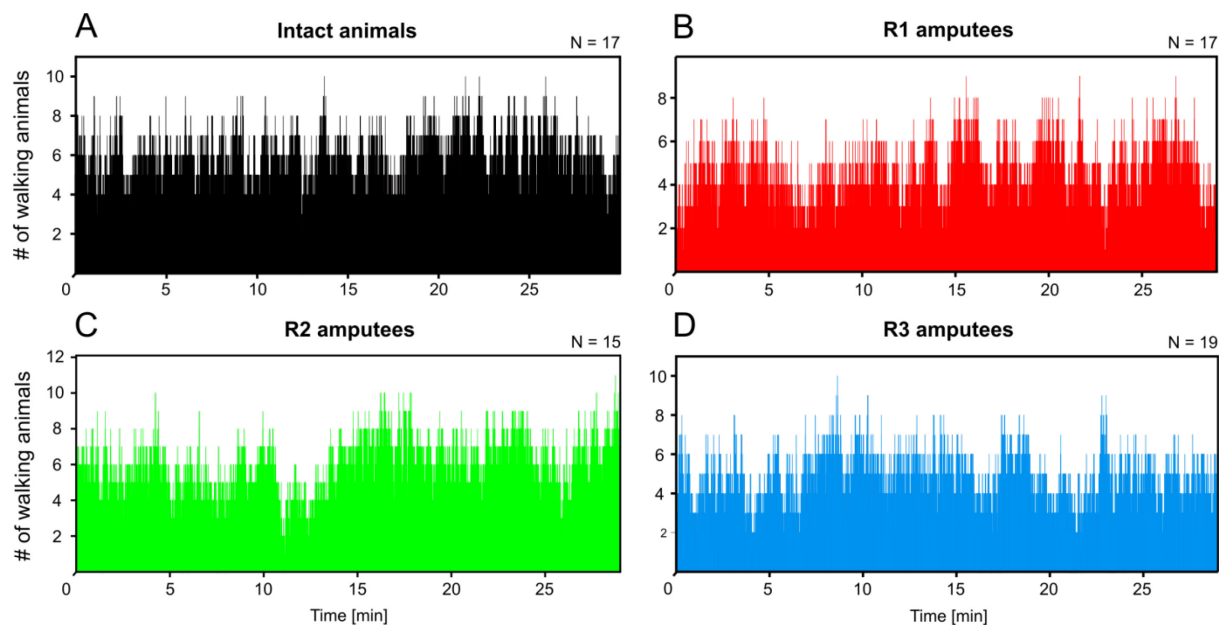


**Fig. 42: Number of walking animals counted for every video frame. The histograms show pooled data for the first 30 minutes of all recorded videos. If an animal showed walking activity during a video frame in any of its recorded trials the activity was counted as 1. If all animals would show walking activity in at least 1 frame of a video the histogram bin of that frame would have a value that equals the number of animals, if no animal would be active at that time point the value would be 0. The data is color coded according to the experimental situation (black: intact animals (A), red: R1 amputees (B), green: R2 amputees (C), blue: R3 amputees (D)).**

### R3 amputees

Data from 19 animals were collected in 13 videos.

The total recording time for all individuals was 602.4 min, for 18.2 % (109.6 min) of this time the flies showed an activity that was classified as walking (Fig. 38 D). They spend 5.6 % (33.6 min of the total recorded time) for walks in the center of the arena (Fig. 39 Di) and 12.5 % (75.1 min of the total recorded time) for walks close to the rim (Fig. 39 Dii). With this values the activity level of R3 amputees was comparable to R1 amputees (17.5 %), but lower than in intact animals (28.9 %) and R2 amputees (30.4 %). A preference for walks close to the rim of the enclosure was also found for intact animals and all other tested amputees. R3 amputees showed the largest range of recorded walking speeds of all amputees (Fig. 38 D) with values ranging up to 20 mm/s. However, most of the recorded speeds were in a range below 7 mm/s and the values between 7 and 20 mm/s were found with a decreasing probability. In agreement to findings in intact animals and R1 and R2 amputees, the highest speeds were recorded in the center of the arena (Fig. 39 Di), whereas the animals showed a preference for slower walks close to the rim (Fig. 39 Dii). The majority of the recorded walking bouts had a duration below 2 s, this was true for pooled data (Fig. 40 D) as well as data separated for the area in the center of the arena (Fig. 41 Di) and at the rim of the enclosure (Fig. 41 Dii). These results were consistent to the findings for intact animals (Fig. 40 A) and the other amputees (Fig. 40 A, B and C). The accumulated activity of all animals showed a uniform distribution throughout the the first 30 min of all recorded videos (Fig. 42 D) with no preferred time spent walking at the center (Fig. 43 Di) or the rim area of the arena (Fig. 43 Dii).

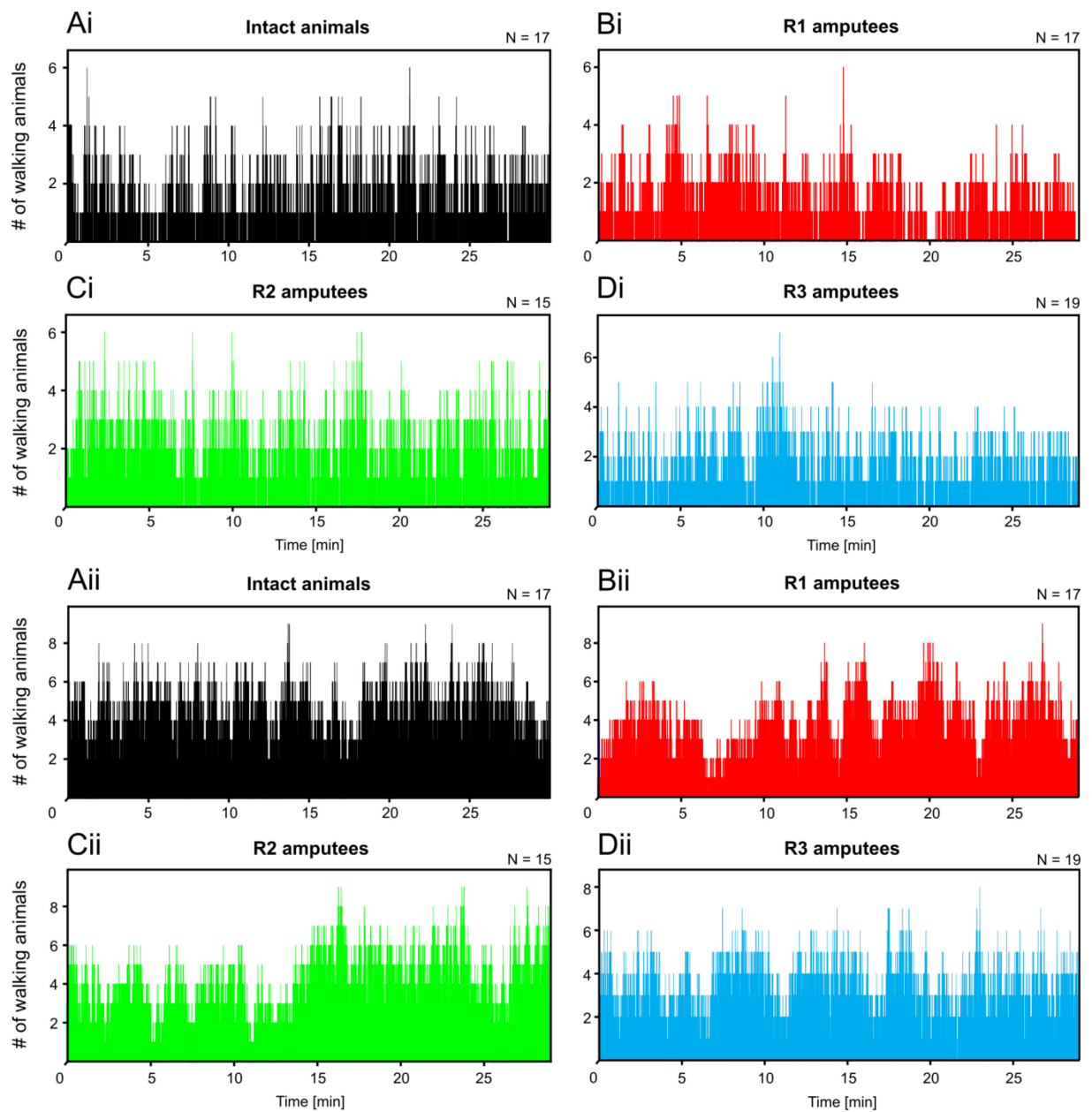


**Fig. 43: Number of walking animals counted for each video frame. The histograms show pooled data for the first 30 minutes of all recorded videos. In contrast to (Fig. 39) this figure shows the data separated for the center of the arena (panels i) and the rim area (panels ii). If an animal showed walking activity during a video frame in any of its recorded trials the activity was counted as 1. If all animals would show walking activity in at least 1 frame of a video the histogram bin of that frame would show a value that equals the number of animals, if no animal would be active at that time point the value would be 0. The data is color coded according to the experimental situation (black: intact animals (A), red: R1 amputees (B), green: R2 amputees (C), blue: R3 amputees (D)).**

## 4. Discussion

Parts of this section are included in a paper draft with the working title: "**Speed-dependent interplay between local, pattern generating activity and sensory feedback during walking in *Drosophila***" that has recently been submitted for publication in Journal of Experimental Biology.

For the current work several aspects of walking behavior have been investigated in intact and single leg amputated *Drosophilae*. In the first section the motor activity of leg stumps was studied during tethered walking on top of an air-cushioned ball. Special focus was drawn here on the temporal and kinematic characteristics of the stump and its coordination with respect to the remaining intact legs of the animal.

It was observed that single leg amputees still showed coordinated walking activity with their remaining intact legs, while they were tethered atop the ball. Compared to intact animals the walking speed range in amputees was somewhat reduced (Fig. 17). The stumps of front, middle and hind leg amputees showed rhythmic oscillations while the intact legs were walking. These oscillatory movements consisted of a pro- and retraction as well as a levation and depression component (Fig. 16).

The frequency of stump oscillations was often much higher than the stepping frequency in intact legs (Fig. 19, Fig. 28, Fig. 18 and Fig. 26). Additionally, it was on average constant over the whole range of recorded walking speeds, with periods that ranged around 100 ms (approx. 10 Hz). This contrasted with the behavior of intact legs in both amputees and intact flies. In intact legs there was a clear correlation between walking speed and stepping period (Fig. 19 and Fig. 30). This relation has been observed in previous studies on several insect species (cockroaches and beetles: Hughes, 1952; stick insect: Wendler, 1964; *Drosophila*: Mendes et al., 2013; Wosnitza et al., 2013) and can be regarded as a relatively strict invariant its therefore noteworthy if this relation is absent. As the stump oscillated with such a high and almost constant frequency its movements were largely independent of the intact legs during slow walking, which made a cycle-to-cycle coupling between stumps and intact legs impossible. Nevertheless there was a preferred temporal delay between PEP events in intact legs and subsequent DEP and VEP in the stump (Fig. 23 and Fig. 24).

During fast walking the stepping frequency in intact legs (Fig. 17 and Fig. 28) became similar to frequency of stump oscillations, thus that the occurrence of multiple stump oscillations during single steps of the intact legs ceased (Fig. 18 and Fig. 26). This leads to a decrease in the variability of phase relations between intact legs and the stump (Fig. 21, Fig. 32 and Fig. 33), which could also be quantified by an increase of the corresponding mean resultant vector length (Fig. 22, Fig. 37 and Fig. 34). The transitional speed range in which this happens was very narrow namely between 5 and 6



BL/s. At this walking speed the stepping frequency of the intact legs becomes similar to the frequency of the stump (approx. 10 Hz).

To investigate the role of sensory influences from the intact legs on the movements of the stumps, experiments with R2 amputees of the *nan[36a]* mutant were conducted. All chordotonal organs of these mutants are defective due to a P-element insertion in the *nanchung* gene that codes for a mechanosensory transducer channel (Kim et al., 2003). Chordotonal organs are used in insect legs to monitor the position, and relative motion, of individual leg segments (for review see Field and Matheson, 1998; Kavlie and Albert, 2013). R2 amputees of the *nan[36a]* mutant showed coordinated walking activity on the ball (Fig. 19 Di and Diii) and the stump oscillated with approx. 10 Hz (Fig. 19 Dii) despite the lack of sensory information from chordotonal organs. In contrast to *CS* wildtype flies an increase in walking speed of the *nan[36a]* mutants did not lead to a decrease in the variability of phase relations between intact legs and the R2 stump. This is also reflected in the corresponding mean resultant vector length, which remained on a low level for the whole range of recorded walking speeds (Fig. 22 D). However, a preferred temporal delay between PEP events in intact legs and subsequent DEP and VEP in the stump (Fig. 23 and Fig. 24) was still found, but it was more variable in chordotonal organ defective *nan[36a]* mutants.

#### 4.1 Rhythmic Motor Activity of Leg Stumps in Walking *Drosophila*

For the amputation experiments in the current study the legs were removed at the mid-femur, additionally the animal was tethered so that the remaining stump could not touch the ground during any phase of its movement. The amputation leads to a removal of all sensory structures distal to the lesion. Those structures therefore cannot provide sensory feedback to the nervous system. On the other hand sensory structures on the remaining leg stump, such as campaniform sensilla (Zill et al., 2009; Zill et al., 2011), hair plates (Dean and Schmitz, 1992; Schmitz, 1986b), chordotonal organs (Bässler, 1965; Bässler, 1977; Büschges, 1994; Füller A., 1973) and multipolar stretch receptors (Schmitz and Schöwerling, 1992) are still present and probably functional in this situation. This interpretation is supported by the observation that the leg stumps can be used in an effective and coordinated manner if the stump makes contact with a substrate (Noah et al., 2004). Due to the missing ground contact of the stump at least the campaniform sensilla are not likely to signal anything as in cockroaches and stick insects they were shown to be only activated when the leg is loaded or when movements are resisted (Zill, 2010; 2011; 2013). This means that most of the intra-leg sensory signals, which are known to dominate motor output during walking, such as the angular information provided by the femoral chordotonal organ and load information provided by the campaniform sensilla (for rev see Büschges, 2005; Büschges and Gruhn, 2007), are not present in the leg affected by the amputation.

---

Given all these limitations in sensory feedback available for the neural network controlling the leg stump, the question arises why the stump still showed oscillatory movements during the experiments.

One possible explanation might be that rhythmic inter-segmental influences of sensory information generated by the intact legs of the animal might give rise to the stump oscillations. Another possibility is that the stump oscillations are driven by local pattern generating networks, which are situated in the associated hemi-ganglion. These networks could probably use the sensory information on movement and position of the coxo-trochanteral and thoraco-coxal joints that is provided by the hair plates, chordotonal organs and multipolar stretch receptors that are still present on the stump. Movements of the stump toward levation of the coxa-trochanter joint would be detected by the trochanteral hair plate. In the cockroach (Pearson et al., 1976) and stick insect, for example, the hair plate is known to mono-synaptically excite motor neurons to the depressor muscle (Schmitz, 1986a). In walking, this connection is thought to contribute to the onset of depressor activity at the start of the stance phase (Wong and Pearson, 1976). In the stump, movement of the leg toward extreme levation could generate depressor firing that would produce rapid and unimpeded movement toward the extreme of joint depression. This movement could be detected by internal receptors monitoring leg position and movement, such as the levator stretch receptor and coxal chordotonal organ (Bräunig et al., 1981; Schmitz and Schöwerling, 1992). These receptors have been shown to activate levator motor neurons and could contribute to the termination of the stance phase and onset of swing. Thus, the receptors remaining in the stump could generate sequential activation of motor neurons to produce rapid alternating movements of the leg. This hypothesis is supported by the finding that the rate of movement of the stump remains constant over a range of walking speeds (Fig. 19 Bi, Cii, Eiii and Fig. 30 Cii).

In other insects the existence of local, i.e. segmental, central pattern generating networks responsible for rhythmic motor activity of the legs is well established, e.g. in the hawk moth (Johnston and Levine, 1996b), locust (Ryckebusch and Laurent, 1993), and stick insect (Büschges et al., 1995). For the stick insect it has been shown that there are independent pattern generating networks for each leg joint (Büschges et al., 1995). These findings, however, are based on much reduced preparations. Due to the presence of remaining proximal sensory structure, it is likely that the stump oscillations observed here result from activities in the CPG in concert with sensory signals from the leg segments that remain intact after the partial amputation. This notion is also supported by previous studies using electromyography recordings in single leg amputated cockroaches (Delcomyn, 1988).

## 4.2 Descending Control of Walking Speed in *Drosophila*

If the oscillations of the of the stump largely reflect a rhythmicity that is provided by local, pattern-generating networks one could hypothesize that a putative central descending drive activates and controls walking in *Drosophila* in at least two different ways.

At first, there is a qualitative influence that only induces activity of local CPGs or CPG-like networks in the thorax. It thereby acts as a switch, which activates and deactivates local pattern generating networks, but does not modulate their activity. This would mean that descending influences, which originate most likely from the gnathal (former: sub-esophageal) ganglion or the brain, activate networks in the ventral nerve cord (VNC), which in turn drive the leg muscles in a rhythmic fashion with an inherent frequency. This frequency seems to be in the order of 10 Hz. Previous studies in stick insects support this idea as they suggest the existence of a central control mechanism that influences the global state of the animal by inducing qualitative changes not only in local CPGs (Büschges et al., 2004) but also in how sensory information is processed (Bässler, 1986; Bässler, 1988; for review see Büschges and Bässler, 1998). This is further substantiated by anecdotal observations during the current study, where several instances of stump oscillations were found shortly before or after a walking sequence in the intact legs was recorded. In these cases the animal seemed active and the stump oscillated with a similar frequency although no stepping was observed in the intact legs (Fig. 20).

As indicated by literature findings (e.g Mendes et al., 2013; Wosnitza et al., 2013) and the behavior of the intact legs in the current study (Fig. 17 A-C, Fig. 19 and Fig. 28) walking speed is mainly controlled by changes in stepping frequency. This suggests a second, quantitative influence of the descending signal able to modulate the stepping frequency. However, during the current work oscillation periods of front, middle and hind leg stumps were found to be largely independent of walking speed (Fig. 17 and Fig. 28). If an increase in walking speed is associated with an increase in movement frequency of the intact legs, but not with those of the stump the question arises how the nervous system of the animal changes walking speed. A putative central command that might change the walking speed of the animal does not seem to have a direct influence on the oscillatory networks, which drive the stump movements. In contrast to the first influence of the central drive, which might act as a switch and directly targets rhythm generating networks, the second influence might have a more indirect effect in the VNC. Hypothetically, it might act via gain modulation of sensory feedback; especially those associated with the stance phase, because only during stance phase a legs movement speed can influence the walking speed of an animal. A likely target for such a stance phase-specific influence would be sensory information provided by load sensors, i.e. campaniform sensilla. In the intact insect leg campaniform sensilla are active at the transition from swing to stance phase and during the stance phase (Zill et al., 2009) signaling touch-down and reliable ground contact. In leg

stumps these load-related signals are probably completely absent, because the distal campaniform sensilla were removed during amputation and the proximal campaniform sensilla that remain on the stump were never stimulated due to absence of ground contact. This notion is supported by a previous study in the stick insect where changes in the synaptic drive to stance phase motor neurons only become effective and correlated to walking speed well after the beginning of the stance phase (Gabriel and Büschges, 2007).

### 4.3 Speed-dependence of coordination strength

The results of this thesis point towards a speed dependent increase of coordination between intact legs and leg stumps.

If the coupling strength between different legs of the animal is only loose the frequency of the oscillatory systems that are investigated here is of particular importance. During slow walking the frequency difference between an intact leg and the stump is large. Weakly coupled oscillators with very different frequencies cannot entrain each other in a 1:1 ratio (Kuramoto, 1984; Pikovsky et al., 2003). This might be the reason why there is no clear coordination between the stump and either intact leg (see Fig. 16 C and Fig. 26 B). However, if the animal accelerates the stepping frequency of the intact legs increases and at a certain point it gets similar to the oscillation frequency of the stump. At this point the frequencies of the stump and intact legs are sufficiently similar to allow for cycle-to-cycle synchrony and a 1:1 entrainment occurs (see Fig. 16 D and Fig. 18 D).

Several findings support this idea. First, the increase in coordination is relatively sudden. There is a small range of walking speeds in which the coordination strength between a stump and the ipsilateral intact legs tends to rise quickly (Fig. 21 Fig. 21 and Fig. 37). This was found in all leg stumps and, to a certain extent, also in intact animals. In addition, this increase occurred at a walking speed at which the stepping frequency in intact legs becomes similar to the natural stump frequency of approximately 10 Hz. Finally, during slow walking, the cycle-to-cycle coupling between stumps and intact legs is lost and, consequently, there is no preferred phase relation (Fig. 22 and Fig. 32). However, there was a preferred absolute time interval between PEPs in intact legs and the subsequent onset of depression (DEP) or levation (VEP) in the stump even in slowly walking animals (Fig. 23 and Fig. 24). This means that there is an information transfer between sensory events in intact legs and the behavior of the stump. These findings are consistent with the idea that the legs are weakly coupled oscillators that entrain in a 1:1 ratio only if their frequencies are very similar.

The high natural frequency of stump oscillations might be explained as an adaptation to the requirements of fast walking. To prevent instability, a leg can only execute its swing phase during the

stance phases of its neighboring legs. This concept is captured in the *Cruse rules* (for review see Cruse, 1990; Dürr et al., 2004). In addition, stance phases, but not swing phases, become shorter with increasing walking speed, as shown for *Drosophila* (Wosnitza et al., 2013) as well as several other walking insects (locust and grasshopper: Burns, 1973; cockroach: Delcomyn, 1971; stick insect: Wendler, 1964). As a consequence the timing of swing phase execution is particularly important during fast walking, as the time in which a swing phase can be executed, i.e. during the stance phase of neighboring legs, is short and therefore the margin of error is small. Hence, neural signals mediating coordination have to be more effective during fast walking, thereby increasing strictness in coordination. A natural oscillatory frequency of a segmental pattern generating network that is similar to the stepping frequency at high walking speeds will facilitate such strictness. Facilitation of precise timing via the natural frequency of the rhythm generating networks might occur in all insects, even in species that infrequently walk at high-speed. Based on this it might be informative to examine this issue in walking insects that, due to ecological constraints, often have to walk fast, e.g. the desert ant (Wahl et al., 2015; Zollikofer, 1994) or the cockroach (Full and Tu, 1990; 1991).

#### 4.4 Differences between the ball setups

For this thesis the kinematics and timing of walking behavior in intact animals and single leg amputees was studied on two different setups.

The side-view setup (Fig. 6) provided a rostral view on the walking behavior of the tethered flies and allowed a precise manual analysis of the pro- and retraction as well as the levation and depression component of the intact leg and stump movement (Fig. 16). Since the amplitude of pro- and retraction was comparatively small only the levation/depression component (Fig. 18) was analyzed during the experiments on the side-view setup where both movements were visible. For the temporal analysis of leg movements the dorsal extreme position (DEP) was chosen as a reference event. This choice was made for technical reasons as most of the single leg stumps showed a movement trajectory (Fig. 16) with a sharp DEP at the superior end, which made it easier and more reliable to detect this extreme value in the manually tracked trajectories. During walking in intact legs the swing phase was shorter than the stance phase and on average constant for the whole range of recorded walking speeds (Fig. 25). The depression period of the stump was on average slightly shorter than the levation period. Nevertheless, the ratio of depression period and stump oscillation period (Fig. 25 Bi, Cii, Dii and Eiii) showed broadly distributed values with no clear preference for either the levation or the depression to dominate the oscillation cycle of the stump.

The top-view setup (Fig. 7) allowed analyzing the behavior of all six legs of an intact animal or all five intact legs of an amputee, but, because of the camera view from above (Fig. 7), only the pro- and retraction component of leg or stump movements was visible. Furthermore, due to their kinematics, the stumps of front and hind legs were occluded by either the head or the abdomen of the animal during parts of their movement trajectory, which made it impossible to extract reliable data for these stumps (Fig. 27). The only stump movements studied in the top-view setup were those of the middle leg stump. The pro- and retraction movements of this stump were tracked manually and the last video frame before the onset of protraction was termed sPEP event. This was arbitrarily chosen as a reference event for the temporal analysis.

A technical necessity of the ball setups was that the flies had to be tethered during walking to maintain a stable position atop the ball. As a consequence the flies do not have to carry their own body weight. On the one hand this is an advantage for the current study because flies with leg amputations cannot suffer from stability issues during walking, which allows the leg stumps to move freely without contacting the ground. On the other hand there is no need for the tethered animal to change the stepping pattern of the remaining intact legs in order to maintain stability during walking. Such possible adaptations that a free walking animal might show in response to the amputation can probably not be studied on the ball setups.

For the temporal analysis of the stump movements DEP (side-view setup) or sPEP (top-view setup) events in the stump have been substituted for PEP events in intact legs. However, this does not mean that a DEP or a sPEP event in the stump necessarily corresponds to a PEP event in the intact legs. In fact it is unknown which position on the stumps' movement trajectory corresponds to a PEP in intact legs.

#### **4.5 Differences between free and tethered walking**

Walking speeds between 5 and 16 BL/s (see Fig. 17 D) were published for intact *CS* flies during untethered walking in a tunnel setup (Wosnitza et al., 2013), whereas during the current study only walking speeds between 1.4 and 9.8 BL/s were found for intact animals during tethered walking on a ball (Fig. 17 A-C).

This could have several different reasons. The simplest explanation might be that the temperature to which the flies were exposed on the ball setup was lower than the temperature in the tunnel setup used by Wosnitza and colleagues (2013). Such a temperature difference seems likely as the tunnel setup forms an enclosure around the fly, whereas the ball setup is open to the laboratory environment. Additionally, the air cushion of the ball uses a constant flow of air and thereby provides additional

cooling. Temperature was not constantly controlled or monitored during the experiments of the current study, the same holds for several literature studies (Mendes et al., 2013; Mendes et al., 2014; Strauss and Heisenberg, 1990; Wosnitza et al., 2013). As flies are poikilothermic animals a lower temperature during the experiments of the current study would explain the lower walking speed range (Gilchrist et al., 1997). Another explanation might be the different visual environment of the flies during the experiments. The ball setup was open to the laboratory environment and no special visual cues were presented to the fly. In the tunnel setup both ends of the walking tunnel might have been an optical stimulus for the flies inducing walking behavior, similar to the optical cues used in the Buridans paradigm (Bülthoff et al., 1982). During the current study the flies were slightly touched at the abdomen or air puffs were applied to induce walking. During the tunnel experiments walking behavior was often induced using the natural negative gravitaxis behavior (e.g. Armstrong et al., 2006) of the flies. This was achieved by holding the tunnel in a vertical orientation before it was placed in the horizontal holder for video capture (Dr. Till Bockemühl, personal communication). If the flies started walking when the tunnel was held upright they often continued walking in the horizontal plane (personal experience during a practical course).

The aforementioned reasons would just affect the walking speed exhibited by the animals during the experiments and in the worst case only coordination at low walking speeds could be studied on the ball setups. Another reason for the flies to exhibit slower walks might be the ball mass of 100 mg, which is 142 times larger than the mass of 0.7 mg reported for male *CS* flies (Wosnitza et al., 2013). This mass has to be turned on an air cushion by the animals during walking and might create a coordination of the legs that is never present under free walking conditions. However, due to their small body size *Drosophila* has a much greater ratio of muscle cross-sectional area to limb mass compared to larger animals, such as for example humans (Hooper et al., 2009 Fig. 9). This biomechanical property allows them to move masses that are many times larger than their own body mass. Furthermore, as mentioned earlier the flies showed coordinated walking activity atop the ball and a large range of walking speeds was observed. The leg periods that were found in intact animals showed a similar dependence on walking speed than those found by Wosnitza and colleagues (2013) (Fig. 17). Also parameters concerning inter leg coordination were quite comparable to literature findings. For example, the phase relation of swing onset with regard to L1, which was calculated for all intact legs of intact animals (Fig. 29) and R3 amputees (Fig. 35), showed only minor, if any, differences to published values (Wosnitza et al., 2013 Fig. 2 C and Fig. 8 C). The differences found for R3 amputees might be explained by the fact that tethered animals do not have to carry their body weight, whereas free walking animals suffer from stability issues during walking with only 5 remaining legs. Literature findings reveal a large degree of similarity between untethered and tethered walking also for other insect species such as the cockroach (Delcomyn, 1973).



---

To address the question whether the reduced range of walking speeds was just a chance find or a result of the special experimental situation during tethered walking on an air-cushioned ball, a series of long term experiments was carried out in the second section of this thesis. For these experiments a behavioral setup was created to record the walking behavior of up to nine flies in separate petridish enclosures. Additionally, software was developed that allowed an automated analysis of the recorded videos and a visualization of the results. Similar setups and software has already been developed and used for several studies that can be found in the literature (e.g. Bender et al., 2010; Branson et al., 2009; Martin, 2004; Valente et al., 2007).

Software such as CTrax (Branson et al., 2009), which is available in the internet for free and also other commercially available systems allow to distinguish a wide variety of behavioral parameters, like grooming and mating behavior and several others that are not that are not necessarily related to walking and that are therefore not required for the present study.

In order to be perfectly adapted to the requirements of the recent work, software and hardware for this study was developed from scratch. It was designed to record and evaluate the walking behavior of single flies in separate enclosures extracting the time they spend walking, their walking speed and the length of single walking bouts. All these parameters could be recorded and evaluated with the resulting hard- and software.

It was found that compared to intact animals the occurrence of walking speeds above 5 mm/s was strongly reduced in amputees. During voluntary untethered walking R3 amputees showed the highest speed range of all amputees. A reduced level of walking activity was found in R1 and R3 amputees whereas R2 amputees showed the same probability to walk as the intact animals. Walking activity in intact animals and R2 amputees was found for about 30% of the total recorded time R1 and R3 amputees walked for less than 30%. Consistent with literature findings (Valente et al., 2007) most of the flies' walking activity was recorded close to the wall of the enclosures (Fig. 39).

The findings coincide, with results obtained on the ball setups where amputees showed a reduced range of walking speeds compared to intact animals. Of course, a one by one comparison of both situations is not possible as stability might be strongly affected during untethered walking with a leg amputation. R2 amputees perform surprisingly well with their lesion, taken into consideration that one leg of a tripod group is missing, which should affect stability during untethered walking. However due to the reduced walking speed range middle leg amputees might never walk in tripod coordination. For a fly length of about 2 mm, which was mostly found during the experiments of the current thesis, a walking speed of 5 mm/s would correspond to 2.5 BL/s. Results of Wosnitza and colleagues (2013) indicate that walking in strict tripod coordination is rather rare in speed range below 10 BL/s.

## 4.6 New insights and open questions

Several previous amputation studies for example in cockroach (Delcomyn, 1988; Delcomyn, 1991b; Delcomyn, 1991c; Hughes, 1957) and stick insects (Buddenbrock, 1921; Wendler, 1964) reported oscillations or muscle activity of a single leg stump in otherwise intact walking animals.

Most of these studies showed multiple stump oscillations during single step cycles in intact legs. These observations were often only qualitative and they rather focus on effects of amputations on the kinematics and coordination of the remaining intact legs. For the current study oscillations were recorded in single leg stumps of the fruit flies front, middle and hind legs. A special focus was drawn here on walking speed dependence and the temporal coordination of the stump movements with regard to intact legs of the animal. The present study also tries to differentiate between local CPG-like activity and inter-segmental sensory influence during walking. Due to *Drosophila*'s status as a model organism and its genetic accessibility the present study is an important baseline for the investigation of sensory mutants and VNC networks in the context of walking.

During fast walking stumps become highly coordinated with respect to intact legs. This can be explained by either an increased similarity of the frequencies of the rhythm-generating networks and their subsequent entrainment. In that case a direct influence between the involved networks would exist. Alternatively, the entrainment effect might be explained by rhythmic sensory information from the intact legs, entraining the stump. This second alternative is supported by results of experiments with middle leg amputated *nan[36a]* mutant flies in the current thesis. These flies lack sensory input from their chordotonal organs and fail to entrain the stump in a 1:1 fashion at high walking speeds (Fig. 21 Fig. 21 Dii and Fig. 22 Dii). Obviously, sensory input from the chordotonal organs in the intact legs is important for inter-leg coordination and serves to entrain the stump during fast walking. This also coincides with findings of Mendes and colleagues (2014), who could show that chordotonal organs are important for plasticity during walking, e.g. the adaption to additional load.

While the results are consistent with a bipartite effect of descending signals, it is unclear how this is implemented in the nervous system. The descending drive controlling initiation of walking and speed could either be one global signal originating in higher centers which is then split up into its two putative components locally in the ganglia. Alternatively, there might be two anatomically different descending channels that originate in two higher centers and influence CPG activity and walking speed independently from each other. Although the second alternative is probably more complex and requires more neuronal wiring it is supported by recent findings. It has been shown that octopamine-deficient *Drosophila* mutants are able to walk coordinately but do so at much lower average walking speeds (Wosnitza et al., 2013). This is consistent with the hypothesis that descending gain modulation of sensory influences required for higher walking speeds does not function in these mutants and might

therefore be dependent on octopamine. Octopaminergic candidate neurons (Hsu and Bhandawat, 2016) that might constitute such a channel for gain modulation are the so-called DUM neurons, whose modulatory functions have been shown in other insect species (locust: Bräunig M., 1998; Hoyle et al., 1974; for review see Roeder, 2005; Stevenson and Spörhase-Eichmann, 1995; Bräunig and Pflüger, 2001).

As a genetically accessible model organism *Drosophila* offers the opportunity to gain detailed insights into the neural and sensory bases of walking behavior by a specific activation, inhibition or ablation of the involved neurons and sensory structures. Sensory-deprived *Drosophila* lines might play an important role in that regard (e.g. Desai et al., 2014; Kernan et al., 1994; Mendes et al., 2013). In such lines it is, in principle, possible to completely ablate all leg sensory structures genetically, while otherwise leaving the legs completely intact. It has been shown that sensory mutants that lack many sensory structures, but are otherwise intact, are still able to walk coordinately; the complete absence of all sensory information in these mutants has not been shown explicitly, though (Mendes et al., 2013). Using such *Drosophila* sensory mutants might offer a way of distinguishing between centrally and sensory-mediated coupling. Additionally, more specific lines could be created in which a subset of sensory structures or even single ones are silenced or activated by the use of optogenetic tools (Fiala et al., 2010). This tools in principle allow for a phasic activation (Klapoetke et al., 2014) or inactivation (Chuong et al., 2014) of the investigated structures during any part of the step cycle in a millisecond range (Boyden et al., 2005; Hsiao et al., 2016; Tuthill and Wilson, 2016). Such an approach might help to investigate the contributions of sensory structures and even interneurons for the coordination of all six legs during walking.

## Bibliography

- Akay, T., Bässler, U., Gerharz, P. and Büschges, A.** (2001). The role of sensory signals from the insect coxa-trochanteral joint in controlling motor activity of the femur-tibia joint. *J. Neurophysiol.* **85**, 594–604.
- Akay, T., Haehn, S., Schmitz, J. and Büschges, A.** (2004). Signals From Load Sensors Underlie Interjoint Coordination During Stepping Movements of the Stick Insect Leg. *J. Neurophysiol.* **92**, 42–51.
- Armstrong, J. D., Texada, M. J., Munjaal, R., Baker, D. A. and Beckingham, K. M.** (2006). Gravitaxis in *Drosophila melanogaster*: a forward genetic screen. *Genes. Brain. Behav.* **5**, 222–39.
- Bacqué-Cazenave, J., Chung, B., Cofer, D. W., Cattaert, D. and Edwards, D. H.** (2015). The effect of sensory feedback on crayfish posture and locomotion: II. Neuromechanical simulation of closing the loop. *J. Neurophysiol.* **113**, 1772–83.
- Bässler, U.** (1965). Propriozeptoren am Subcoxal- und Femur-Tibia-Gelenk der Stabheuschrecke *Carausius morosus* und ihre Rolle bei der Wahrnehmung der Schwerkraftichtung. *Kybernetik* **2**, 168–193.
- Bässler, U.** (1977). Sense organs in the femur of the stick insect and their relevance to the control of position of the femur-tibia-joint. *J. Comp. Physiol. A Neuroethol. Sensory, Neural, Behav. Physiol.* **121**, 99–113.
- Bässler, U.** (1986). Afferent control of walking movements in the stick insect *Cuniculina impigra*. *J. Comp. Physiol. A* **158**, 345–349.
- Bässler, U.** (1988). Steuerung von Laufbewegungen. *Verh.Dtsch.Zool.Ges.* **81**, 47–57.
- Bender, J. A., Simpson, E. M. and Ritzmann, R. E.** (2010). Computer-assisted 3D kinematic analysis of all leg joints in walking insects. *PLoS One* **5**, e13617.
- Benezeth, Y., Jodoin, P. M., Emile, B., Laurent, H. and Rosenberger, C.** (2008). Review and evaluation of commonly-implemented background subtraction algorithms. In *2008 19th International Conference on Pattern Recognition*, pp. 1–4. IEEE.
- Berendes, V., Dübbert, M., Bockemühl, T., Schmitz, J., Büschges, A. and Gruhn, M.** (2013). A laser-supported lowerable surface setup to study the role of ground contact during stepping. *J. Neurosci. Methods* **215**, 224–233.

- Berlin, S., Carroll, E. C., Newman, Z. L., Okada, H. O., Quinn, C. M., Kallman, B., Rockwell, N. C., Martin, S. S., Lagarias, J. C. and Isacoff, E. Y.** (2015). Photoactivatable genetically encoded calcium indicators for targeted neuronal imaging. *Nat. Methods* **12**, 852–858.
- Bidaye, S. S., Machacek, C., Wu, Y. and Dickson, B. J.** (2014). Neuronal control of *Drosophila* walking direction. *Science* **344**, 97–101.
- Borgmann, A., Hooper, S. L. and Büschges, A.** (2009). Sensory feedback induced by front-leg stepping entrains the activity of central pattern generators in caudal segments of the stick insect walking system. *J Neurosci* **29**, 2972–2983.
- Borgmann, A., Toth, T. I., Gruhn, M., Daun-Gruhn, S. and Büschges, A.** (2012). Dominance of local sensory signals over inter-segmental effects in a motor system: experiments. *Biol Cybern.*
- Boyden, E. S., Zhang, F., Bamberg, E., Nagel, G. and Deisseroth, K.** (2005). Millisecond-timescale, genetically targeted optical control of neural activity. *Nat. Neurosci.* **8**, 1263–1268.
- Branson, K., Robie, A. A., Bender, J., Perona, P. and Dickinson, M. H.** (2009). High-throughput ethomics in large groups of *Drosophila*. *Nat Methods* **6**, 451–457.
- Bräunig, P. and Eder, M.** (1998). Locust dorsal unpaired median (dum) neurones directly innervate and modulate hindleg proprioceptors. *J. Exp. Biol.* **201**, 3333.
- Bräunig, P. and Pflüger, H.-J.** (2001). *The unpaired median neurons of insects.*
- Bräunig, P., Hustert, R. and Pflüger, H. J.** (1981). Distribution and specific central projections of mechanoreceptors in the thorax and proximal leg joints of locusts. I. Morphology, location and innervation of internal proprioceptors of pro- and metathorax and their central projections. *Cell Tissue Res* **216**, 57–77.
- Brown, T. G.** (1911). The Intrinsic Factors in the Act of Progression in the Mammal. *Proc. R. Soc. London. Ser. B, Contain. Pap. a Biol. Character* **84**, 308–319.
- Buddenbrock, W. von** (1921). Der Rhythmus d. Schreitbewegungen der Stabheuschrecke *Dyxippus*. *Biol. Zent. Bl.* **41**, 41–48.
- Bülthoff, H., Götz, K. G. and Herre, M.** (1982). Recurrent inversion of visual orientation in the walking fly, *Drosophila melanogaster*. *J. Comp. Physiol. A* **148**, 471–481.
- Burns, M. D.** (1973). The control of walking in orthoptera. *J. Exp. Biol.* **58**, 45–58.

- Büschges, A.** (1994). THE PHYSIOLOGY OF SENSORY CELLS IN THE VENTRAL SCOLOPARIUM OF THE STICK INSECT FEMORAL CHORDOTONAL ORGAN. *J. Exp. Biol.* **189**, 285–92.
- Büschges, A.** (2005). Sensory control and organization of neural networks mediating coordination of multisegmental organs for locomotion. *J Neurophysiol* **93**, 1127–1135.
- Büschges, A.** (2012). Lessons for circuit function from large insects: Towards understanding the neural basis of motor flexibility. *Curr. Opin. Neurobiol.* **22**, 602–608.
- Büschges, A. and Bässler, U.** (1998). Pattern generation for stick insect walking movements--multisensory control of a locomotor program. *Brain Res Rev* **27**, 65–88.
- Büschges, A. and Gruhn, M.** (2007). Mechanosensory Feedback in Walking: From Joint Control to Locomotor Patterns. In *Advances in Insect Physiology* (ed. Casas, J.) and Simpson, S. J.), pp. 193–230. Academic Press.
- Büschges, A., Schmitz, J. and Bässler, U.** (1995). Rhythmic patterns in the thoracic nerve cord of the stick insect induced by pilocarpine. *J. Exp. Biol.* **198**, 435–56.
- Büschges, A., Ludwar, B. C., Bucher, D., Schmidt, J. and DiCaprio, R. A.** (2004). Synaptic drive contributing to rhythmic activation of motoneurons in the deafferented stick insect walking system. *Eur. J. Neurosci.* **19**, 1856–62.
- Chung, Y. D., Zhu, J., Han, Y. G. and Kernan, M. J.** (2001). *nompA* encodes a PNS-specific, ZP domain protein required to connect mechanosensory dendrites to sensory structures. *Neuron* **29**, 415–428.
- Chung, B., Bacqué-Cazenave, J., Cofer, D. W., Cattaert, D. and Edwards, D. H.** (2015). The effect of sensory feedback on crayfish posture and locomotion: I. Experimental analysis of closing the loop. *J. Neurophysiol.* **113**, 1763–71.
- Chuong, A. S., Miri, M. L., Busskamp, V., Matthews, G. a C., Acker, L. C., Sørensen, A. T., Young, A., Klapoetke, N. C., Henninger, M. A., Kodandaramaiah, S. B., et al.** (2014). Noninvasive optical inhibition with a red-shifted microbial rhodopsin. *Nat. Neurosci.* **17**, 1123–1129.
- Cruse, H.** (1990). What mechanisms coordinate leg movement in walking arthropods? *Trends Neurosci.* **13**, 15–21.
- Cruse, H., Bartling, C., Cymbalyuk, G., Dean, J. and Dreifert, M.** (1995). A modular artificial neural net for controlling a six-legged walking system. *Biol. Cybern.* **72**, 421–30.

- Daun-Gruhn, S. and Toth, T. I.** (2011). An inter-segmental network model and its use in elucidating gait-switches in the stick insect. *J. Comput. Neurosci.* **31**, 43–60.
- Daun-Gruhn, S., Toth, T. I. and Borgmann, A.** (2012). Dominance of local sensory signals over inter-segmental effects in a motor system: modeling studies. *Biol. Cybern.*
- Dean, J. and Schmitz, J.** (1992). The two groups of sensilla in the ventral coxal hairplate of *Carausius morosus* have different roles during walking. *Physiol. Entomol.* **17**, 331–341.
- Delcomyn, F.** (1971). The Locomotion of the Cockroach *Periplaneta Americana*. *J. Exp. Biol.* **54**, 443–452.
- Delcomyn, F.** (1973). Motor Activity During Walking in the Cockroach *Periplaneta Americana* II. Tethered Walking. *J. Exp. Biol.* **59**, 643–654.
- Delcomyn, F.** (1987). Motor activity during searching and walking movements of cockroach legs. *J Exp Biol* **133**, 111–120.
- Delcomyn, F.** (1988). Motor activity in the stump of an amputated leg during free walking in cockroaches. *J. Exp. Biol.* **140**, 465–76.
- Delcomyn, F.** (1989). Walking in the American cockroach: the timing of motor activity in the legs during straight walking. *Biol Cybern* **60**, 373–384.
- Delcomyn, F.** (1991a). Gait instability after leg amputation during walking in cockroaches.
- Delcomyn, F.** (1991b). Perturbation of the motor system in freely walking cockroaches. II. The timing of motor activity in leg muscles after amputation of a middle leg. *J Exp Biol* **156**, 503–517.
- Delcomyn, F.** (1991c). Perturbation of the motor system in freely walking cockroaches. I. Rear leg amputation and the timing of motor activity in leg muscles. *J Exp Biol* **156**, 483–502.
- Desai, B. S., Chadha, A. and Cook, B.** (2014). The stum gene is essential for mechanical sensing in proprioceptive neurons. *Science.* **343**, 1256–1259.
- Dhooria, M. S.** (2008). *Ane's Encyclopedic Dictionary of General Applied Entomology*. 7th ed. Dordrecht: Springer Netherlands.
- Dickinson, M. H., Farley, C. T., Full, R. J., Koehl, M. A., Kram, R. and Lehman, S.** (2000). How animals move: an integrative view. *Science* **288**, 100–6.
- Dürr, V., Schmitz, J. and Cruse, H.** (2004). Behaviour-based modelling of hexapod locomotion: linking biology and technical application. *Arthropod Struct. Dev.* **33**, 237–250.



- Fiala, A., Suska, A. and Schluter, O. M.** (2010). Optogenetic approaches in neuroscience. *Curr. Biol.* **20**, R897–903.
- Field, L. H. and Matheson, T.** (1998). Chordotonal Organs of Insects. *Adv. Insect Physiol.* **27**, 1–56.
- Foth, E. and Bässler, U.** (1985a). Leg movements of stick insects walking with five legs on a treadmill and with one leg on a motor-driven belt. II. Leg coordination when step-frequencies differ from leg to leg. *Biol. Cybern.* **51**, 319–24.
- Foth, E. and Bässler, U.** (1985b). Leg movements of stick insects walking with five legs on a treadmill and with one leg on a motor-driven belt. I. General results and 1:1-coordination. *Biol. Cybern.* **51**, 313–318.
- Fuchs, E., Holmes, P., David, I. and Ayali, A.** (2012). Proprioceptive feedback reinforces centrally generated stepping patterns in the cockroach. *J. Exp. Biol.* **215**, 1884–1891.
- Full, R. J. and Tu, M. S.** (1990). Mechanics of six-legged runners. *J. Exp. Biol.* **148**, 129–146.
- Full, R. J. and Tu, M. S.** (1991). Mechanics of a rapid running insect: two-, four- and six-legged locomotion. *J Exp Biol* **156**, 215–231.
- Füller A., H. . E.** (1973). Die Ultrastruktur der femoralen Chordotonalorgane von *Carausius morosus* BR. *Zool.Jb.Anat.* **91**, 574–601.
- Gabriel, J. P. and Büschges, A.** (2007). Control of stepping velocity in a single insect leg during walking. *Philos. Trans. R. Soc. A Math. Phys. Eng. Sci.* **365**, 251–271.
- Gal, R. and Libersat, F.** (2006). New vistas on the initiation and maintenance of insect motor behaviors revealed by specific lesions of the head ganglia. *J Comp Physiol A Neuroethol Sens Neural Behav Physiol* **192**, 1003–1020.
- Gilchrist, G. W., Huey, R. B. and Partridge, L.** (1997). Thermal sensitivity of *Drosophila melanogaster*: evolutionary responses of adults and eggs to laboratory natural selection at different temperatures. *Physiol. Zool.* **70**, 403–414.
- Grabowska, M., Godlewska, E., Schmidt, J. and Daun-Gruhn, S.** (2012). Quadrupedal gaits in hexapod animals - inter-leg coordination in free-walking adult stick insects. *J. Exp. Biol.* **215**, 4255–66.
- Graham, D.** (1972). A behavioural analysis of the temporal organisation of walking movements in the 1st instar and adult stick insect (*Carausius morosus*). *J. Comp. Physiol.* **81**, 23–52.

- Graham, D.** (1977). The Effect of Amputation and Leg Restraint on the Free Walking Coordination of the Stick Insect *Carausius morosus*. *J. Comp. Physiol. A* **116**, 91–116.
- Graham, D.** (1979). Effects of circum-oesophageal lesion on the behaviour of the stick insect *Carausius morosus*. I. Cyclic behaviour patterns. *Biol. Cybern.* **32**, 139–145.
- Graham, D.** (1985). Pattern and Control of Walking in Insects. In *Advances in Insect Physiology* (ed. M.J. Berridge, J. E. T.) and Wigglesworth, V. B.), pp. 31–140. Academic Press.
- Grillner, S.** (1985). Neurobiological bases of rhythmic motor acts in vertebrates. *Science* **228**, 143–149.
- Gruhn, M., von Uckermann, G., Westmark, S., Wosnitza, A., Büschges, A. and Borgmann, A.** (2009). Control of stepping velocity in the stick insect *Carausius morosus*. *J. Neurophysiol.* **102**, 1180–92.
- Hamada, F. N., Rosenzweig, M., Kang, K., Pulver, S. R., Ghezzi, A., Jegla, T. J. and Garrity, P. A.** (2008). An internal thermal sensor controlling temperature preference in *Drosophila*. *Nature* **454**, 217–U55.
- Hess, D. and Büschges, A.** (1999). Role of proprioceptive signals from an insect femur-tibia joint in patterning motoneuronal activity of an adjacent leg joint. *J Neurophysiol* **81**, 1856–1865.
- Hooper, S. L., Guschlbauer, C., Blümel, M., Rosenbaum, P., Gruhn, M., Akay, T. and Büschges, A.** (2009). Neural control of unloaded leg posture and of leg swing in stick insect, cockroach, and mouse differs from that in larger animals. *J. Neurosci.* **29**, 4109–19.
- Hoyle, G., Dagan, D., Moberly, B. and Colquhoun, W.** (1974). Dorsal unpaired median insect neurons make neurosecretory endings on skeletal muscle. *J. Exp. Zool.* **187**, 159–165.
- Hoyt, D. F. and Taylor, C. R.** (1981). Gait and the energetics of locomotion in horses. *Nature* **292**, 239–240.
- Hsiao, P.-Y., Wu, M.-C., Lin, Y.-Y., Fu, C.-C. and Chiang, A.-S.** (2016). Optogenetic Manipulation of Selective Neural Activity in Free-Moving *Drosophila* Adults. *Methods Mol. Biol.* **1408**, 377–87.
- Hsu, C. T. and Bhandawat, V.** (2016). Organization of descending neurons in *Drosophila melanogaster*. *Sci. Rep.* **6**, 20259.

- Hughes, G. M.** (1952). The Co-Ordination of Insect Movements: I The Walking Movements of Insects. *J. Exp. Biol.* **29**, 267–285.
- Hughes, G. M.** (1957). The Co-Ordination of Insect Movements: 11. The Effect of Limb Amputation and the Cutting of Commissures In The Cockroach (*Blatta Oiuentalis*). *J. Exp. Biol.* **34**, 306–333.
- Jennings, B. H.** (2011). *Drosophila*-a versatile model in biology & medicine. *Mater. Today* **14**, 190–195.
- Johnston, R. M. and Levine, R. B.** (1996a). Crawling motor patterns induced by pilocarpine in isolated larval nerve cords of *Manduca sexta*. *J Neurophysiol* **76**, 3178–3195.
- Johnston, R. M. and Levine, R. B.** (1996b). Locomotory behavior in the hawkmoth *Manduca sexta*: kinematic and electromyographic analyses of the thoracic legs in larvae and adults. *J. Exp. Biol.* **199**, 759–774.
- Kain, J., Stokes, C., Gaudry, Q., Song, X., Foley, J., Wilson, R. and de Bivort, B.** (2013). Leg-tracking and automated behavioural classification in *Drosophila*. *Nat Commun* **4**, 1910.
- Kavlie, R. G. and Albert, J. T.** (2013). Chordotonal organs. *Curr. Biol.* **23**, R334–R335.
- Kernan, M., Cowan, D. and Zuker, C.** (1994). Genetic dissection of mechanosensory transduction: mechanoreception-defective mutations of *Drosophila*. *Neuron* **12**, 1195–206.
- Kien, J. and Altman, J. S.** (1984). Descending interneurons from the brain and suboesophageal ganglia and their role in the control of locust behaviour. *J. Insect Physiol.* **30**, 59–72.
- Kien, J. and Williams, M.** (1983). Morphology of neurones in locust brain and suboesophageal ganglion involved in initiation and maintenance of walking. *Proc. R. Soc. London B* **219**, 175–192.
- Kim, J., Chung, Y. D., Park, D.-Y., Choi, S., Shin, D. W., Soh, H., Lee, H. W., Son, W., Yim, J., Park, C.-S., et al.** (2003). A TRPV family ion channel required for hearing in *Drosophila*. *Nature* **424**, 81–84.
- Klapoetke, N. C., Murata, Y., Kim, S. S., Pulver, S. R., Birdsey-Benson, A., Cho, Y. K., Morimoto, T. K., Chuong, A. S., Carpenter, E. J., Tian, Z., et al.** (2014). Independent optical excitation of distinct neural populations. *Nat. Methods* **11**, 338–346.
- Knoppien, P., Pers, J. N. C. Van Der and Delden, W. Van** (2000). Quantification of Locomotion and the Effect of Food Deprivation on Locomotor Activity in *Drosophila*. **13**, 27–43.

- Kuramoto, Y.** (1984). *Chemical Oscillations, Waves, and Turbulence*. Berlin, Heidelberg: Springer Berlin Heidelberg.
- Laurent, G. and Burrows, M.** (1989). Distribution of intersegmental inputs to nonspiking local interneurons and motor neurons in the locust. *J Neurosci* **9**, 3019–3029.
- Ludwar, B. C.** (2004). Intersegmental Coordination of Walking Movements in Stick Insects. *J. Neurophysiol.* **93**, 1255–1265.
- Marder, E. and Calabrese, R. L.** (1996). Principles of rhythmic motor pattern generation. *Physiol. Rev.* **76**, 687–717.
- Martin, J. R.** (2004). A portrait of locomotor behaviour in *Drosophila* determined by a video-tracking paradigm. *Behav. Processes* **67**, 207–219.
- Mendes, C. S., Bartos, I., Akay, T., Marka, S. and Mann, R. S.** (2013). Quantification of gait parameters in freely walking wild type and sensory deprived *Drosophila melanogaster*. *Elife* **2**, e00231.
- Mendes, C. S., Rajendren, S. V., Bartos, I., Márka, S. and Mann, R. S.** (2014). Kinematic responses to changes in walking orientation and gravitational load in *drosophila melanogaster*. *PLoS One* **9**,
- Noah, J. A., Quimby, L., Frazier, S. F. and Zill, S. N.** (2004). Walking on a “peg leg”: extensor muscle activities and sensory feedback after distal leg denervation in cockroaches. *J Comp Physiol A Neuroethol Sens Neural Behav Physiol* **190**, 217–231.
- Nusbaum, M. P., Otto Friesen, W., Kristan, W. B. and Pearce, R. A.** (1987). Neural mechanisms generating the leech swimming rhythm: Swim-initiator neurons excite the network of swim oscillator neurons. *J. Comp. Physiol. A* **161**, 355–366.
- Orlovsky** (1999). Neuronal Control of Locomotion. In *Neuronal Control of Locomotion From Mollusc to Man* (ed. C.N.Orlovsky and Grillner, T. G. D.), New York: Oxford University INC.
- Pearson, K. G.** (1993). Common Principles of Motor Control in Vertebrates and Invertebrates. *Annu. Rev. Neurosci.* **16**, 265–297.
- Pearson, K. G.** (2004). Generating the walking gait: role of sensory feedback. *Prog Brain Res* **143**, 123–129.

- Pearson, K. G. and Iles, J. F.** (1973). Nervous Mechanisms Underlying Intersegmental Coordination of Leg Movements During Walking in the Cockroach. *J. Exp. Biol.* **58**, 725–744.
- Pearson, K. G., Wong, R. K. and Fourtner, C. R.** (1976). Connexions between hair-plate afferents and motoneurons in the cockroach leg. *J Exp Biol* **64**, 251–266.
- Pikovsky, A., Rosenblum, M. and Kurths, J.** (2003). *Synchronization A Universal Concept in Nonlinear Sciences*. Cambridge university press.
- Ridgel, A. L. and Ritzmann, R. E.** (2005). Insights into age-related locomotor declines from studies of insects. *Ageing Res Rev* **4**, 23–39.
- Robertson, G. A., Mortin, L. I., Keifer, J. and Stein, P. S.** (1985). Three forms of the scratch reflex in the spinal turtle: central generation of motor patterns. *J. Neurophysiol.* **53**, 1517–1534.
- Roeder, K. D.** (1937). The control of tonus and locomotor activity in the praying mantis (*Mantis religiosa* L.). *J. Exp. Zool.* **76**, 353–374.
- Roeder, T.** (2005). Tyramine and octopamine: ruling behavior and metabolism. *Annu. Rev. Entomol.* **50**, 447–77.
- Rubin, G. M.** (1988). *Drosophila melanogaster* as an Experimental Organism. *Science (80- )*. **240**, 1453–1459.
- Ryckebusch, S. and Laurent, G.** (1993). Rhythmic patterns evoked in locust leg motor neurons by the muscarinic agonist pilocarpine. *J Neurophysiol* **69**, 1583–1595.
- Sauer, A. E., Driesang, R. B., Büschges, A. and Bässler, U.** (1996). Distributed processing on the basis of parallel and antagonistic pathways simulation of the femur-tibia control system in the stick insect. *J Comput Neurosci* **3**, 179–198.
- Schilling, M., Hoinville, T., Schmitz, J. and Cruse, H.** (2013). Walknet, a bio-inspired controller for hexapod walking. *Biol. Cybern.* **107**, 397–419.
- Schmitz, J.** (1986a). The depressor trochanteris motoneurons and their role in the coxo-trochanteral feedback loop in the stick insect *Carausius morosus*. *Biol. Cybern.* **55**, 25–34.
- Schmitz, J.** (1986b). Properties of the feedback system controlling the coxa-trochanter joint in the stick insect *Carausius morosus*. *Biol. Cybern.* **55**, 35–42.

- Schmitz, J. and Schöwerling, H.** (1992). No effects of coxo-trochanteral proprioceptors on extensor tibiae motor neurons in posture control. *Proc. 20 th Göttingen Neurobiol. Conf.* 1992.
- Schmitz, J., Gruhn, M. and Büschges, A.** (2015). The role of leg touchdown for the control of locomotor activity in the walking stick insect. *J. Neurophysiol.* **113**, 2309–2320.
- Seelig, J. D. and Jayaraman, V.** (2013). Feature detection and orientation tuning in the *Drosophila* central complex. *Nature*.
- Seelig, J. D., Chiappe, M. E., Lott, G. K., Dutta, A., Osborne, J. E., Reiser, M. B. and Jayaraman, V.** (2010). Two-photon calcium imaging from head-fixed *Drosophila* during optomotor walking behavior. *Nat Meth* **7**, 535–540.
- Spirito, C. P. and Mushrush, D. L.** (1979). Interlimb Coordination During Slow Walking in the Cockroach: I. Effects of Substrate Alterations. *J Exp Biol* **78**, 233–243.
- Stevenson, P. A. and Spörhase-Eichmann, U.** (1995). Localization of octopaminergic neurones in insects. *Comp. Biochem. Physiol. A. Physiol.* **110**, 203–15.
- Strauss, R. and Heisenberg, M.** (1990). Coordination of legs during straight walking and turning in *Drosophila melanogaster*. *J. Comp. Physiol. A.* **167**, 403–412.
- Tuthill, J. C. and Wilson, R. I.** (2016). Parallel Transformation of Tactile Signals in Central Circuits of *Drosophila*. *Cell* **164**, 1046–59.
- Valente, D., Golani, I. and Mitra, P. P.** (2007). Analysis of the trajectory of *Drosophila melanogaster* in a circular open field arena. *PLoS One* **2**,.
- Wahl, V., Pfeffer, S. E. and Wittlinger, M.** (2015). Walking and running in the desert ant *Cataglyphis fortis*. *J. Comp. Physiol. A* 645–656.
- Wallén, P. and Williams, T. L.** (1984). Fictive locomotion in the lamprey spinal cord in vitro compared with swimming in the intact and spinal animal. *J. Physiol.* **347**, 225–239.
- Wendler, G.** (1964). Laufen und Stehen der Staubheuschrecke *Carausius morosus*: Sinnesborstenfelder in den Beingelenken als Glieder von Regelkreisen. *Z. Versl.Physil.* **48**, 197–250.
- Wendler, G.** (1965). The co-ordination of walking movements in arthropods. *Symp. Soc. Exp. Biol.* **20**, 229–249.
- Wilson, D. M.** (1966). Annual Reviews [www.annualreviews.org/aronline](http://www.annualreviews.org/aronline). *Annu. Rev. Entomol.* **11**, 103–122.

- Wong, R. K. and Pearson, K. G.** (1976). Properties of the trochanteral hair plate and its function in the control of walking in the cockroach. *J Exp Biol* **64**, 233–249.
- Wosnitza, A., Bockemühl, T., Dübbert, M., Scholz, H. and Büschges, A.** (2013). Inter-leg coordination in the control of walking speed in *Drosophila*. *J. Exp. Biol.* **216**, 480–491.
- Yamaguchi, S., Desplan, C. and Heisenberg, M.** (2010). Contribution of photoreceptor subtypes to spectral wavelength preference in *Drosophila*. *Proc. Natl. Acad. Sci.* **107**, 5634–5639.
- Zhang, F., Wang, L.-P., Brauner, M., Liewald, J. F., Kay, K., Watzke, N., Wood, P. G., Bamberg, E., Nagel, G., Gottschalk, A., et al.** (2007). Multimodal fast optical interrogation of neural circuitry. *Nature* **446**, 633–9.
- Zill, S.** (2010). Invertebrate neurobiology: brain control of insect walking. *Curr Biol* **20**, R438–40.
- Zill, S., Schmitz, J. and Büschges, A.** (2004). Load sensing and control of posture and locomotion. *Arthropod Struct Dev* **33**, 273–286.
- Zill, S. N., Keller, B. R. and Duke, E. R.** (2009). Sensory signals of unloading in one leg follow stance onset in another leg: transfer of load and emergent coordination in cockroach walking. *J Neurophysiol* **101**, 2297–2304.
- Zill, S. N., Büschges, A. and Schmitz, J.** (2011). Encoding of force increases and decreases by tibial campaniform sensilla in the stick insect, *Carausius morosus*. *J. Comp. Physiol. A. Neuroethol. Sens. Neural. Behav. Physiol.* **197**, 851–67.
- Zill, S. N., Chaudhry, S., Büschges, A. and Schmitz, J.** (2013). Directional specificity and encoding of muscle forces and loads by stick insect tibial campaniform sensilla, including receptors with round cuticular caps. *Arthropod Struct. Dev.* **42**, 455–67.
- Zollikofer, C.** (1994). Stepping patterns in ants. III. Influence of load. *J Exp Biol* **192**, 119–127.



## Appendix

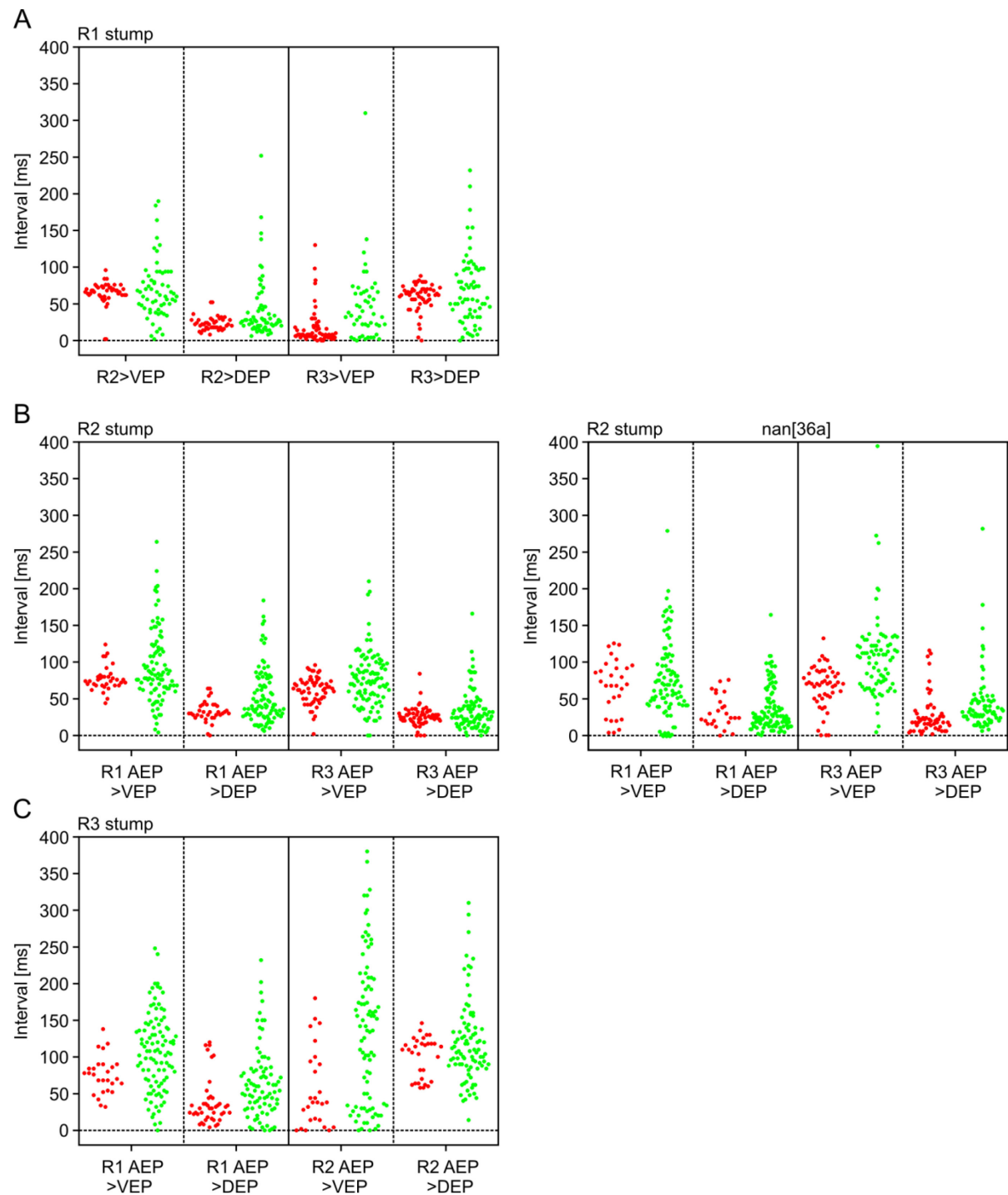
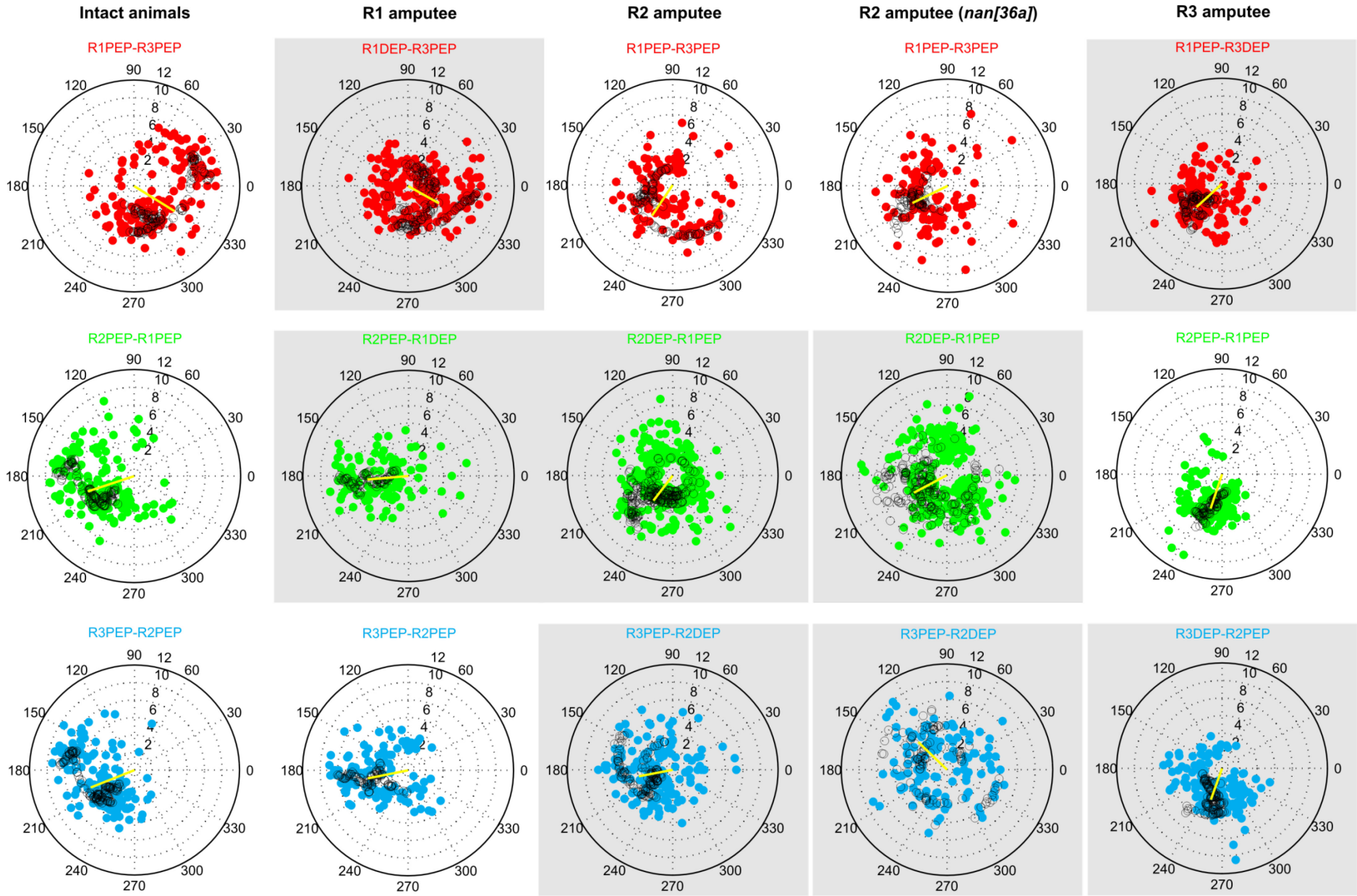


**Fig. 44:** Time intervals between AEPs in intact legs and stump VEPs and DEPs, respectively. Panel A shows data for front leg amputees, panel B shows data for middle leg amputees, and panel D shows data for hind leg amputees. Panel C shows data for middle leg amputees of the chordotonal organ defective *nan[36a]* mutant. Each data point refers to the first VEP or DEP event in a stump following a AEP in an intact leg; for instance, R2>VEP in Panel A refers to the time that elapsed between a AEP in the middle leg (R2) and the next VEP in the front leg stump. Data has been subdivided into those associated with a walking speed equal to or above 5 BL/s (red dots) and those associated with walking speeds below 5 BL/s. If multiple stump movements occurred during the step period of an intact leg only the first DEP or VEP of the stump after the AEP in the reference leg was taken in consideration.



---

**Fig. 45: Circular plot showing the relative phase relation of an event in one leg (PEP) or stump (DEP) versus a reference event in another leg or stump. The panel titles depict the dependent leg and event first and the reference leg and event last. For instance, R2PEP-R1DEP indicates a PEP in the right middle leg as the dependent event and a DEP in the stump of the right front leg as the reference event. A yellow line in each plot indicates the circular mean of the data. The length of the vector is a measure for circular spread. Color coded dots show the phase relation values calculated for each event plotted versus the walking speed [BL/s] of the animal during the period of the reference leg (speed increases from the center to the outside). The color of the dots represents the first leg in the plot titles, the dependent leg during phase relation calculation (front leg or stump: red, middle leg or stump: green, hind leg or stump: blue). Black circles indicate mean values (circular means for the phase relation versus arithmetic means for the speed) calculated for a sliding window of 15 values that has been applied on the speed sorted data.**

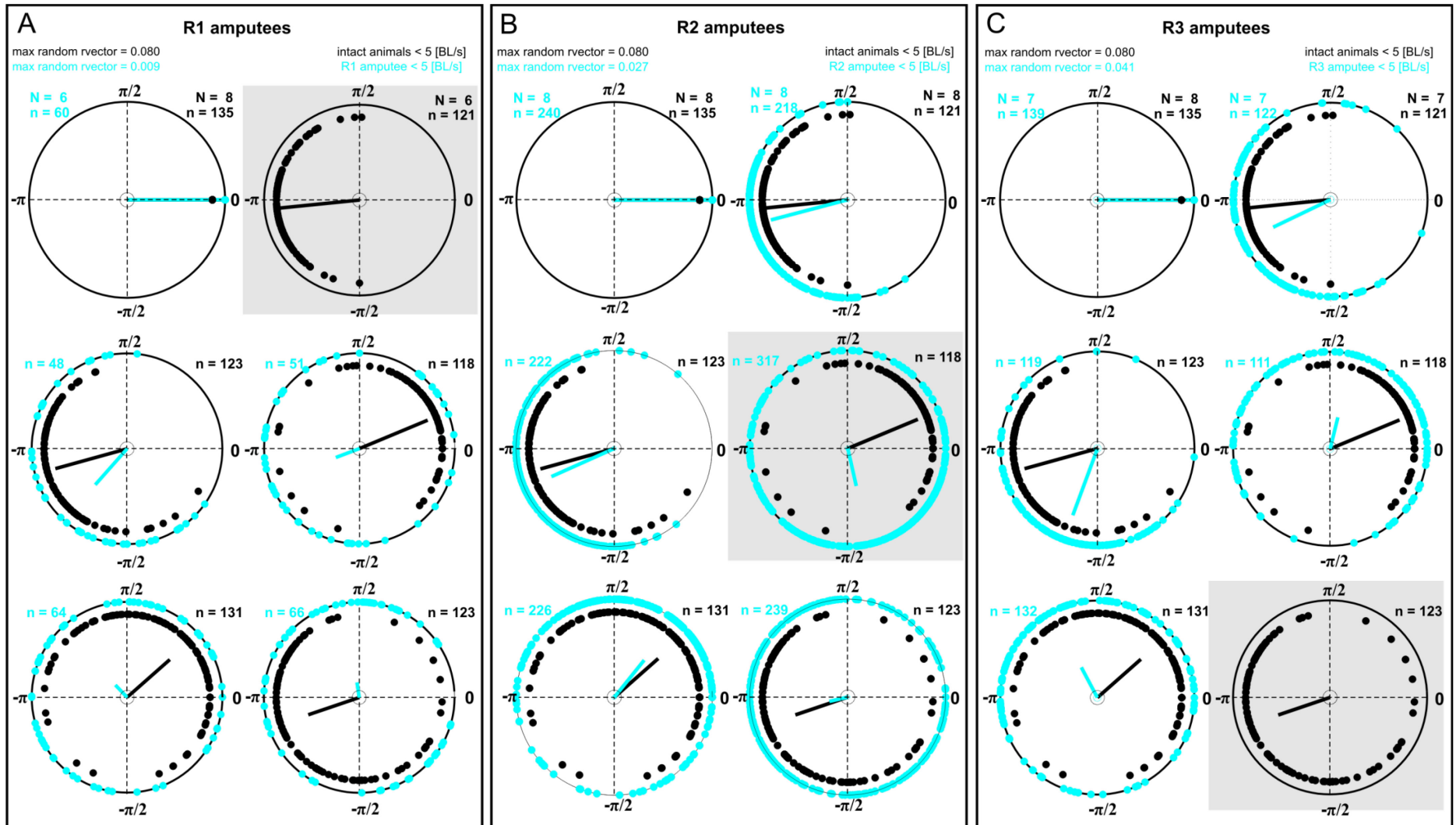
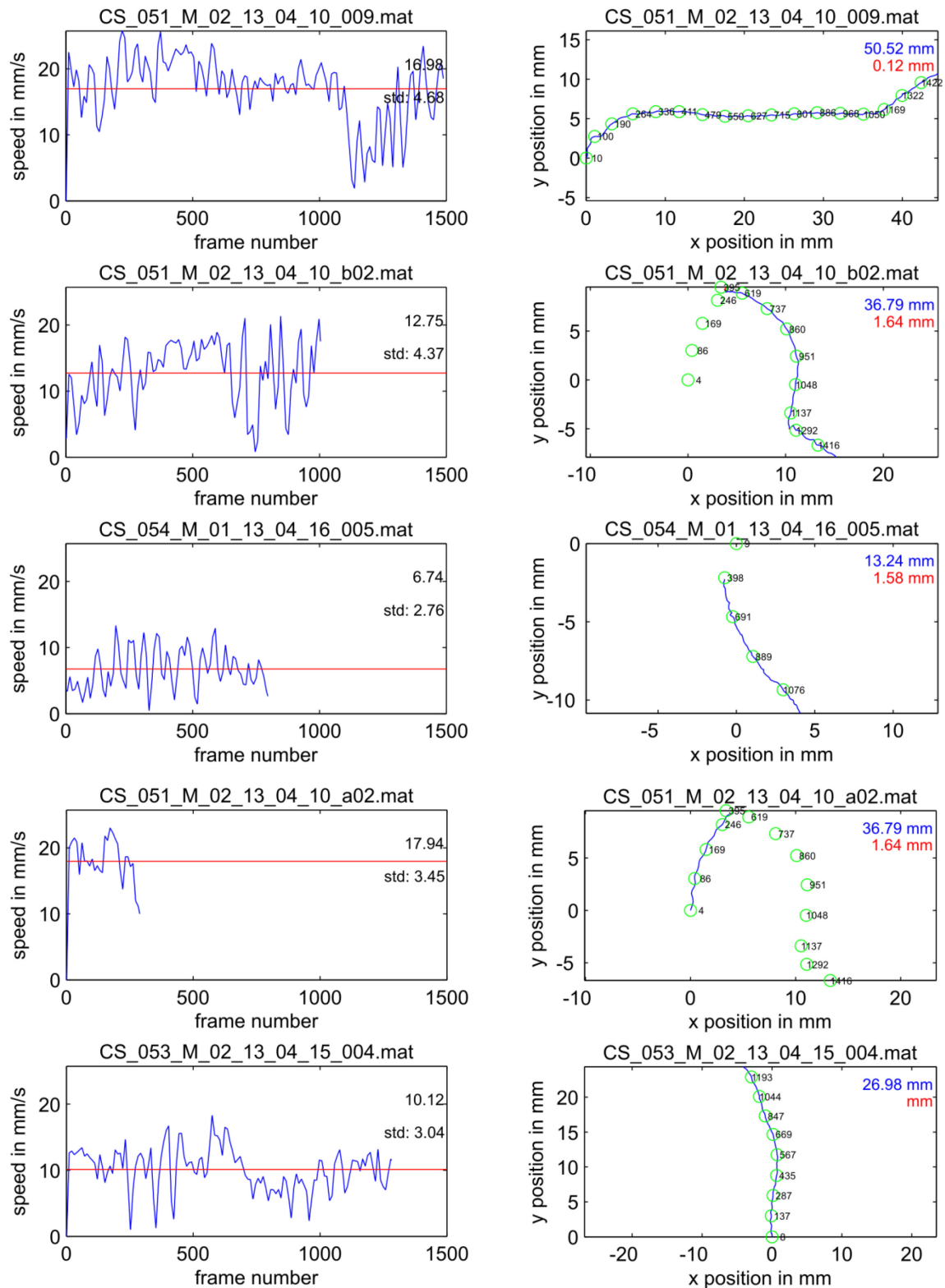


Fig. 46: Circ plots showing the phase relations of swing onset for all legs of intact animals (black dots) and single leg amputees (cyan dots) in a speed range below 5 BL/s ( $N$  = number of animals;  $n$  = number of steps). The swing onset (PEP) in L1 served as a reference in all plots. Black and Cyan lines indicate average phase relation and mean resultant vector length for the phase relations in intact animals and amputees, respectively. Black and cyan circles in the center of the plots indicate the length of a mean resultant vector for the average phase relation between a triangle signal (10 Hz shifted 100 x for 5 video frames) and the L1 reference in intact animals and amputees, respectively.





## Intact animals side-view



**Fig. 48:** Walking speed time course (mm/s vs. frame number) and walking trajectory of evaluated single walks from intact animals. A solid line indicates the evaluated part on the walking path of the flies in the panels on the right. This line indicates positive velocity in blue and negative velocity in red. Green circles divide the walking path in segments of 2 mm length each. Blue numbers indicate the length of the walking trajectory segments with a positive velocity. Red numbers those with a negative velocity. A solid blue line in the speed plots on the left indicates the walking speed time course for the evaluated walking sequence. A red line in the same plots indicates average walking speed of the analyzed walking sequence. Video frame rate was 500 fps (one frame every two ms).

## Intact animals side-view

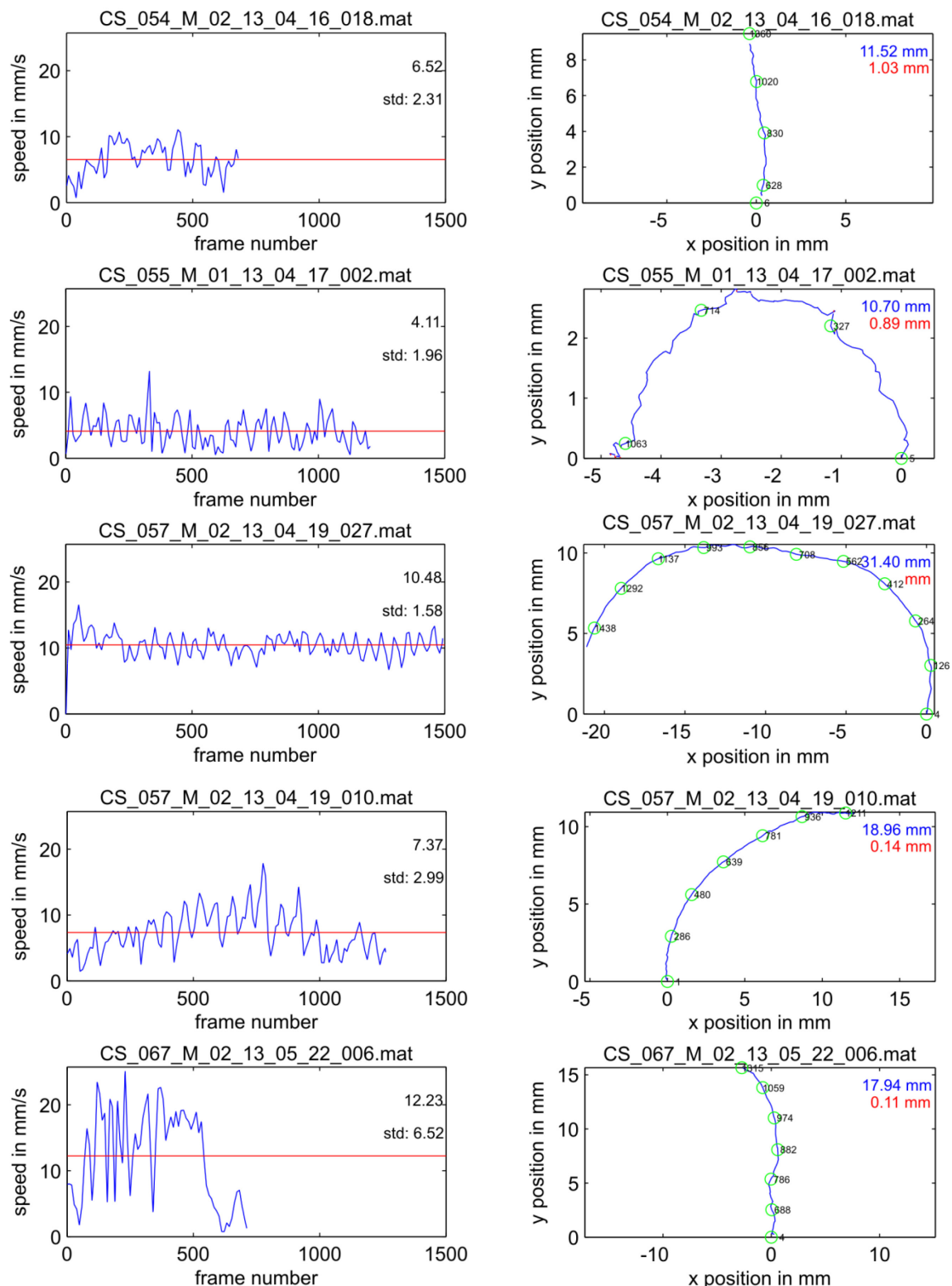


**Fig. 49: Walking speed time course (mm/s vs. frame number) and walking trajectory of evaluated single walks from intact animals. A solid line indicates the evaluated part on the walking path of the flies in the panels on the right. This line indicates positive velocity in blue and negative velocity in red. Green circles divide the walking path in segments of 2 mm length each. Green circles without a solid line indicate segments of the walking trajectory that have not been evaluated. Blue numbers indicate the length of the walking trajectory with a positive velocity. Red numbers those with a negative velocity. A solid blue line in the speed plots on the left indicates the walking speed time course for the evaluated walking sequence. A red line in the same plots indicates average walking speed of the analyzed walking sequence. Video frame rate was 500 fps (one frame every two ms).**



## R1 amputees side-view

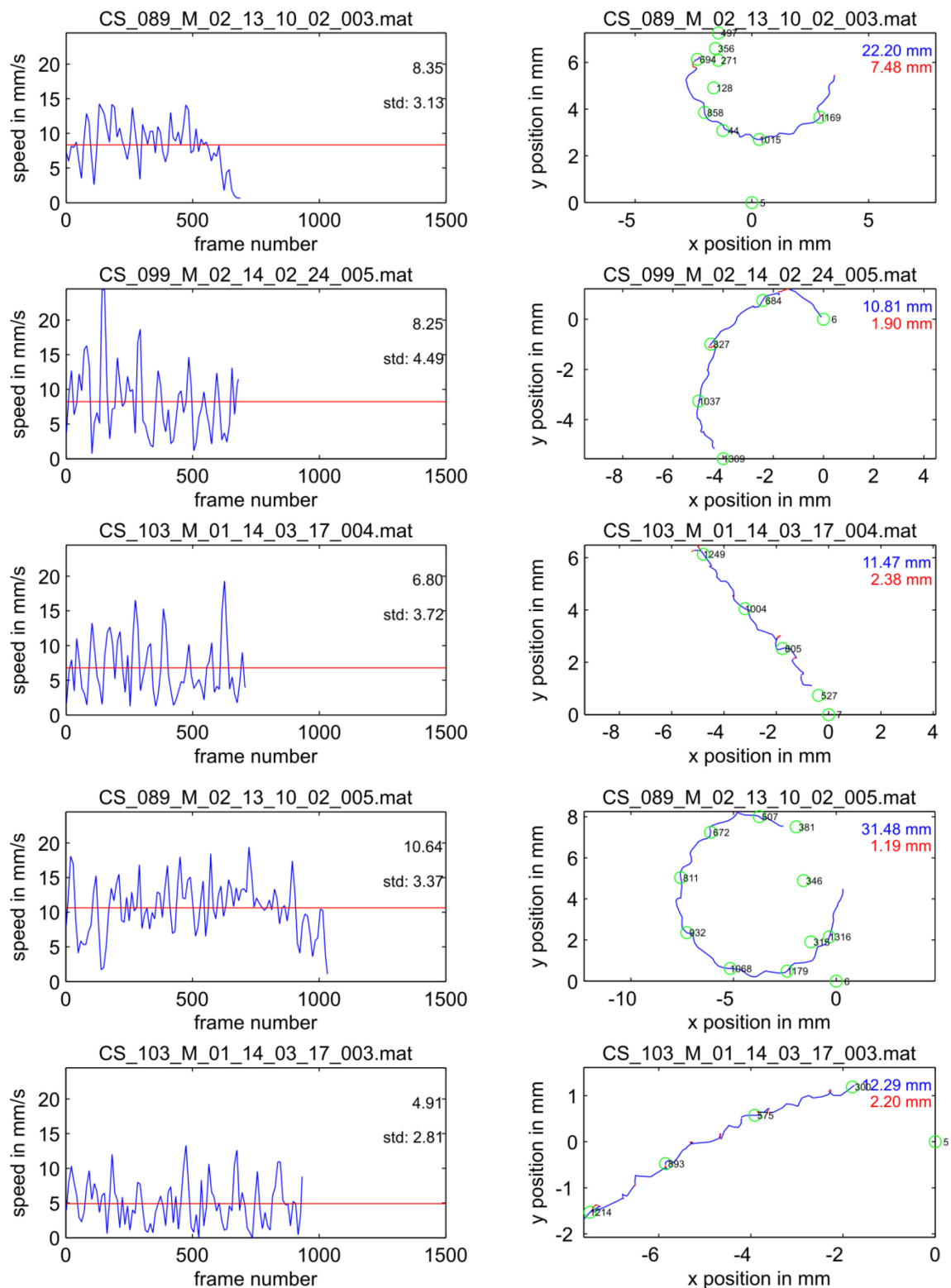


**Fig. 50: Walking speed time course (mm/s vs. frame number) and walking trajectory of evaluated single walks from R1 amputees. A solid line indicates the evaluated part on the walking path of the flies in the panels on the right. This line indicates positive velocity in blue and negative velocity in red. Green circles divide the walking path in segments of 2 mm length each. Green circles without a solid line indicate segments of the walking trajectory that have not been evaluated. Blue numbers indicate the length of the walking trajectory with a positive velocity. Red numbers those with a negative velocity. A solid blue line in the speed plots on the left indicates the walking speed time course for the evaluated walking sequence. A red line in the same plots indicates average walking speed of the analyzed walking sequence. Video frame rate was 500 fps (one frame every two ms).**

## R1 amputees side-view

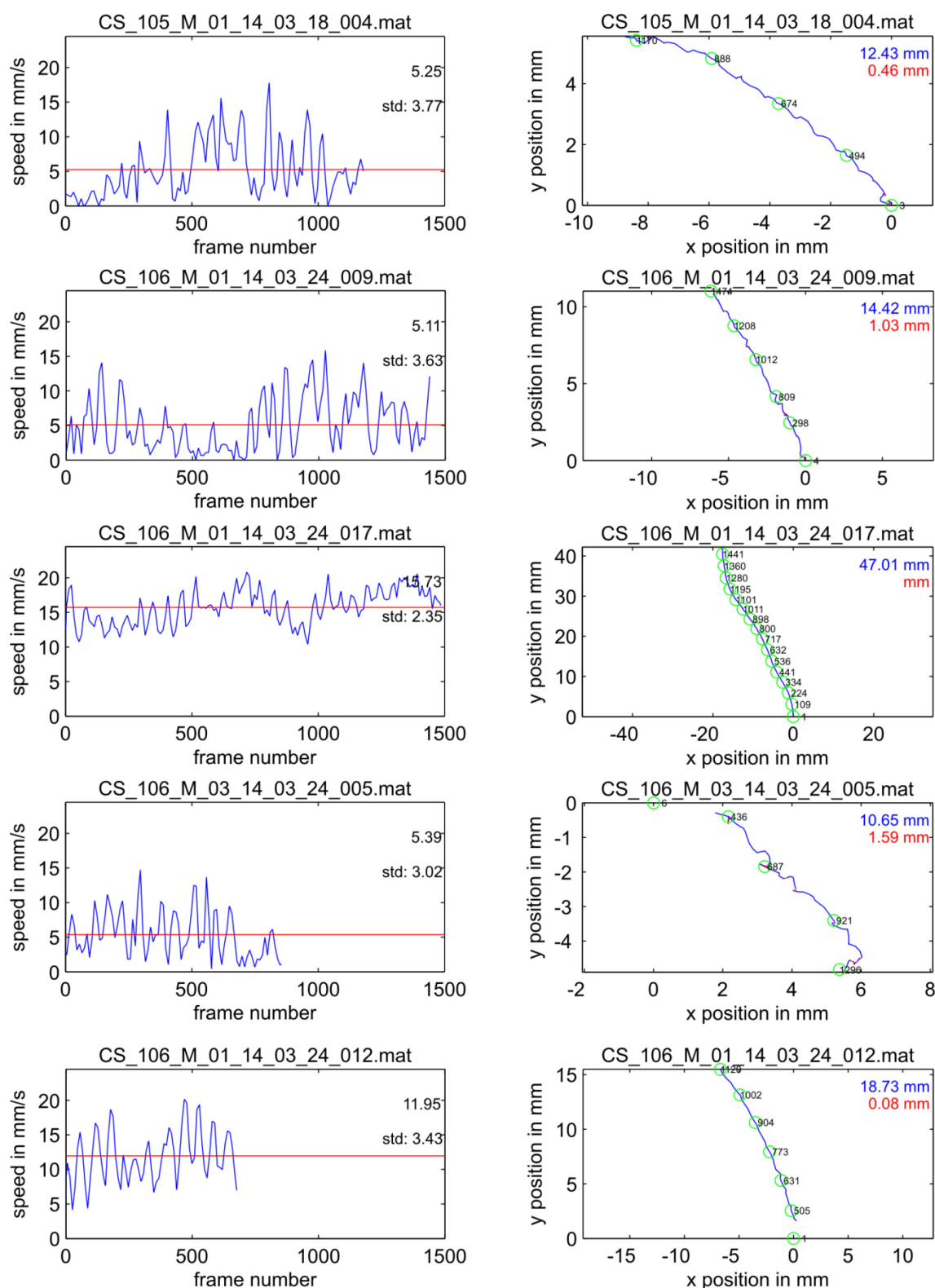


**Fig. 51: Walking speed time course (mm/s vs. frame number) and walking trajectory of evaluated single walks from R1 amputees. A solid line indicates the evaluated part on the walking path of the flies in the panels on the right. This line indicates positive velocity in blue and negative velocity in red. Green circles divide the walking path in segments of 2 mm length each. Green circles without a solid line indicate segments of the walking trajectory that have not been evaluated. Blue numbers indicate the length of the walking trajectory with a positive velocity. Red numbers those with a negative velocity. A solid blue line in the speed plots on the left indicates the walking speed time course for the evaluated walking sequence. A red line in the same plots indicates average walking speed of the analyzed walking sequence. Video frame rate was 500 fps (one frame every two ms).**

## R1 amputees side-view

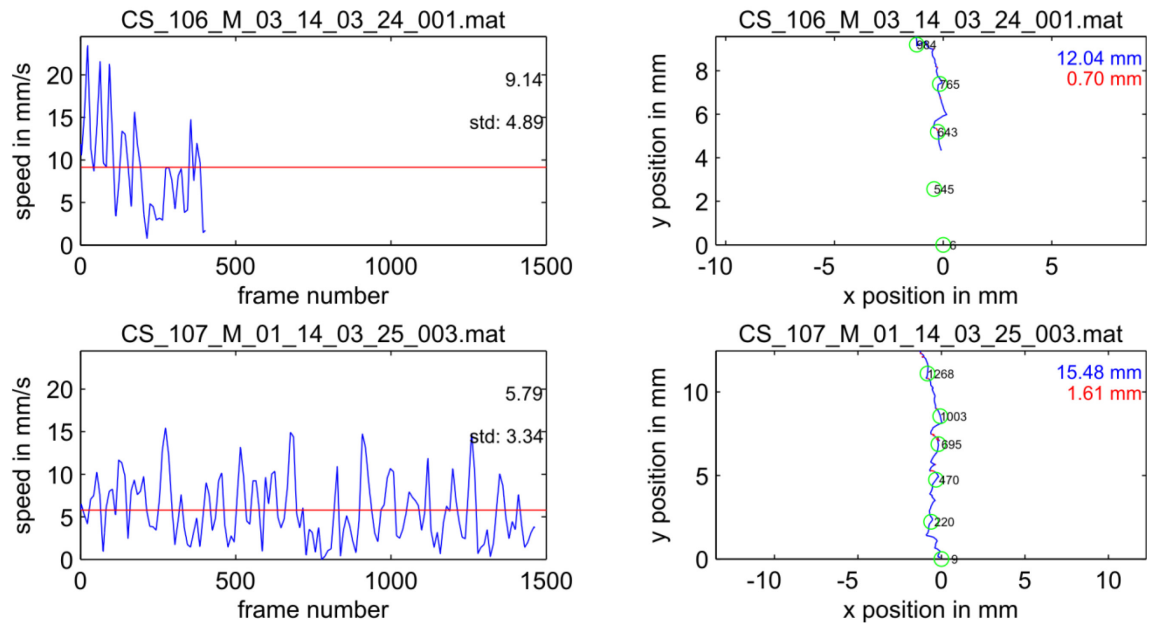


**Fig. 52: Walking speed time course (mm/s vs. frame number) and walking trajectory of evaluated single walks from R1 amputees. A solid line indicates the evaluated part on the walking path of the flies in the panels on the right. This line indicates positive velocity in blue and negative velocity in red. Green circles divide the walking path in segments of 2 mm length each. Green circles without a solid line indicate segments of the walking trajectory that have not been evaluated. Blue numbers indicate the length of the walking trajectory with a positive velocity. Red numbers those with a negative velocity. A solid blue line in the speed plots on the left indicates the walking speed time course for the evaluated walking sequence. A red line in the same plots indicates average walking speed of the analyzed walking sequence. Video frame rate was 500 fps (one frame every two ms).**

## R2 amputees side-view

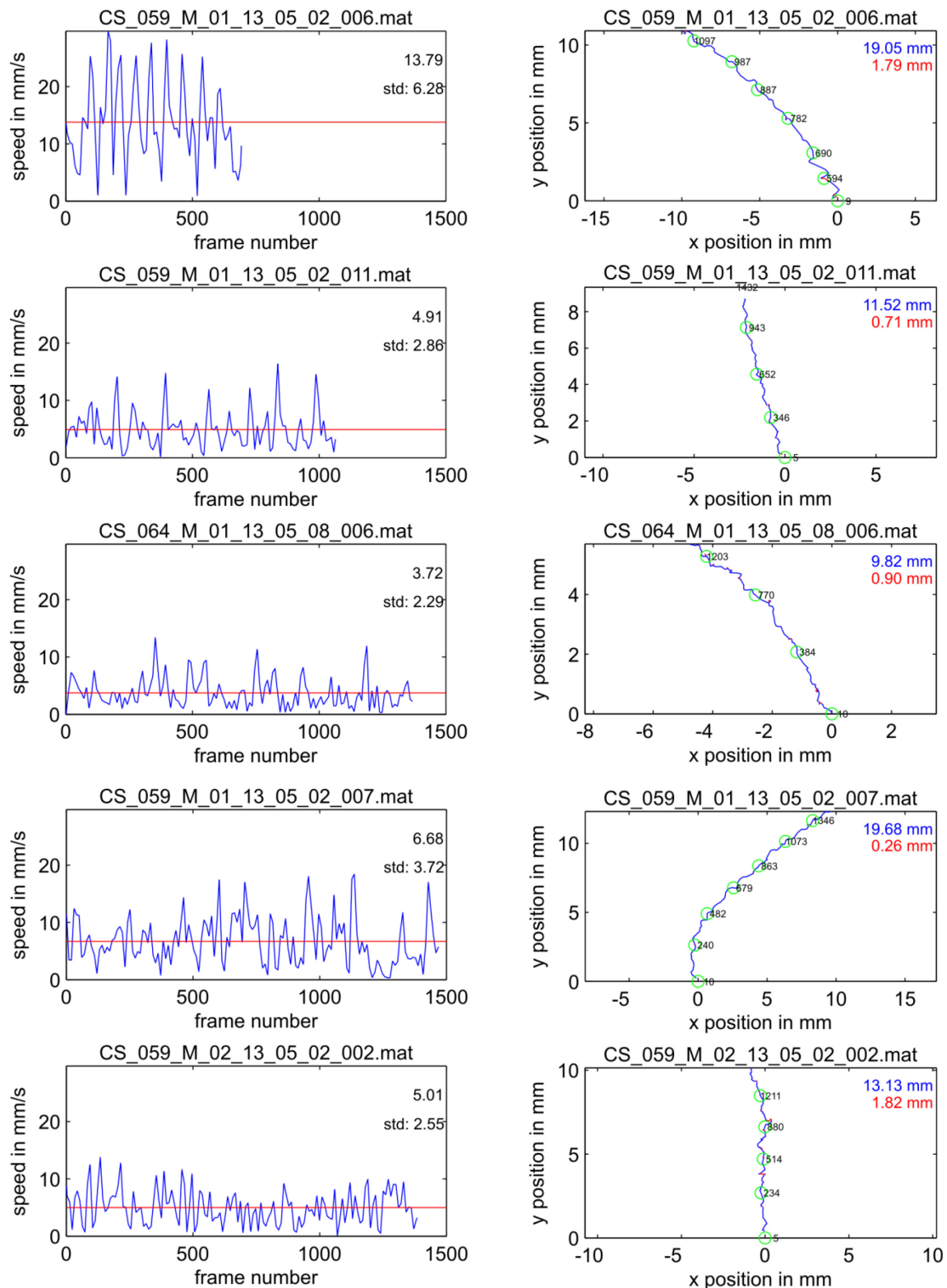


Fig. 53: Walking speed time course (mm/s vs. frame number) and walking trajectory of evaluated single walks from R2 amputees. A solid line indicates the evaluated part on the walking path of the flies in the panels on the right. This line indicates positive velocity in blue and negative velocity in red. Green circles divide the walking path in segments of 2 mm length each. Green circles without a solid line indicate segments of the walking trajectory that have not been evaluated. Blue numbers indicate the length of the walking trajectory with a positive velocity. Red numbers those with a negative velocity. A solid blue line in the speed plots on the left indicates the walking speed time course for the evaluated walking sequence. A red line in the same plots indicates average walking speed of the analyzed walking sequence. Video frame rate was 500 fps (one frame every two ms).

## R2 amputees side-view

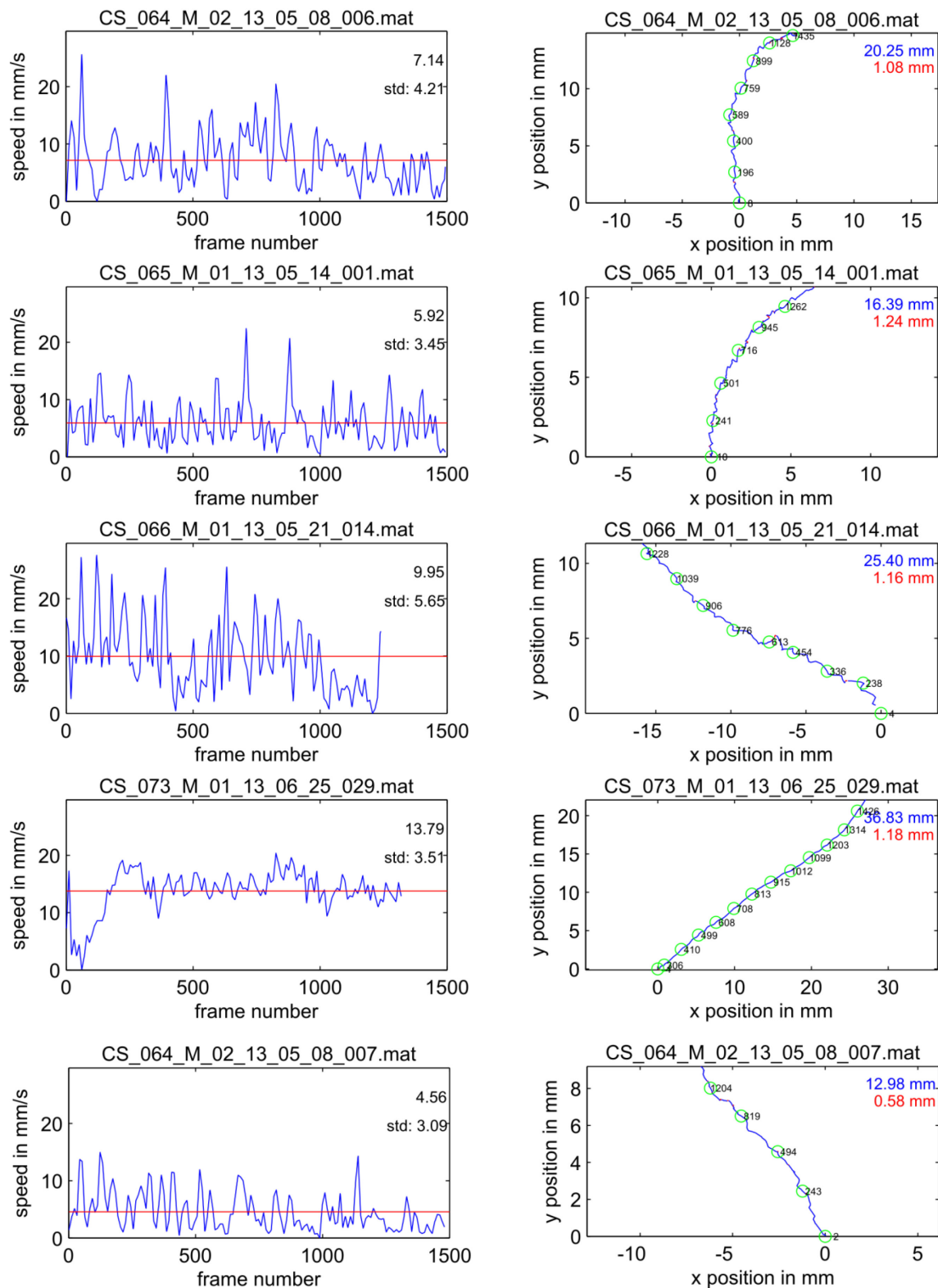
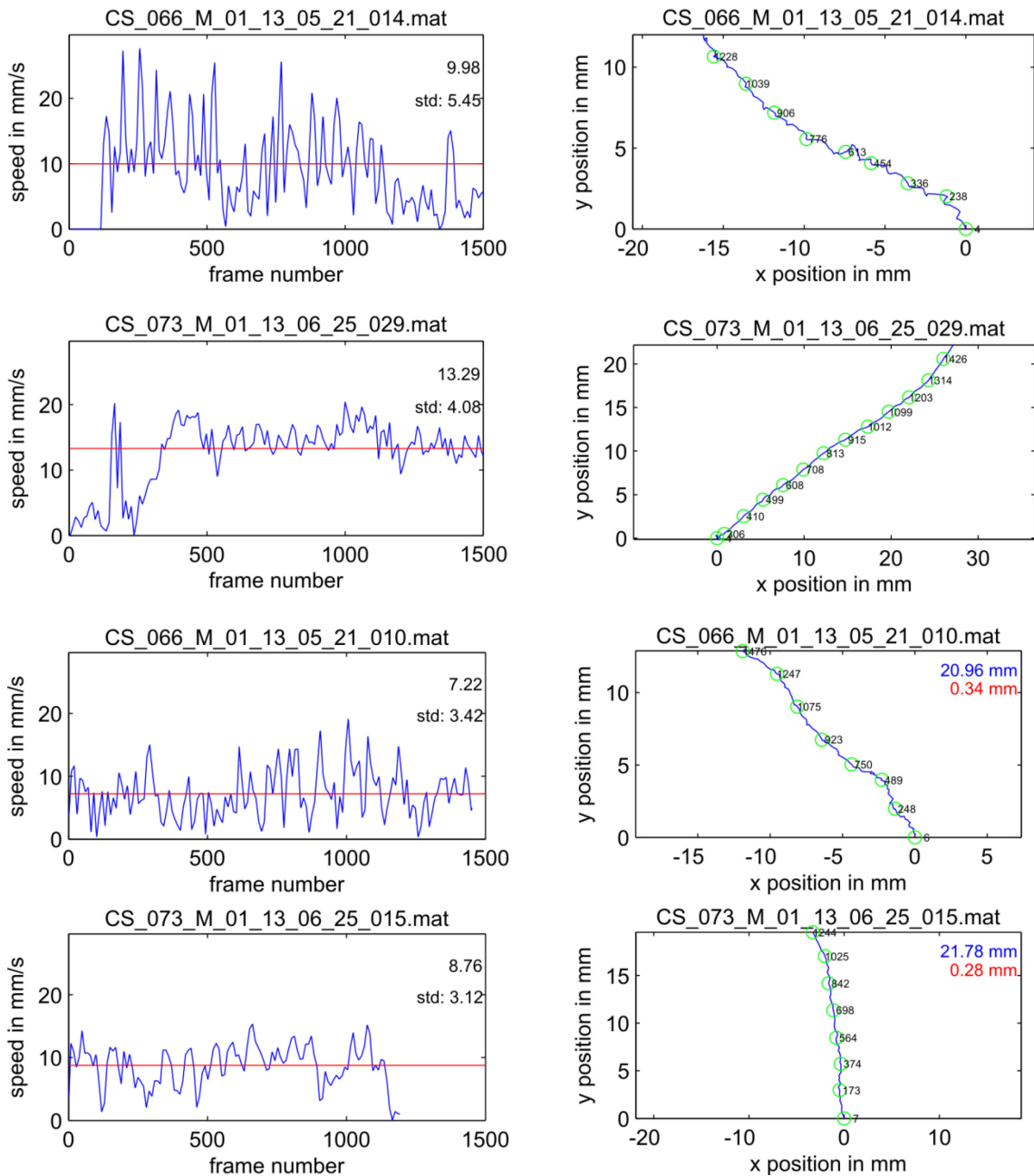


Fig. 54: Walking speed time course (mm/s vs. frame number) and walking trajectory of evaluated single walks from R2 amputees. A solid line indicates the evaluated part on the walking path of the flies in the panels on the right. This line indicates positive velocity in blue and negative velocity in red. Green circles divide the walking path in segments of 2 mm length each. Green circles without a solid line indicate segments of the walking trajectory that have not been evaluated. Blue numbers indicate the length of the walking trajectory with a positive velocity. Red numbers those with a negative velocity. A solid blue line in the speed plots on the left indicates the walking speed time course for the evaluated walking sequence. A red line in the same plots indicates average walking speed of the analyzed walking sequence. Video frame rate was 500 fps (one frame every two ms).



## R2 amputees side-view



**Fig. 55: Walking speed time course (mm/s vs. frame number) and walking trajectory of evaluated single walks from R2 amputees. A solid line indicates the evaluated part on the walking path of the flies in the panels on the right. This line indicates positive velocity in blue and negative velocity in red. Green circles divide the walking path in segments of 2 mm length each. Green circles without a solid line indicate segments of the walking trajectory that have not been evaluated. Blue numbers indicate the length of the walking trajectory with a positive velocity. Red numbers those with a negative velocity. A solid blue line in the speed plots on the left indicates the walking speed time course for the evaluated walking sequence. A red line in the same plots indicates average walking speed of the analyzed walking sequence. Video frame rate was 500 fps (one frame every two ms).**

## R2 amputees nan[36a] side-view

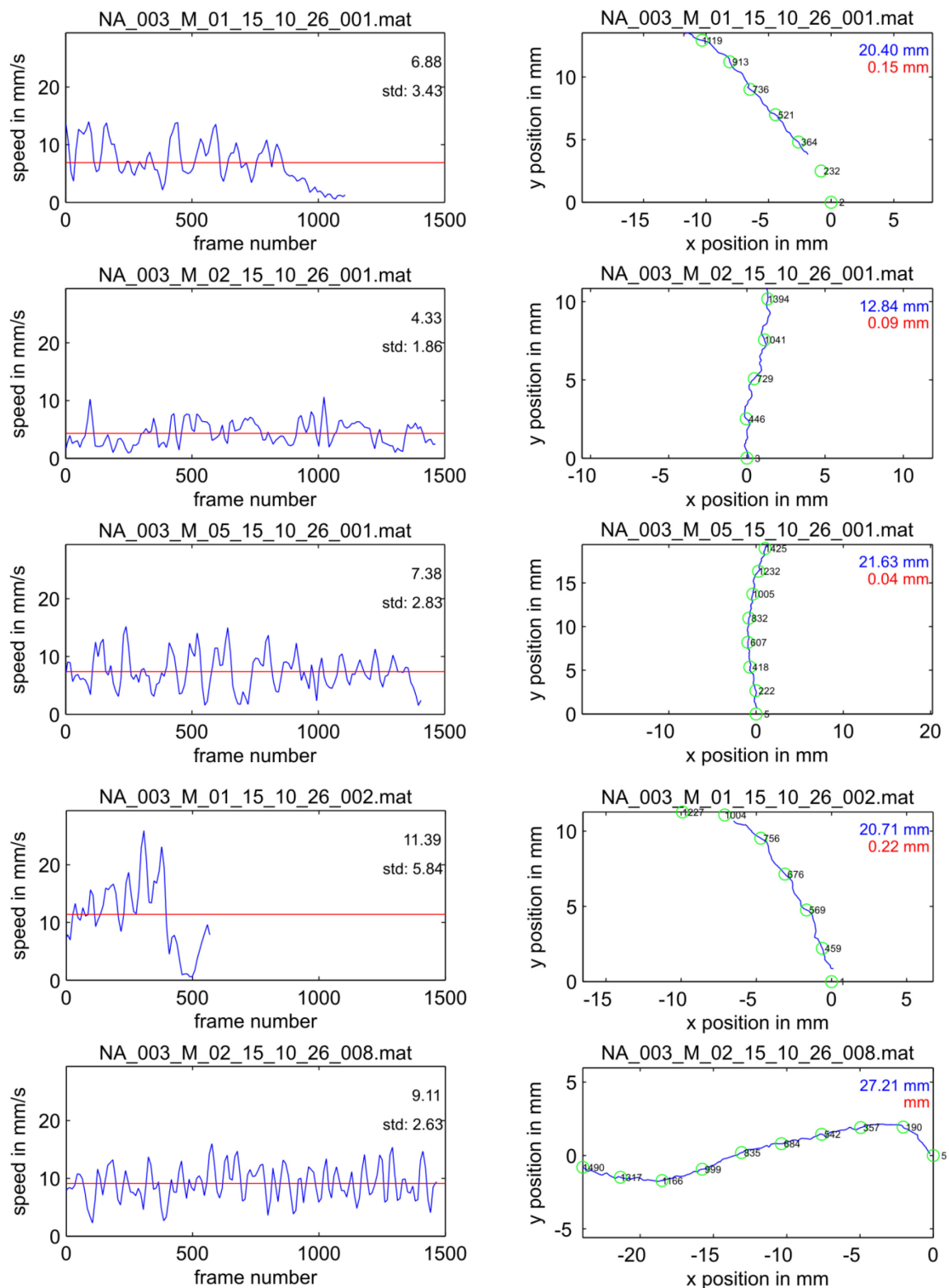
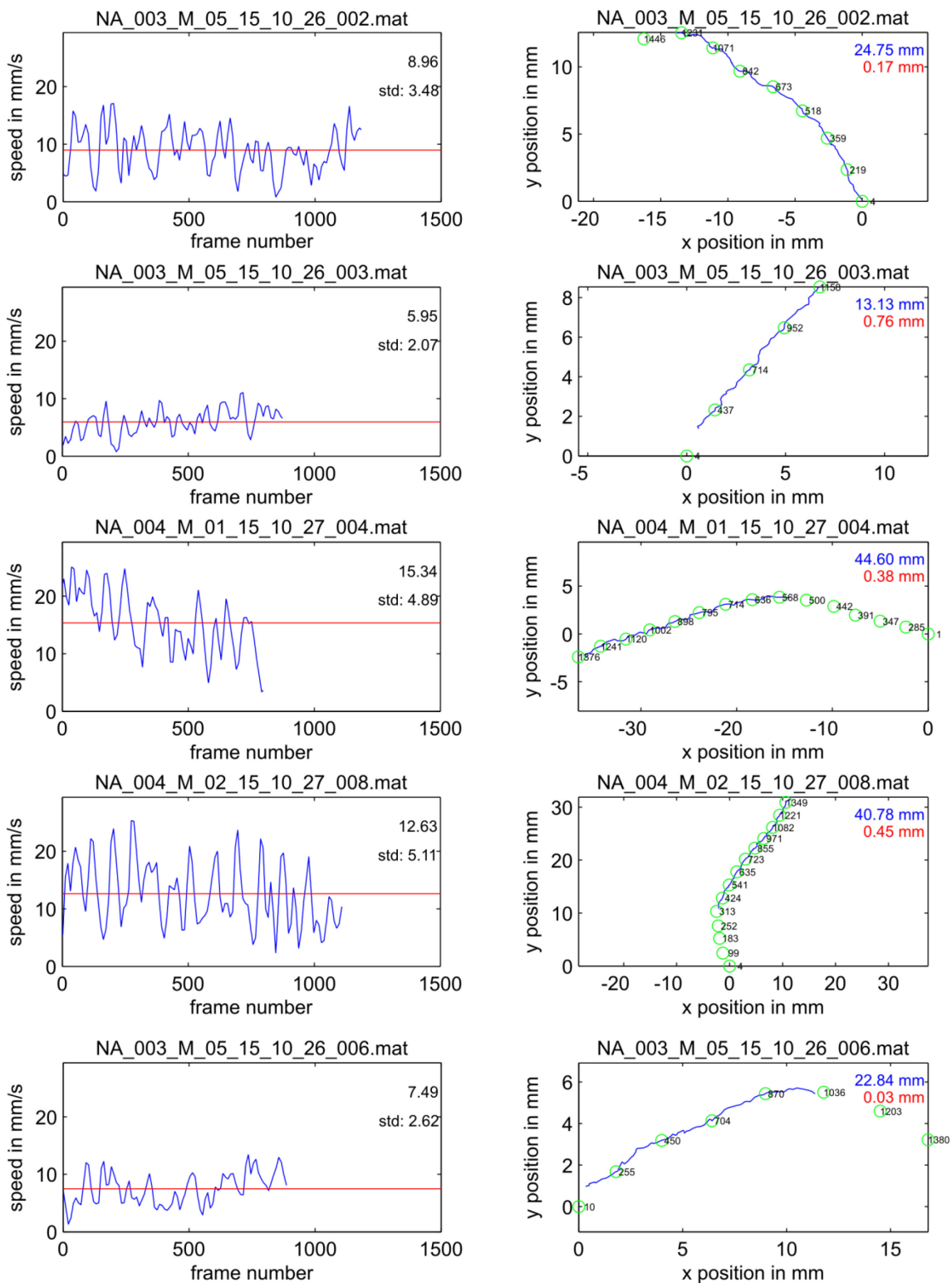


Fig. 56: Walking speed time course (mm/s vs. frame number) and walking trajectory of evaluated single walks from *nan[36a]* R2 amputees. A solid line indicates the evaluated part on the walking path of the flies in the panels on the right. This line indicates positive velocity in blue and negative velocity in red. Green circles divide the walking path in segments of 2 mm length each. Green circles without a solid line indicate segments of the walking trajectory that have not been evaluated. Blue numbers indicate the length of the walking trajectory with a positive velocity. Red numbers those with a negative velocity. A solid blue line in the speed plots on the left indicates the walking speed time course for the evaluated walking sequence. A red line in the same plots indicates average walking speed of the analyzed walking sequence. Video frame rate was 500 fps (one frame every two ms).

## R2 amputees nan[36a] side-view



**Fig. 57:** Walking speed time course (mm/s vs. frame number) and walking trajectory of evaluated single walks from *nan[36a]* R2 amputees. A solid line indicates the evaluated part on the walking path of the flies in the panels on the right. This line indicates positive velocity in blue and negative velocity in red. Green circles divide the walking path in segments of 2 mm length each. Green circles without a solid line indicate segments of the walking trajectory that have not been evaluated. Blue numbers indicate the length of the walking trajectory with a positive velocity. Red numbers those with a negative velocity. A solid blue line in the speed plots on the left indicates the walking speed time course for the evaluated walking sequence. A red line in the same plots indicates average walking speed of the analyzed walking sequence. Video frame rate was 500 fps (one frame every two ms).



## R2 amputees nan[36a] side-view

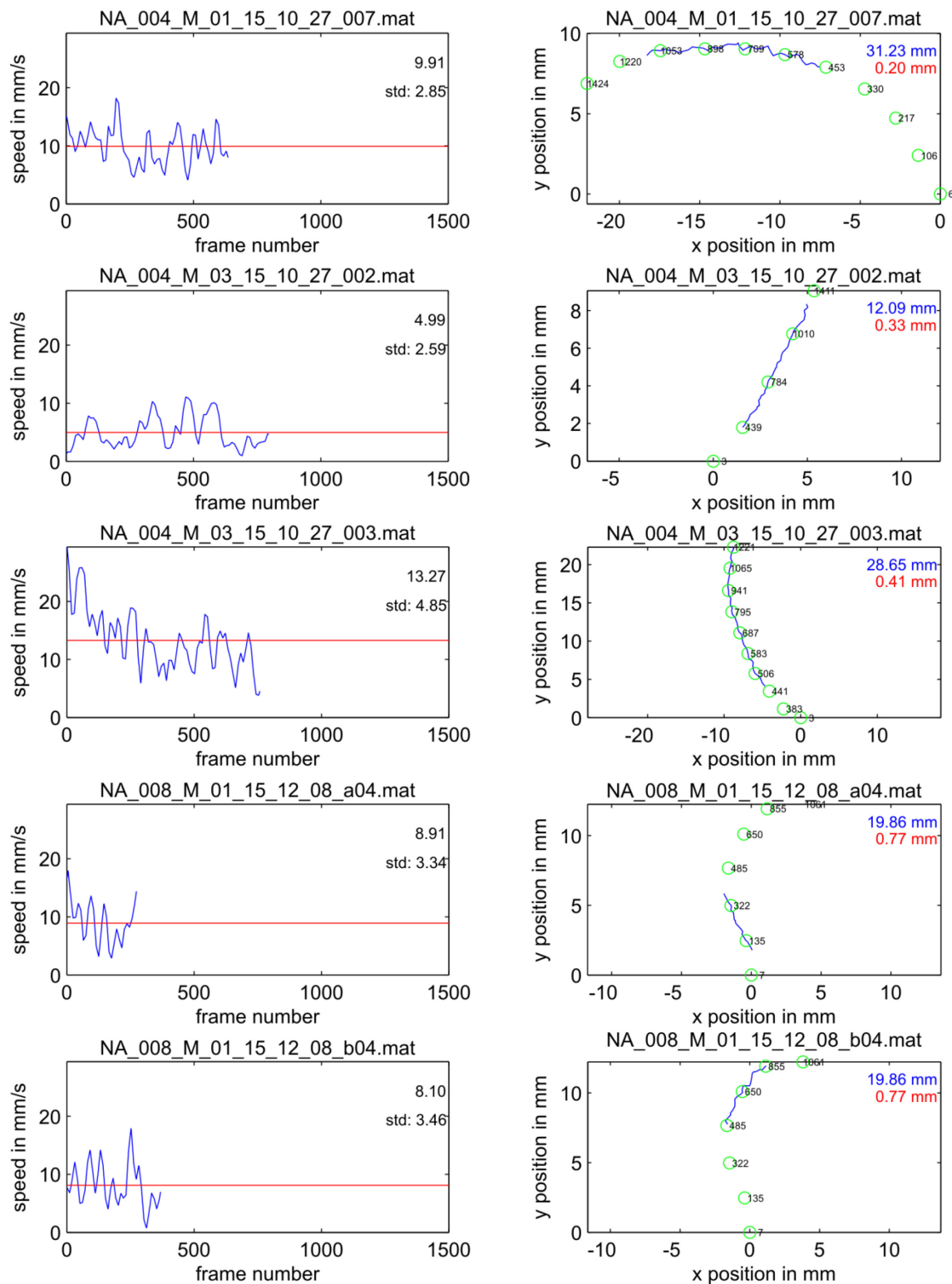
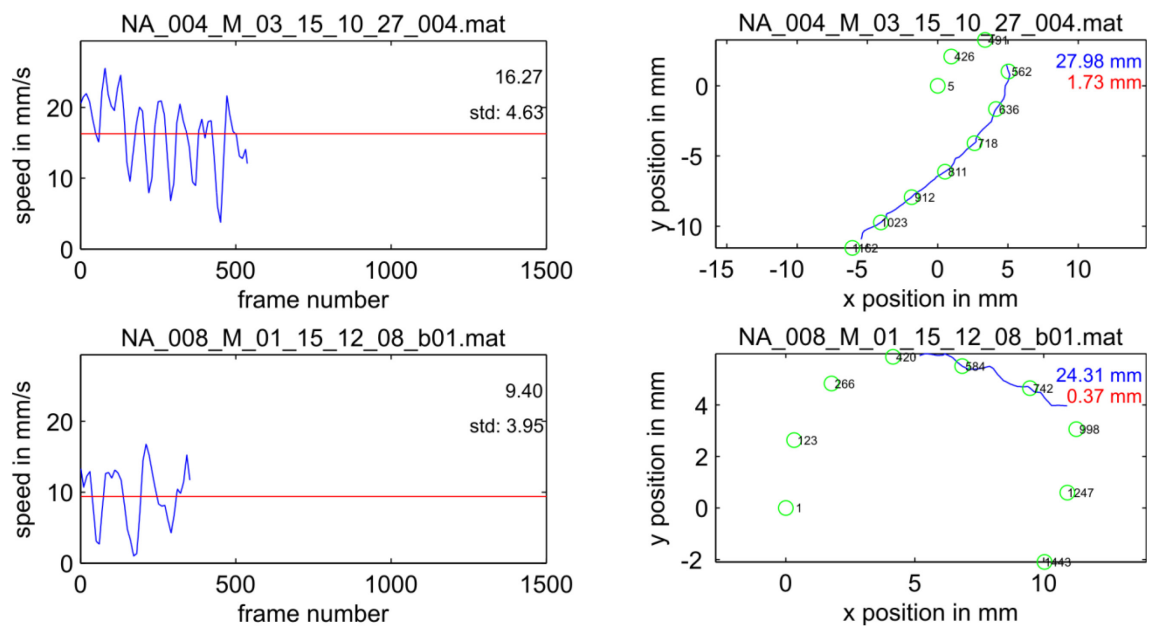


Fig. 58: Walking speed time course (mm/s vs. frame number) and walking trajectory of evaluated single walks from *nan[36a]* R2 amputees. A solid line indicates the evaluated part on the walking path of the flies in the panels on the right. This line indicates positive velocity in blue and negative velocity in red. Green circles divide the walking path in segments of 2 mm length each. Green circles without a solid line indicate segments of the walking trajectory that have not been evaluated. Blue numbers indicate the length of the walking trajectory with a positive velocity. Red numbers those with a negative velocity. A solid blue line in the speed plots on the left indicates the walking speed time course for the evaluated walking sequence. A red line in the same plots indicates average walking speed of the analyzed walking sequence. Video frame rate was 500 fps (one frame every two ms).

## R2 amputees nan[36a] side-view



**Fig. 59: Walking speed time course (mm/s vs. frame number) and walking trajectory of evaluated single walks from *nan[36a]* R2 amputees. A solid line indicates the evaluated part on the walking path of the flies in the panels on the right. This line indicates positive velocity in blue and negative velocity in red. Green circles divide the walking path in segments of 2 mm length each. Green circles without a solid line indicate segments of the walking trajectory that have not been evaluated. Blue numbers indicate the length of the walking trajectory with a positive velocity. Red numbers those with a negative velocity. A solid blue line in the speed plots on the left indicates the walking speed time course for the evaluated walking sequence. A red line in the same plots indicates average walking speed of the analyzed walking sequence. Video frame rate was 500 fps (one frame every two ms).**

## R3 amputees side-view

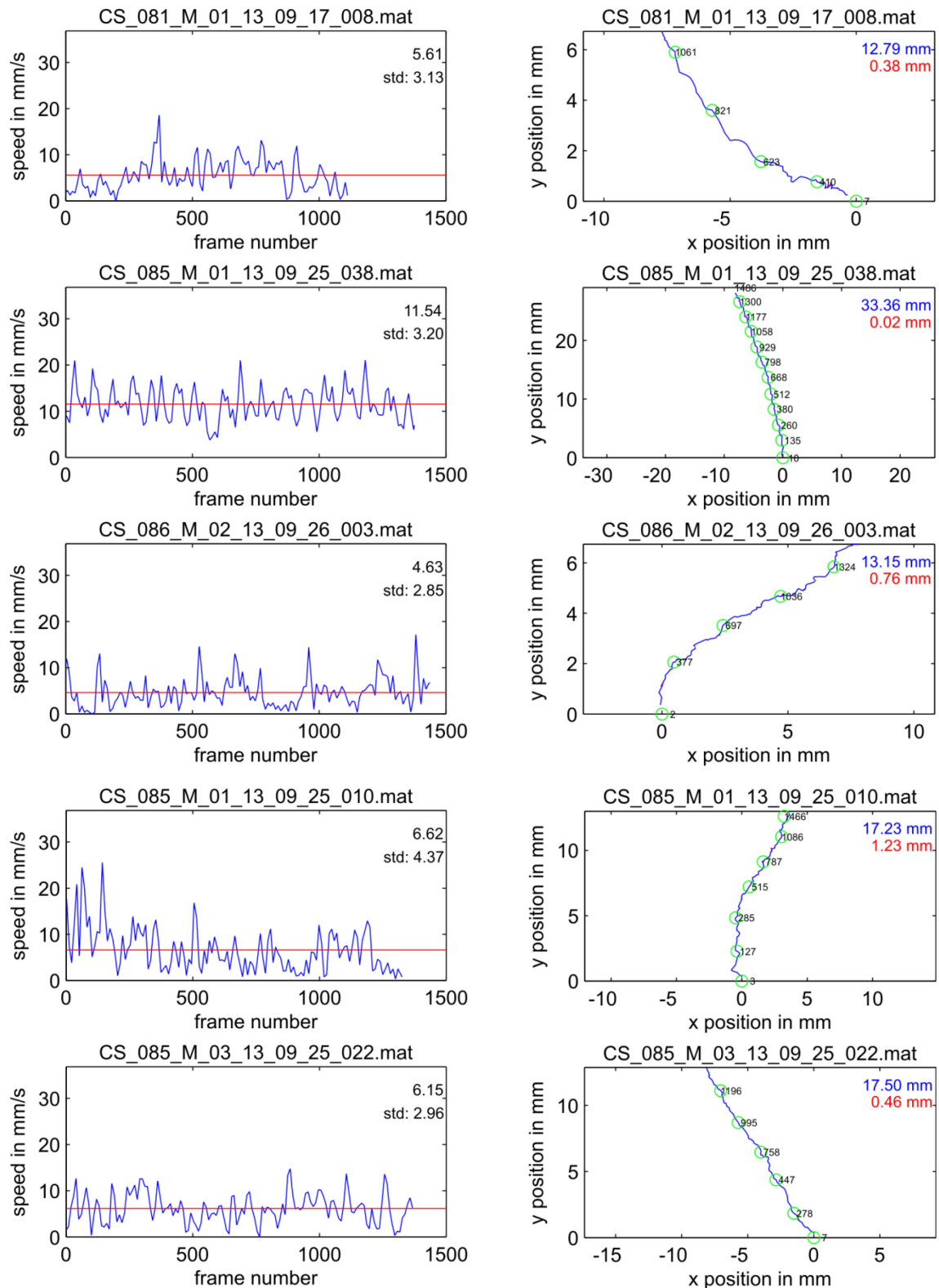


**Fig. 60: Walking speed time course (mm/s vs. frame number) and walking trajectory of evaluated single walks from R3 amputees. A solid line indicates the evaluated part on the walking path of the flies in the panels on the right. This line indicates positive velocity in blue and negative velocity in red. Green circles divide the walking path in segments of 2 mm length each. Green circles without a solid line indicate segments of the walking trajectory that have not been evaluated. Blue numbers indicate the length of the walking trajectory with a positive velocity. Red numbers those with a negative velocity. A solid blue line in the speed plots on the left indicates the walking speed time course for the evaluated walking sequence. A red line in the same plots indicates average walking speed of the analyzed walking sequence. Video frame rate was 500 fps (one frame every two ms).**

## R3 amputees side-view

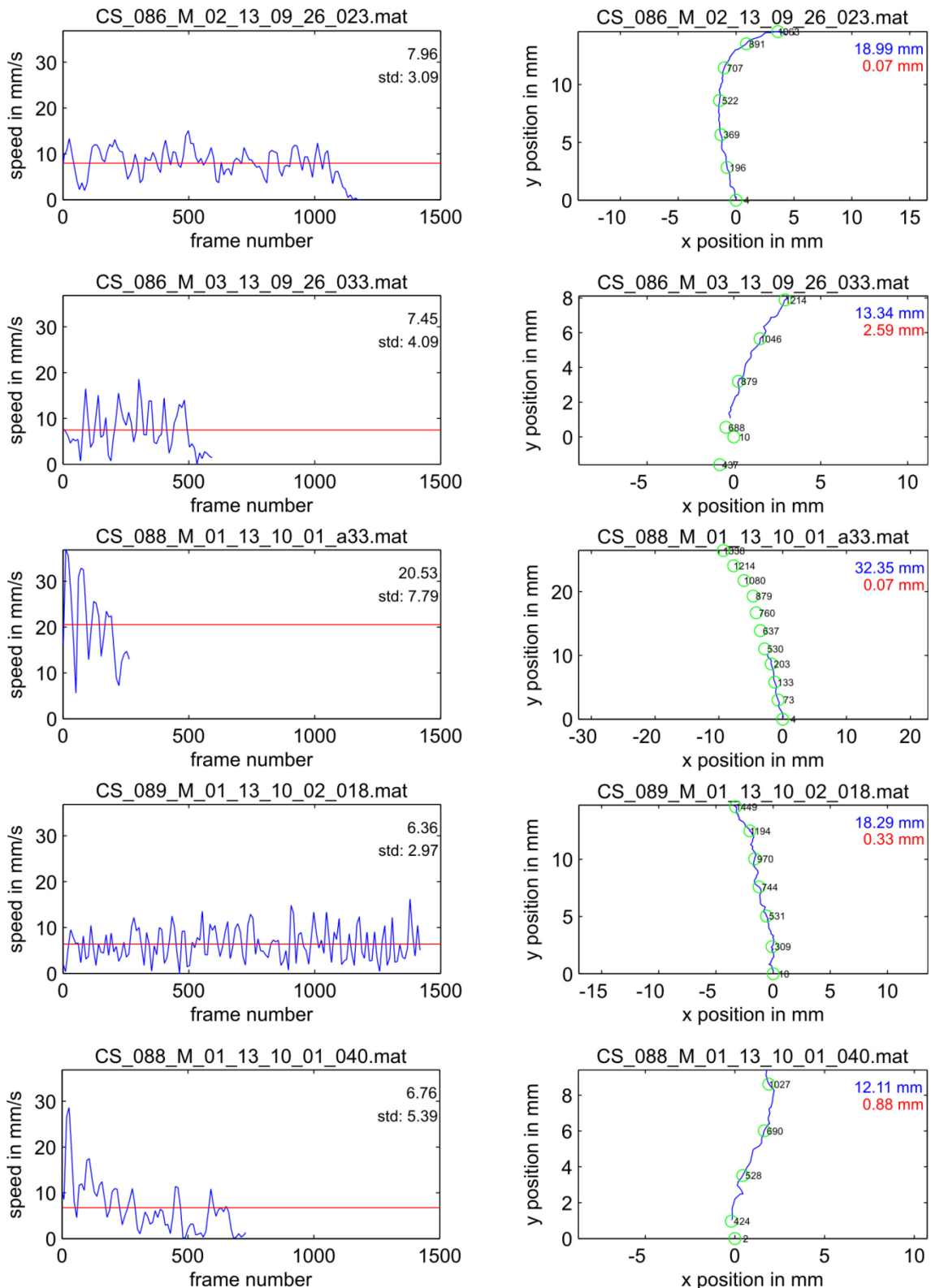


**Fig. 61: Walking speed time course (mm/s vs. frame number) and walking trajectory of evaluated single walks from R3 amputees. A solid line indicates the evaluated part on the walking path of the flies in the panels on the right. This line indicates positive velocity in blue and negative velocity in red. Green circles divide the walking path in segments of 2 mm length each. Green circles without a solid line indicate segments of the walking trajectory that have not been evaluated. Blue numbers indicate the length of the walking trajectory with a positive velocity. Red numbers those with a negative velocity. A solid blue line in the speed plots on the left indicates the walking speed time course for the evaluated walking sequence. A red line in the same plots indicates average walking speed of the analyzed walking sequence. Video frame rate was 500 fps (one frame every two ms).**

## R3 amputees side-view

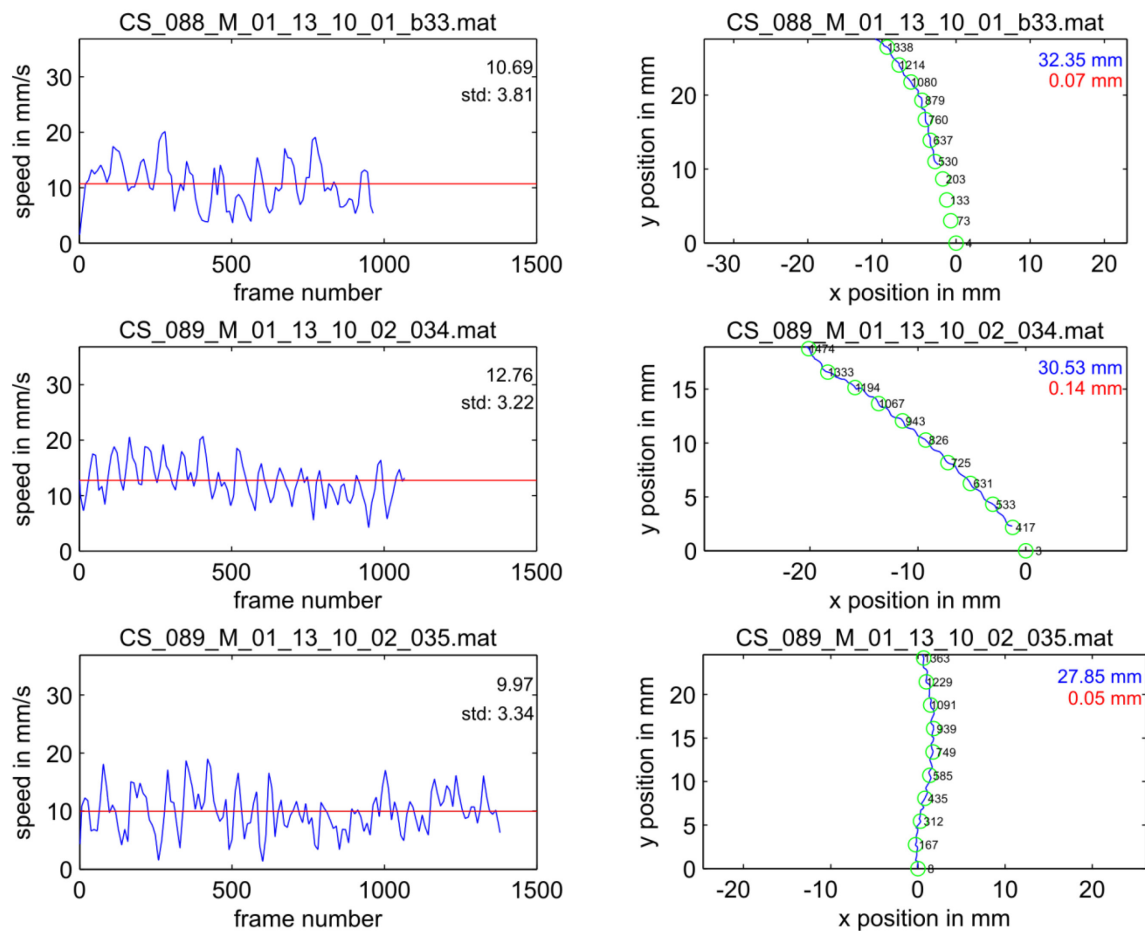


**Fig. 62:** Walking speed time course (mm/s vs. frame number) and walking trajectory of evaluated single walks from R3 amputees. A solid line indicates the evaluated part on the walking path of the flies in the panels on the right. This line indicates positive velocity in blue and negative velocity in red. Green circles divide the walking path in segments of 2 mm length each. Green circles without a solid line indicate segments of the walking trajectory that have not been evaluated. Blue numbers indicate the length of the walking trajectory with a positive velocity. Red numbers those with a negative velocity. A solid blue line in the speed plots on the left indicates the walking speed time course for the evaluated walking sequence. A red line in the same plots indicates average walking speed of the analyzed walking sequence. Video frame rate was 500 fps (one frame every two ms).

## List of Figures

|  |    |
|--|----|
| <b>Fig. 1:</b> Leg modules and their connection via coordination rules (from Dürr et al. 2004).  | 3  |
| <b>Fig. 2:</b> Stereotypic footfall patterns of hexapedal animals.   | 4  |
| <b>Fig. 3:</b> Setups used to study the walking behavior in fruit flies.   | 6  |
| <b>Fig. 4:</b> Exemplary image of a male <i>Drosophila</i> tethered with dental glue and a copper wire on top of a 6 mm polypropylene (PP) ball.                                   | 10 |
| <b>Fig. 5:</b> Flies used had either all legs intact or one leg amputated.   | 11 |
| <b>Fig. 6:</b> Schematic overview of the side-view setup (courtesy of Dr Till Bockemühl).  | 12 |
| <b>Fig. 7:</b> Schematic overview of the top-view setup (courtesy of Dr Till Bockemühl).   | 13 |
| <b>Fig. 8:</b> Scheme illustrating the spatial conventions used in the text.   | 14 |
| <b>Fig. 9:</b> Single video frame of an intact fly walking on a 6 mm polypropylene ball in the top-view setup.   | 16 |
| <b>Fig. 10:</b> Schematic drawing to illustrate the calculation of phase relations in between legs.  | 17 |
| <b>Fig. 11:</b> Scheme illustrating the gliding window approach used to calculate mean phase values for the dataset.   | 18 |
| <b>Fig. 12:</b> Schematic overview of the setup for activity and speed monitoring during voluntary walking.  | 20 |
| <b>Fig. 13:</b> Figure showing the image processing steps involved during background subtraction.  | 22 |
| <b>Fig. 14:</b> User interface displaying the adjustable parameters of the function flytrackingparadigm.   | 23 |
| <b>Fig. 15:</b> User interface of the evaluateflytracking function.  | 24 |
| <b>Fig. 16:</b> (A) Trajectories of all legs on the right body side derived from a single walk of an intact animal.  | 26 |
| <b>Fig. 17:</b> Periods of leg movement vs. walking speed (in mm per second, mm/s) for intact <i>Canton-S</i> flies.   | 27 |
| <b>Fig. 18:</b> Movements (vertical component only) of intact leg tarsi or the tip of stumps   | 28 |
| <b>Fig. 19:</b> Periods of leg movement vs. walking speed (in body lengths per second, BL/s) for the legs ipsilateral to the camera (N = number of animals; n = number of steps).  | 31 |
| <b>Fig. 20:</b> Example trial of a CS R2 amputee during which the animal stopped stepping with the intact legs whereas the stump was still continuously active.                    | 32 |
| <b>Fig. 21:</b> Relative phase relation of an event in one leg (PEP) or stump (DEP) versus a reference event in another leg or stump (N = number of animals; n = number of steps). | 35 |
| <b>Fig. 22:</b> Length of the mean resultant vector plotted versus walking speed [BL/s].   | 38 |
| <b>Fig. 23:</b> Time intervals between PEPs in intact legs and stump VEPs and DEPs.  | 39 |
| <b>Fig. 24:</b> Stump levation and depression movements 100ms before and after a PEP event in intact legs (N = number of animals; n = number of steps).                            | 40 |

|  |           |
|--|-----------|
| <b>Fig. 25:</b> Duty factor as a function of walking speed [BL/s] (N = number of animals; n = number of steps).....  | <b>41</b> |
| <b>Fig. 26:</b> Movements (horizontal component only) of intact leg tarsi or the tip of stumps, respectively, over time for typical slow (A and B) and fast walks (C and D) of a middle leg amputee.....                                     | <b>42</b> |
| <b>Fig. 27:</b> (A) Trajectories of all legs derived from a single walk of an intact animal.....   | <b>43</b> |
| <b>Fig. 28:</b> Leg periods (in ms) as a function of walking speed (in body length per second, BLs) for all legs on the right (panels A) and left (panels B) body side of an intact animal (N = number of animals; n = number of steps)..... | <b>44</b> |
| <b>Fig. 29:</b> Phase relations of swing onset for all legs of intact animals (N = number of animals; n = number of steps).....  | <b>46</b> |
| <b>Fig. 30:</b> Periods of leg movement as a function of walking speed.....  | <b>48</b> |
| <b>Fig. 31:</b> Phase relations between reference legs and dependent legs on the left body side of the animal.....   | <b>49</b> |
| <b>Fig. 32:</b> Phase relations between reference legs and dependent legs on the right body side of the animal (N = number of animals; n = number of steps).....   | <b>50</b> |
| <b>Fig. 33:</b> Relative phase of a PEP event in a leg or stump on the right body side versus a reference PEP in a leg on the left body side (N = number of animals; n = number of steps).....   | <b>52</b> |
| <b>Fig. 34:</b> Length of the mean resultant vector plotted versus walking speed [BL/s].....   | <b>53</b> |
| <b>Fig. 35:</b> Phase relations of swing onset for the five intact legs of R3 amputees (N = number of animals; n = number of steps).....   | <b>55</b> |
| <b>Fig. 36:</b> Length of the mean resultant vector plotted versus walking speed [BL/s], for the legs on the left body side.....   | <b>56</b> |
| <b>Fig. 37:</b> Length of the mean resultant vector plotted versus walking speed [BL/s], for the legs on the right body side.....  | <b>57</b> |
| <b>Fig. 38:</b> Histograms showing the probability with which the animals walked at a certain speed (N = number of animals).....   | <b>58</b> |
| <b>Fig. 39:</b> Histograms showing the probability with which the animals walked at a certain speed (N = number of animals).....   | <b>60</b> |
| <b>Fig. 40:</b> Bouts of walking activity [specified as fraction of bouts = n bouts/total n bouts] that showed a certain length (specified in s).....  | <b>61</b> |
| <b>Fig. 41:</b> Bouts of walking activity (specified as fraction of bouts = n bouts/total n bouts) that showed a certain duration (specified in s).....  | <b>62</b> |
| <b>Fig. 42:</b> Number of walking animals counted for every video frame.....   | <b>63</b> |
| <b>Fig. 43:</b> Number of walking animals counted for each video frame.....  | <b>65</b> |
| <b>Fig. 44:</b> Time intervals between AEPs in intact legs and stump VEPs and DEPs.....  | <b>88</b> |

|  |            |
|--|------------|
| <b>Fig. 45:</b> Circular plot showing the relative phase relation of an event in one leg (PEP) or stump (DEP) versus a reference event in another leg or stump. ....                     | <b>90</b>  |
| <b>Fig. 46:</b> Circ plots showing the phase relations of swing onset for all legs of intact animals (black dots) and single leg amputees (cyan dots) in a speed range below 5 BL/s..... | <b>91</b>  |
| <b>Fig. 47:</b> Circ plots showing the phase relations of swing onset for all legs of intact animals (black dots) and single leg amputees (cyan dots) in a speed range above 5 BL/s..... | <b>92</b>  |
| <b>Fig. 48:</b> Walking speed time course (mm/s vs. frame number) and walking trajectory of evaluated single walks from intact animals. ....   | <b>93</b>  |
| <b>Fig. 49:</b> Walking speed time course (mm/s vs. frame number) and walking trajectory of evaluated single walks from intact animals. ....   | <b>94</b>  |
| <b>Fig. 50:</b> Walking speed time course (mm/s vs. frame number) and walking trajectory of evaluated single walks from R1 amputees.....   | <b>95</b>  |
| <b>Fig. 51:</b> Walking speed time course (mm/s vs. frame number) and walking trajectory of evaluated single walks from R1 amputees.....   | <b>96</b>  |
| <b>Fig. 52:</b> Walking speed time course (mm/s vs. frame number) and walking trajectory of evaluated single walks from R1 amputees.....   | <b>97</b>  |
| <b>Fig. 53:</b> Walking speed time course (mm/s vs. frame number) and walking trajectory of evaluated single walks from R2 amputees.....   | <b>98</b>  |
| <b>Fig. 54:</b> Walking speed time course (mm/s vs. frame number) and walking trajectory of evaluated single walks from R2 amputees.....   | <b>99</b>  |
| <b>Fig. 55:</b> Walking speed time course (mm/s vs. frame number) and walking trajectory of evaluated single walks from R2 amputees.....   | <b>100</b> |
| <b>Fig. 56:</b> Walking speed time course (mm/s vs. frame number) and walking trajectory of evaluated single walks from <i>nan[36a]</i> R2 amputees.....                                 | <b>101</b> |
| <b>Fig. 57:</b> Walking speed time course (mm/s vs. frame number) and walking trajectory of evaluated single walks from <i>nan[36a]</i> R2 amputees.....                                 | <b>102</b> |
| <b>Fig. 58:</b> Walking speed time course (mm/s vs. frame number) and walking trajectory of evaluated single walks from <i>nan[36a]</i> R2 amputees.....                                 | <b>103</b> |
| <b>Fig. 59:</b> Walking speed time course (mm/s vs. frame number) and walking trajectory of evaluated single walks from <i>nan[36a]</i> R2 amputees.....                                 | <b>104</b> |
| <b>Fig. 60:</b> Walking speed time course (mm/s vs. frame number) and walking trajectory of evaluated single walks from R3 amputees.....   | <b>105</b> |
| <b>Fig. 61:</b> Walking speed time course (mm/s vs. frame number) and walking trajectory of evaluated single walks from R3 amputees.....   | <b>106</b> |
| <b>Fig. 62:</b> Walking speed time course (mm/s vs. frame number) and walking trajectory of evaluated single walks from R3 amputees.....   | <b>107</b> |



## Danksagung

### **Mein Besonderer Dank gilt:**

Prof. Dr. Ansgar Büschges für die freundliche Aufnahme in seine Arbeitsgruppe, die Betreuung der vorliegenden Arbeit, seinen Humor und seine Unterstützung sowohl auf wissenschaftlicher als auch auf menschlicher Ebene.

Dr. Silvia Gruhn für die freundliche Übernahme des Zweitgutachtens.

Dr. Till Bockemühl dafür das er mich fürs Programmieren begeistert hat, unzählige wissenschaftliche Ratschläge, das Programmieren vieler von mir benutzter MATLAB Funktionen, viele interessante Gespräche und das Korrekturlesen von Teilen der vorliegenden Arbeit.

Den Elektroboyz Dipl. Ing. Michael Dübbert und Jan Sydow für ihren Humor, viele interessante und lehrreiche Gespräche, Konstruktion und Bau diverser von mir eingesetzter Setups sowie allgemein exzellente technische Unterstützung.

Unsere technischen Assistenten Hans-Peter Bollhagen, Sima Seyed-Nejadi, Sherylane Seeliger und Tierpflegerin Corinna Rosch für technische Unterstützung sowie viele interessante Gespräche.

Thomas Stolz, Charalampos Mantziaris, Alexander Seldon Chockley und besonders Anna C. Schneider für das Korrekturlesen des Manuskripts und viel konstruktive Kritik an der vorliegenden Arbeit.

Joscha Schmitz für seine Hilfe bei der Formatierung des vorliegenden Textes.

Allen aktuellen und ehemaligen Mitgliedern der zwei Büros in denen ich arbeiten durfte für die sehr angenehme Arbeitsatmosphäre.

Überhaupt danke ich allen Mitgliedern der Arbeitsgruppen Büschges, Wellmann und Gruhn für die sehr angenehme und kollegiale Arbeitsatmosphäre, in der Hoffnung das diese von zukünftigen Mitgliedern der Arbeitsgruppen so erhalten wird.

### **Persönlich besonders Danken möchte ich:**

Meiner Familie für ihre Unterstützung während meiner gesamten Ausbildung sowohl in finanzieller als auch in menschlicher Hinsicht.

Meinen Freunden innerhalb und außerhalb der Uni, dafür das ich zu so vielen Veranstaltungen eingeladen war obwohl ich kein einfacher Mensch bin.

## Teilpublikationen

### Conference abstracts

**Berendes V.**, Büschges A., Bockemühl T., (2015) Speed-dependent interplay between CPG activity and sensory feedback during walking in *Drosophila*. *Proc. of the 11th Meeting of the German Neuroscience Society, Göttingen. Conference Abstract T21-12D.*

## Erklärung

Ich versichere, dass ich die von mir vorgelegte Dissertation selbständig angefertigt, die benutzten Quellen und Hilfsmittel vollständig angegeben und die Stellen der Arbeit einschließlich Tabellen, Karten und Abbildungen, die anderen Werken im Wortlaut oder dem Sinn nach entnommen sind, in jedem Einzelfall als Entlehnung kenntlich gemacht habe; dass diese Dissertation noch keiner anderen Fakultät oder Universität zur Prüfung vorgelegen hat; dass sie abgesehen von unten angegebenen Teilpublikationen noch nicht veröffentlicht worden ist, sowie, dass ich eine solche Veröffentlichung vor Abschluss des Promotionsverfahrens nicht vornehmen werde. Die Bestimmungen der Promotionsordnung sind mir bekannt. Die von mir vorgelegte Dissertation ist von Prof. Dr. Ansgar Büschges betreut worden.

Köln, den 2.07.16

## Curriculum vitae

Name: Volker Berendes

Geburtsdatum: 27.12.1983

Geburtsort: Bensberg, heute Bergisch Gladbach

Staatsangehörigkeit: Deutsch

Familienstand: ledig

Vater: Heinrich Berendes  
Beruf: Dipl.-Ing. Maschinenbau

Mutter: Beate Berendes, geb. Balluff  
Beruf: Organisationsprogrammiererin

## Ausbildung

April 2012 - April 2016 Doktorand am Lehrstuhl von Prof. Dr. Büschges

Januar 2012 - April 2012 Arbeit als wissenschaftlicher Mitarbeiter am  
Lehrstuhl von Prof. Dr. Büschges

10.01.2012 Abschluss Master of Science

Juli 2011 - 10.1.2012 Anfertigung einer Masterarbeit am Lehrstuhl  
von Prof. Dr. Büschges

01.10.2009 - Juli 2011 Masterstudium der Biologie

02.09.2009 Abschluss Bachelor of Science

24.03.2009 - 02.09.2009 Anfertigung einer Bachelorarbeit am Lehrstuhl  
von Prof. Dr. Hülskamp

01.10.2004 - 24.03.2009 Bachelorstudium der Biologie

01.10.2004 Zulassung für Biologie Bachelor  
Aufnahme des Studiums WS 04/05

01.10.2003 Immatrikulation an der Uni Köln

WS 03/04 Chemie  
SS 04 Geologie

---

1994 - 2003

Stadtgymnasium Köln-Porz, Abschluss Abitur

1989 - 1994

Kath. Grundschule Kupfergasse

### **Praktika**

19.01.09 - 24.03.09

„Etagenpraktikum“ AG Prof. Dr. Hülkamp  
Botanisches Institut der Universität zu Köln

25.08.08 - 26.09.08

Fortsetzung des berufsorientierenden Praktikums  
am Max-Planck-Institut für Züchtungsforschung

11.08.08 - 22.08.08

Praxisorientierte Lehrveranstaltung

Molecular Cloning (Dr. Reugels, Uni Köln)

01.08.08 - 10.08.08

berufsorientierendes Praktikum am Max-Planck-  
Institut für Züchtungsforschung Abteilung Prof. Dr.  
Coupland (AG Davis)

Köln, den 25.07.16